Food Structure

Volume 7 | Number 2 Article 1

1988

Food Microstructure

ISSN 0730-5419
CODEN – FMICDK
Vol. 7, No. 2, 1988

FOOD MICROSTRUCTURE

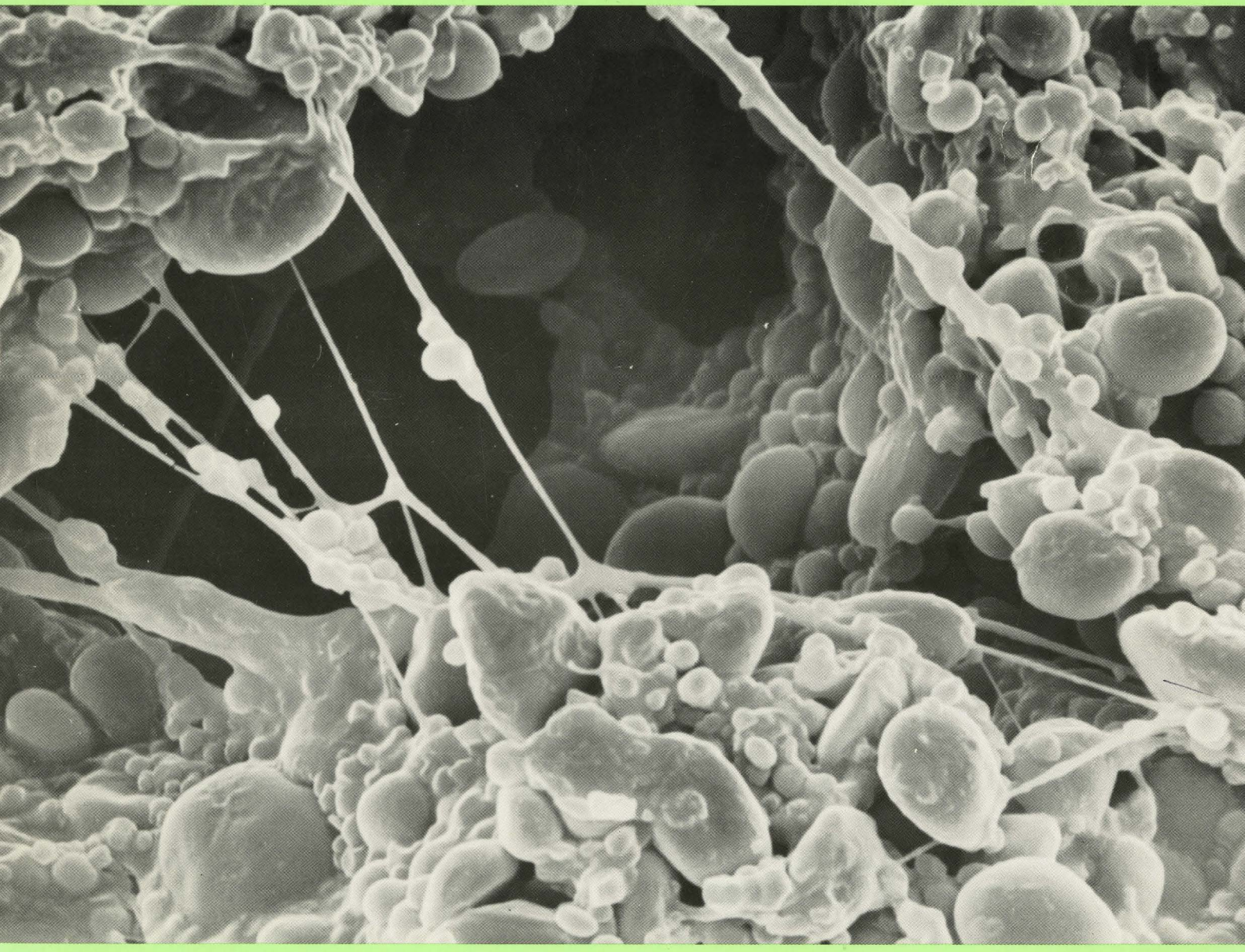

Published By Scanning Microscopy International

FOOD MICROSTRUCTURE

An International Journal on the Microstructure and Microanalysis of Foods, Feeds and their Ingredients

Annual Subscription Rates (including postage and handling by surface mail)

1982 to 1988	U.S. $50.00 (U.S. delivery); U.S. $55 (elsewhere)
1989	U.S. $65.00 (U.S. delivery); U.S. $70.00 (elsewhere)

Business Communications:

Address all communications regarding subscriptions, change of address, etc. to Dr. Om Johari. (See below)

Editorial Correspondence and Inquiries:

Submit papers (see last page), news items, books for review, etc. to one of the editors or to:

Dr. Om Johari, Scanning Microscopy International (SMI)
P.O. Box 66507, Chicago (AMF O'Hare), IL 60666, U.S.A.

FOOD MICROSTRUCTURE, Vol. 7 (1988), pp. 123-135
Scanning Microscopy International, Chicago (AMF O'Hare), IL 60666 USA

0730-5419/88$3.00+.00

M2128

THE APPLICATION OF COLD STAGE SCANNING ELECTRON MICROSCOPY TO FOOD RESEARCH

J.A. Sargent*

Hexland Electron Microscopy Division
Oxford Instruments Limited
Eynsham, Oxford OX8 1TL, U.K.
Phone No. (0865) 882855

Abstract

Most foods and associated microorganisms contain water which in the vacuum of an electron microscope would rapidly evaporate at ambient temperature. In addition constituent fats may melt under the electron beam. Cryopreservation and examination at low temperature avoids these problems. The structure of emulsified or foamed products can be revealed by freeze-fracture techniques. Products such as ice cream which are not stable even under normal pressures at ambient temperature can be prepared rapidly and examined for prolonged periods.

Initial paper received August 09, 1988
Manuscript received November 14, 1988
Direct inquiries to J.A. Sargent
Telephone number: 44-8675-3853

KEY WORDS: Cold stage scanning electron microscopy, hydrated foods, fats, emulsions, foams, spoilage organisms.

* Present address:

Electron Microscopy Consultancy,
Mendota House,
Islip,
Oxford OX5 2SB, U.K. Phone No. (08675) 3853

Introduction

Food scientists have long recognised the value of scanning electron microscopy in the quest to relate the detailed structure of foodstuffs and food products to parameters such as texture, and shelf life. However, the examination of many foods in the SEM has been hampered by the presence within them of fat or water or both. Under ambient temperature conditions most fats would melt under the electron beam (Kalab, 1983, 1984) and the vacuum within the microscope would promote rapid evaporation of the water. Not only would specimen shrinkage and distortion be a consequence but contamination of the microscope would occur. Traditional approaches to the problem of hydrated samples have included freeze-drying or critical point-drying of samples before inserting them into the SEM. Not only are those methods time-consuming, but both may induce unacceptable artefacts in the specimens themselves. Up to 40% shrinkage is not uncommon during freeze-drying and gross distortion can occur (Boyde & Franc, 1981; Boyde & Maconnachie, 1979; Eveling, 1987; Kalab, 1984). Moreover, because critical point-drying involves immersion in solvents, certain components, including fats, can be totally extracted from the specimen (Sargent, 1983).

These problems can be avoided by cold stage electron microscopy (e.g., Bastacky et al, 1987; Pawley and Norton, 1978; Robards and Crosby, 1979; Sargent, 1988a, 1988b). This technique involves freezing the specimen and examining it in the SEM at a temperature (usually around -180°C) at which neither is water lost by sublimation nor fats melted by the energy of the electron beam. The theory and practice of rapid freezing are well reviewed by Robards and Sleytr (1985).Commercially available equipment provides means for rapid specimen cooling and transfer to the SEM in a way which avoids frost contamination (Beckett and Read, 1986; Sargent, 1988a). In addition, specimens can be freeze-fractured or cryo-honed with a cooled steel or tungsten carbide blade which passes through the frozen specimen at a height set by a micrometer screw. A suitable metallic or carbon film is applied to the specimen by diode sputtering or evaporation at low temperature. Controlled heating of the

cooled stage to a predetermined temperature (usually -80°C) permits the controlled sublimation of a naturally occurring surface film of water or etching of a fracture face by careful removal of water. X-ray microanalysis of the specimen on the cold stage presents no problems. Indeed, because soluble components are immobilized at low temperature, greater confidence can be placed in elemental distribution data gained in this way (Echlin, 1984; Marshall, 1988; Roomans, 1988a,b; Wroblewski et al, 1988).

The problems associated with preparing specimens for freeze-fracture and the necessary steps required to reduce artifacts such as the growth of ice crystals within hydrated material are identical with those familiar to electron microscopists who, over the years, have engaged in the laborious practice of making replicas of freeze-fracture faces for transmission electron microscopy. Buchheim (1982a) has reviewed aspects of sample preparation for the preparation of freeze-fracture replicas of food systems.

Of the many advantages conferred by the cryopreservation of SEM samples, an important one for most researchers is its speed. Specimens are commonly frozen, freeze-fractured, coated and prepared for examination within 8 minutes. If they are to be examined uncoated at low accelerating voltages which do not cause charging problems, preparation times are shorter.

The purpose of this paper is to demonstrate how cryopreservation can facilitate the rapid examination of a wide range of basic foodstuffs, how it permits the evaluation of "difficult" products, particularly emulsified and foamed foods, finally, how the presence and development of spoilage agents can be visualized. All the illustrations are of specimens prepared using the Hexland CT1000 A Cryotrans system which can be interfaced to any SEM. Specimens were frozen, without prior treatment, by plunging them into nitrogen slush. If only surface features were to be examined, their size was unimportant, and they were attached, before freezing, to a specimen holder using conducting carbon cement. Liquids or creams, which were to be freeze-fractured, were held between two small rivets and plunged into nitrogen slush. Their cooling rates were thus increased by minimizing the associated mass of metallic support during freezing. The micrographs were taken on a Philips 505 SEM at 25 kV after coating the specimens with gold at -180°C.

Seeds and starch products

Seeds, particularly those of cereals are a major component of the world's food supply and provide the raw products for much of the food processing industry. The importance of baking and brewing to the world's economy is self evident and an understanding of the changes which seed components undergo during processing is of paramount importance in maximizing efficiency during their conversion to acceptable foods and beverages.

Cryopreservation enables seeds such as the imbibed caryopsis of barley shown in figure 1 to be examined without alteration in their hydration state. This specimen was freeze-fractured. The 3-dimensional structure of the starchy endosperm can be readily examined (figure 2). Dry milled flour (figure 3) can be imaged at room temperature in the SEM but should any component be swollen or its structure altered by absorption of water under humid conditions its form will be retained by cryopreservation. The uncertainty about the changes which occur as starch grains become gelatinized is now being resolved (Bowller et al, 1987). The wheat starch shown in figure 4 was soaked in water at 60°C for 10 minutes. The hydrated grains were washed, fast frozen, and freed from surface ice by sublimation. Earlier work based on freeze-dried gelatinized starch grains suggested that this treatment causes grains to become pitted. It is now realised that the pits were artefacts formed during relatively slow freezing and the growth of ice crystals in the hydrated grain surface. Little surface pitting is evident after fast freezing.

Cryopreservation is an ideal method for arresting the development of doughs in order to follow structural changes which occur during their preparation and baking. Figure 5 shows a hydrated, part-baked pizza dough. Even the delicate strands of gluten which originated from the wedge protein are well preserved. In a similar way, the structure of fatty materials such as peanut cotyledon shown in figure 6 can be examined. The technique permits the monitoring of structural changes induced by different roasting regimes or through incorporation into composite foods.

Emulsions

Dairy products were among the first foods to be examined by electron microscopy (Brookeer, 1979; Kalab, 1981; Schmidt, 1982) and many groups throughout the world are now using cold stage scanning electron microscopy to study these materials (Brooker, 1987: Brooker et al., 19886; Heertje et al., 1987; Kalab & Modler, 1985)). Figures 7 and 8 are included to illustrate the value of the low temperature technique in estimating droplet sizes in these products and the spatial relationships between components. Figure 7 shows cream (48% fat) freeze-fractured to reveal the oil-in-water emulsion and figure 8 demonstrates the water-in-oil state after conversion to butter has taken place. Some of the water droplets are very large indeed. Low fat spreads have a high water content (figure 9) and freeze-fracture reveals the extent to which a water phase network can form. Heertje et al. (1987) have described a method for selectively removing the oil phase from these emulsions followed by freeze-fracture and cryo-examination of the aqueous phase in the SEM.

Many salad dressings blended with a variety of flavouring components are produced commercially. The SEM examination of freeze-fracture faces can reveal much about their structure and emulsion stability. Figure 10 shows a Blue cheese salad dressing. The

dispersed oil droplets occur in a variety of sizes in this preparation. Time course studies show that throughout the shelf life of products like these it is common for the oil droplets to coalesce progressively. Ultimately the phases separate and layer. Low temperature scanning electron microscopy thus offers a rapid means of monitoring the ageing of emulsions and the efficiency of means aimed at delaying phase separation. The surfaces of some of the droplets shown in figure 10 appear rough, others are smooth. This probably indicates the presence of a membrane-like material surrounding the droplets which is likely to influence the emulsion's stability. Whether the droplet appears rough or smooth depends on whether the fracture plane occurred on the water or oil side of the interfacial material. Crystallization of oils is, of course, temperature-dependent. Rapid freezing followed by freeze-fracture enables evaluation of oil crystallization at the temperature at which the sample was held just prior to cooling. Mayonnaise (figure 11) contains oil droplets on the surface of which are plaque-like objects.

Of all the emulsified food products which the food technologist wished to examine in the SEM, perhaps ice cream presented, in the past, the greatest challenge. It is a multi-phase system of oil-in-water with suspended air bubbles and ice crystals whose stability is maintained only at sub-zero temperatures. Until the advent of low temperature scanning electron microscopy, an approach to understanding ice cream structure was only possible through the observation of freeze-fracture replicas. Now freeze-fracture faces of ice cream can be prepared and imaged directly in just a few minutes. Care must be taken to maintain the ice cream just below 0°C prior to rapid freezing to ensure that the ice crystals neither melt nor grow before they are examined. Figure 12 demonstrates how such a preparation enables parameters like oil droplet size, bubble diameter range and distribution, and ice crystal size to be determined.

Powders

Powders are ingredients of many products. Much work has been done on examining spray-dried milk at ambient temperature to determine the effect of its water and fat content on certain physical properties and structure (Kalab, 1984; Saito, 1985; Saltmarch & Labuza, 1980). At low temperature, this material can now be examined over prolonged periods with the assurance that its initial level of hydration will not change and its constituent fat droplets (Buchheim, 1982b) will not melt (figures 13 & 14).

Chocolate

Cocoa powder (figures 15 & 16) is incorporated into many products. The existence of polymorphic forms of cocoa butter fat is well known (Hicklin et al, 1985; Jewell, 1972; Manning & Dimick, 1985). These beam-sensitive crystals can be studied at length on a cold stage and steps in their progressive transformation to the stable form VI can be followed both on the surface of conched chocolate (figure 17) and within it (figure 18). Freeze-fractured preparations of chocolate can indicate whether liquid or powdered milk was used in its manufacture, the effectiveness of tempering on fat stability and the size of sugar crystals used as bulk. Figure 19 shows fractured sugar crystals. These are surrounded by a delicate network, possibly protein (Heathcock, 1985), whose presence is probably only revealed after the recrystallization and migration of cocoa butter fat away from the sugar.

Foams

The texture of many products can be markedly altered by processing them in such a way as to produce a stable foam. Figure 20 shows part of a freeze-fractured foamed chocolate bar. Bubble size and distribution are readily assessed and the structure of the chocolate between the bubbles is clear (figure 21). The composite nature of some of the bubbles is evident (figure 22). Large protrusions into the bubbles such as that in figure 23 are probably caused by milk crumb particles which have not been adequately broken up.

Meringue, a solid sugar foam, is another product which degrades on an uncooled SEM stage. From figure 24 it is clear that during cooking or cooling, most of the larger, thin walled cells of the foam have become perforated. The perforations occur either as slits or as rounded holes (figure 25), and a clue to their origin is gained at higher magnification. On the cell walls are well defined areas which appear to be subject to collapse, and "stress" lines exist between which slits can form (figure 26). Perhaps poor mixing of the egg white and sugar or an additive in the sugar is responsible.

The foam texture of potato crisps is achieved by deep-frying hydrated potato slices at a temperature well above the boiling point of water. The product has a fat content of 23 to 40% which makes imaging at ambient temperature virtually impossible. Many factors influence the formation of an acceptable, crispy, foamed product and certain properties can be defined as desirable in a good crisp. These include foam cell size and cell wall thickness and the nature of the starch. Figures 27 to 30 demonstrate how cold stage examination of fractured crisps facilitates the rapid assessment of these parameters. Figure 27 shows a good foam having an even expansion. Foam cells should be thin walled (figure 28) and the starch should be well gelatinized (figure 29). Poor crisps may be unacceptable as a result of having expanded unevenly or having thick cell walls (figure 30).

Meat

Interest is developing in the use of the cold stage to relate meat structure to texture (Dobraszczyk et al,1987). A particularly novel approach has been to separate muscle into component myofibrils for examination after

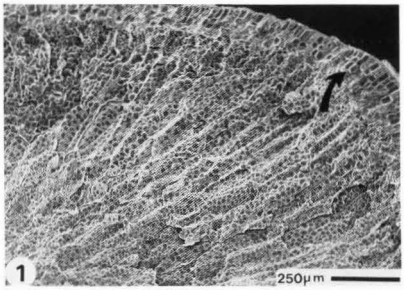

Figure 1. An imbibed barley caryopsis freeze-fractured to reveal the starchy endosperm surrounded by cells of the aleurone layer (arrowed).

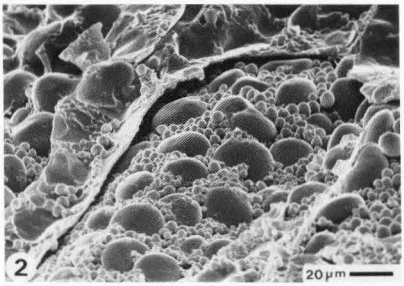

Figure 2. Detail of an endosperm cell from an imbibed barley caryopsis.

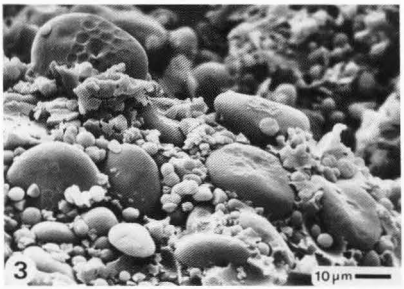

Figure 3. Milled wheat endosperm cryopreserved at its natural level of hydration.

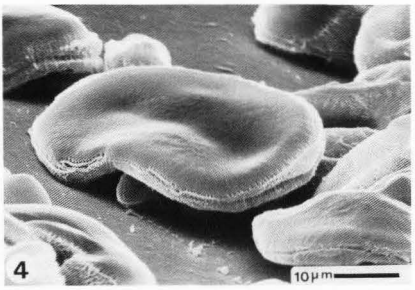

Figure 4. Gelatinized starch grains. Surface pitting caused by ice crystal growth has been minimized by fast freezing.

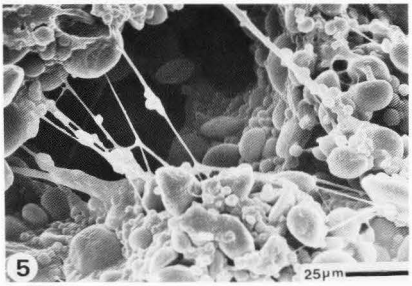

Figure 5. Part-baked pizza dough.

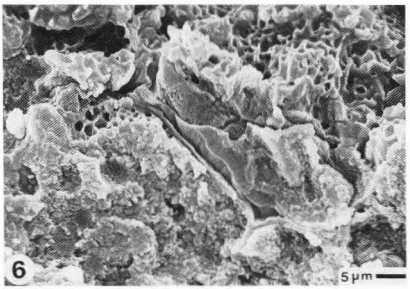

Figure 6. Fatty storage cells from peanut cotyledon.

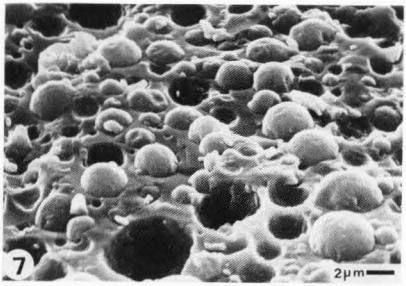

Figure 7. A freeze-fracture face of dairy cream (48% fat).

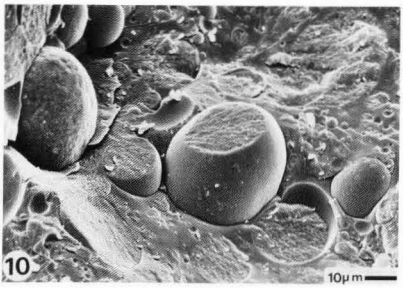

Figure 10. Blue cheese salad dressing, freeze-fractured.

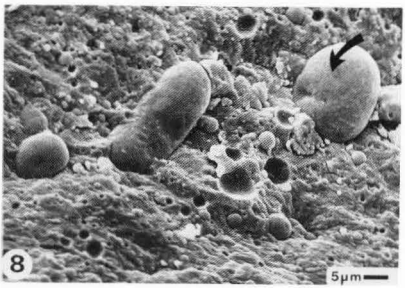

Figure 8. Conversion of cream to butter involves inversion to a water (arrowed)-in-oil emulsion. Very small droplets of oil are present in the fat phase.

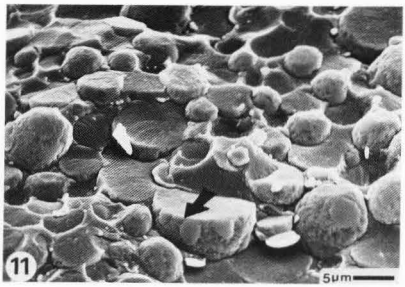

Figures 11. Freeze-fractured mayonnaise. Plaque-like bodies (arrowed) occur at the oil/water interface.

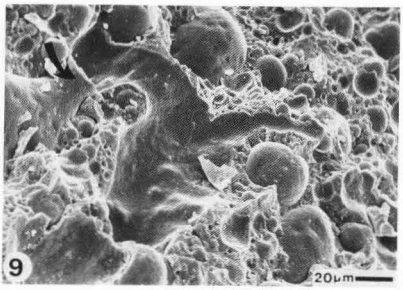

Figure 9. A low-fat spread freeze-fractured to reveal the high proportion of water dispersed in the fat phase. An extensive aqueous phase network (arrowed) can occur in low-fat spreads.

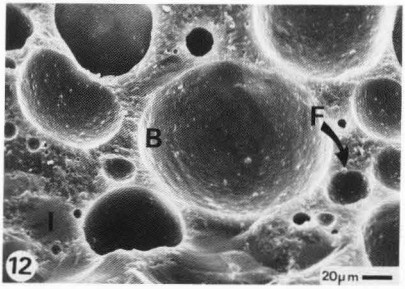

Figure 12. Ice cream, freeze-fractured. Bubble (B) and fat (F) droplet size can be assessed and ice crystals (I) identified.

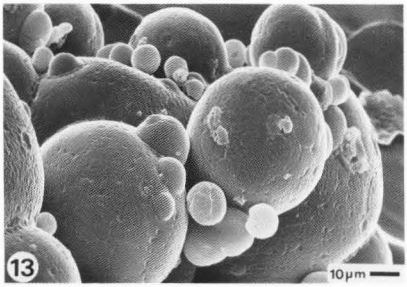

Figure 13. Full cream spray-dried milk powder.

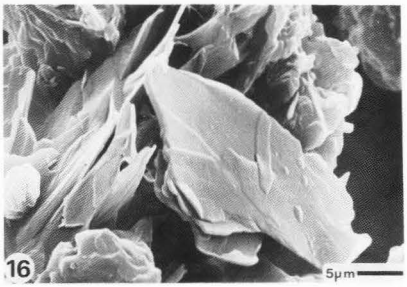

Figure 16. Cocoa butter fat crystals (form VI) in cocoa powder.

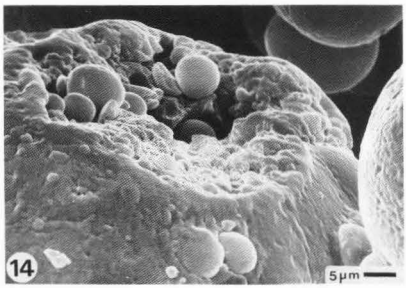

Figure 14. Fat droplets within a fractured dried milk particle.

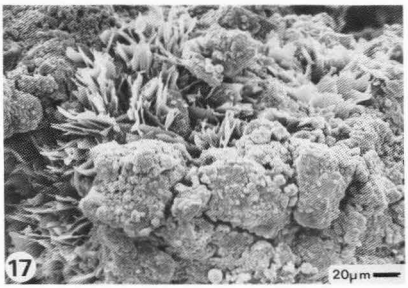

Figure 17. Fat crystals developing as a bloom on the surface of conched chocolate.

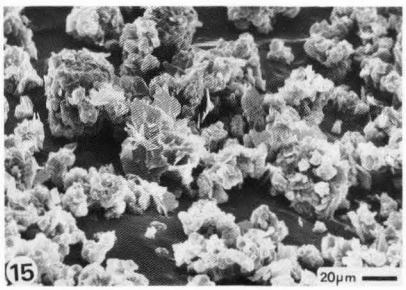

Figure 15. Cocoa powder.

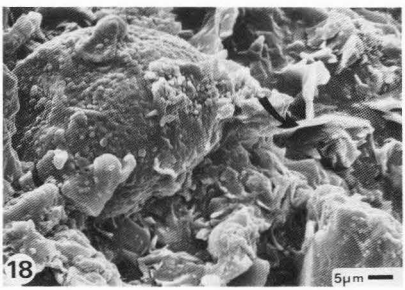

Figure 18. Fat crystals (arrowed) within conched, untempered chocolate.

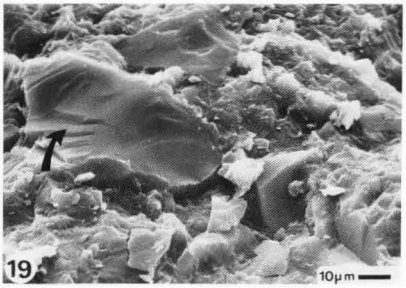

Figure 19. Fractured sugar crystals (arrowed) within chocolate.

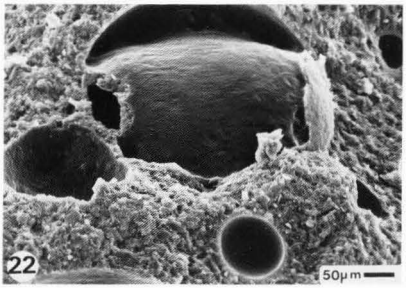

Figure 22. A composite bubble in foamed chocolate.

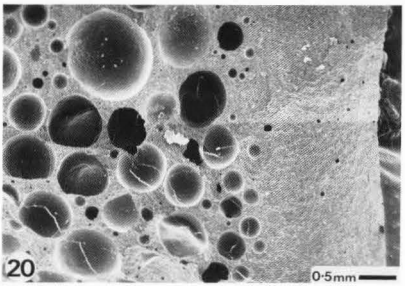

Figure 20. A freeze-fractured foamed chocolate bar.

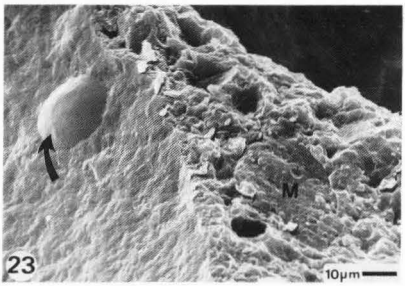

Figure 23. A protrusion (arrowed) into a bubble in foamed chocolate. It is probably formed by an underlying, fat-covered particle of milk crumb, another of which (M) is shown fractured.

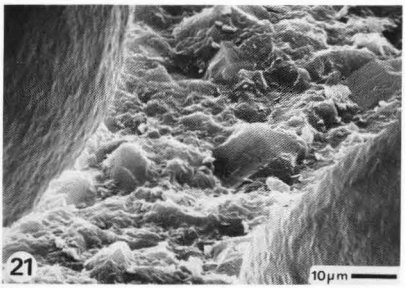

Figure 21. Freeze-fractured chocolate between two bubbles.

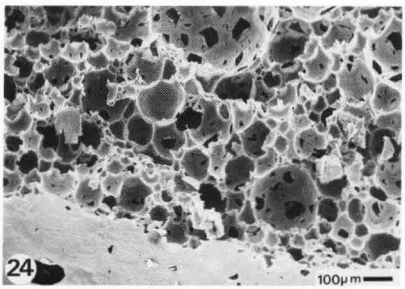

Figure 24. A fracture face of meringue.

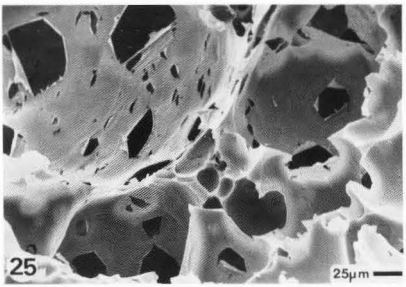

Figure 25. Meringue, fractured to reveal the perforated cell walls.

Figure 28. Thin cell walls of an acceptable potato crisp.

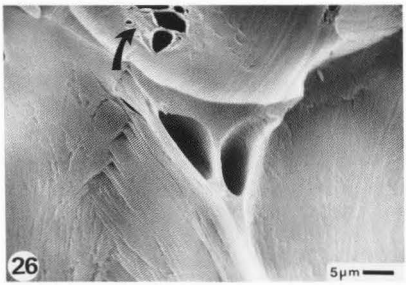

Figure 26. An area (arrowed) on a meringue cell wall subject to collapse.

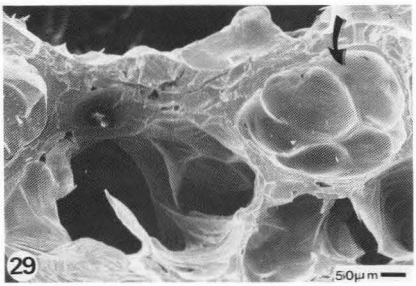

Figure 29. Starch grains (arrowed) within a potato crisp.

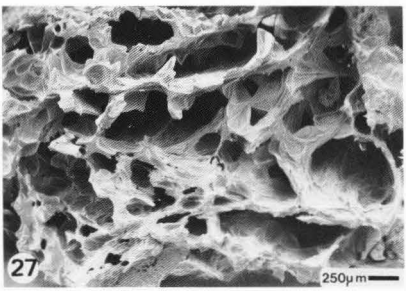

Figure 27. An acceptable potato crisp fractured to show its evenly expanded foam structure.

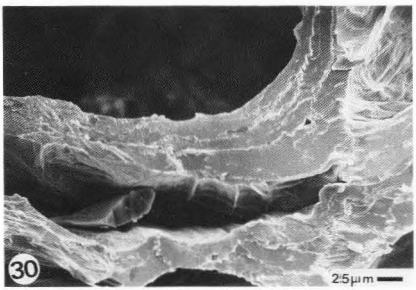

Figure 30. Thick cell walls within a poor crisp.

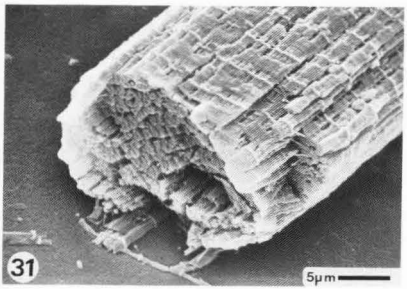

Figure 31. A fractured muscle fibre collected on a membrane filter and surface etched to reveal its component myofibrils.

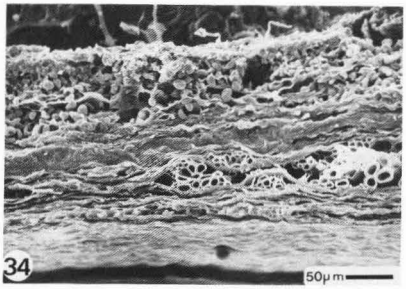

Figure 34. A fractured cocoa bean testa supporting microorganisms.

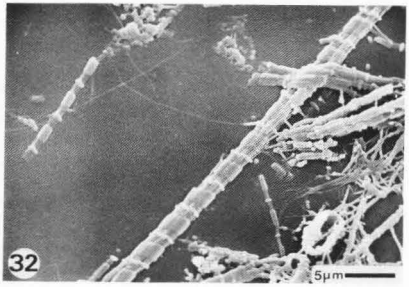

Figure 32. Separated myofibrils.

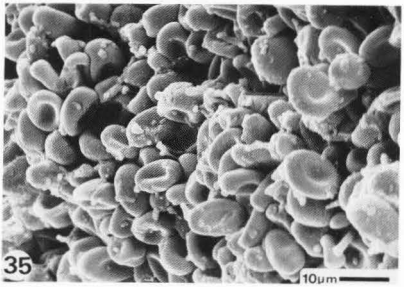

Figure 35. A dense population of microorganisms in the testa of cocoa bean.

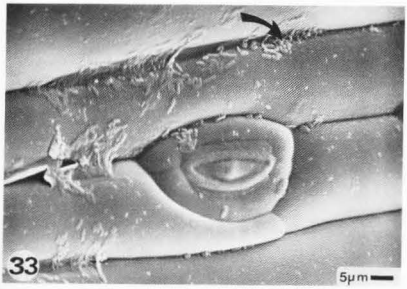

Figure 33. Bacteria (arrowed) on the surface of a fresh cress leaf.

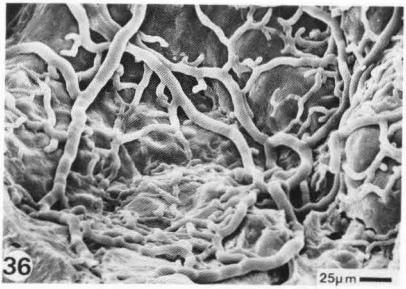

Figure 36. Hyphae of Rhizopus on bread.

collection on a membrane filter while they are fully hydrated. Careful sublimation of surface water from the specimen reveals their components and the extent to which pretreatment has promoted the separation of these (figures 31 and 32).

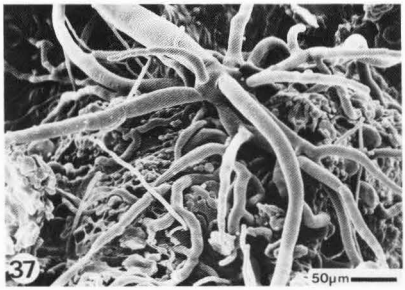

Figure 37. Rhizoids developing on the mycelium of Rhizopus.

Spoilage organisms

Screening foodstuffs for spoilage organisms can be crucial in the production of a safe and consistent product. The low temperature technique can give a rapid indication of the level of contamination and its nature (Allan-Wojtas and Yang, 1987; McMeekin et al, 1986). Salad crops are obvious candidates for transmitting unwanted microorganisms. Figure 33 shows the surface of a cress leaf from a batch thought to have contaminated other food. After sublimation of the surface film of water, a population of bacteria is evident. It is particularly dense in the valleys above the anticlinal walls of the epidermis.

Cocoa beans, following harvest, are usually dried and fermented in their country of origin under poorly controlled conditions. It is not unusual for the beans, on export, to be highly infected with microorganisms (figure 34). Sometimes the density of microorganisms reaches a very high level (figure 35) and they may be located deep in the testa.

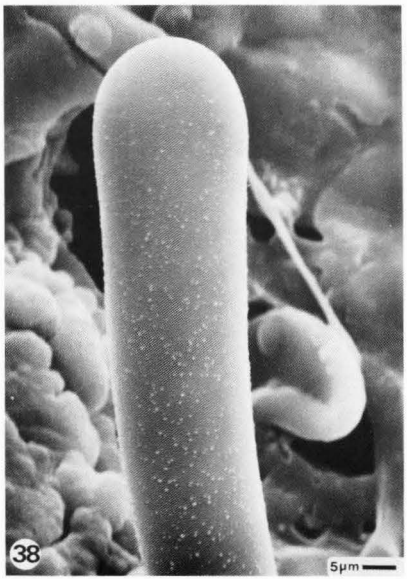

Figure 38. An extending sporangiophore of Rhizopus.

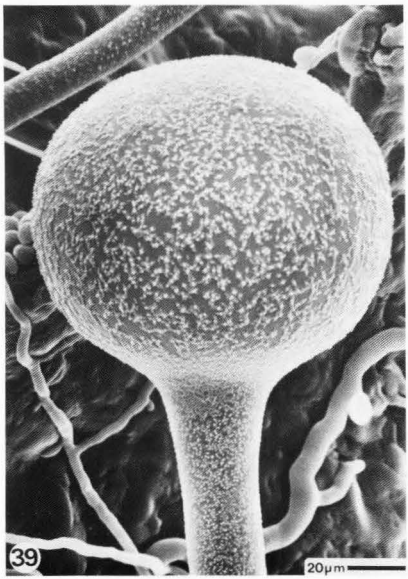

Figure 39. An enlarging sporangium of Rhizopus.

An understanding of the way in which spoilage organisms develop, multiply and spread is crucial if effective strategies are to be adopted to protect foods during production and storage. The cold stage technique is, in most cases, ideal in tracing the development of these organisms and their interaction with substrates. Hydration levels of both microorganism and substrate are maintained in the SEM and cryopreservation enables growth stages to be captured and examined throughout a developmental sequence. This approach is well demonstrated by figures 36 to 43. They show stages in the development of the mould Rhizopus on bread.

Figure 40. A maturing sporangium of Rhizopus.

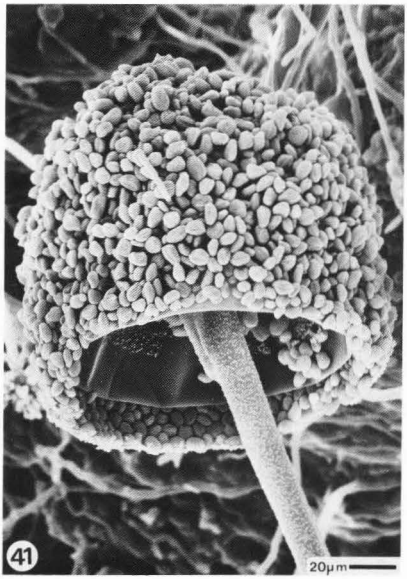

Figure 41. A mature sporangium of Rhizopus.

Figure 42. Sporangiospores of Rhizopus.

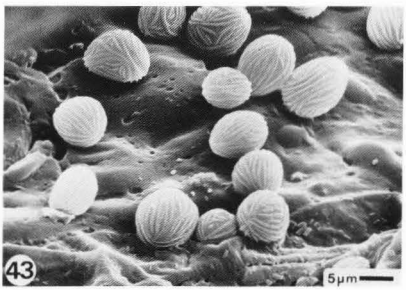

Figure 43. Sporangiospores of Rhizopus on bread.

Hyphae of the mould grow throughout the cellular structure of the bread (figure 36). When the mycelium is sufficiently dense, rhizoids form (figure 37) and from these, sporangiophores arise (figure 38). The tip of each of these swells to form a sporangium (figure 39), its base invaginates (figure 40), its wall autolyses (figure 41) and the spores within it (figure 42 are released. Some of these drift on to uninfected substrate (figure 43).

Conclusion

In illustrating the range of applications of low temperature scanning electron microscopy within the food industry, this paper has necessarily drawn upon a number of disparate examples. They represent but a few of the projects within this vast research field which until the availability of the SEM cold stage were difficult, if not impossible, to tackle with confidence.

Acknowledgement

Figures 3, 5, 11, 18, 19, 27, 28, 29, 30, 33, 34, and 35 are published by kind permission of Dr. Philip Randles, United Biscuits (UK) Ltd. Research and Development Centre, High Wycombe, UK.

References

Allan-Wojtas P, Yang AF (1987) Solutions to difficulties encountered in low-temperature SEM of some frozen hydrated specimens: Examination of Penicillium nalgiovense cultures. J. Electron Microsc. Tech. **6:** 325-333.

Bastacky J, Hook GR, Finch GL, Goerke J, Hayes TL (1987) Low-temperature scanning electron microscopy of frozen hydrated mouse lung. Scanning **9:** 57-70.

Beckett A, Read ND (1986) Low-temperature scanning electron microscopy. Ultrastructural techniques for microorganisms. Ed. Aldrich HC, Todd WJ. 45-86, Plenum Press, New York.

Bowler P, Evers AD, Sargent J (1987) Dehydration artefacts in gelatinized starches. Starch/Stärke **39:** 46-49.

Boyde A, Franc F (1981) Freeze-drying shrinkage of glutaraldehyde fixed liver. J. Microsc. **122:** 75-86.

Boyde P, Maconnachie E (1979) Volume changes during preparation of mouse embryonic tissue for scanning electron microscopy. Scanning **2:** 149-163.

Brooker BE (1979) Milk and its products, In: Food Microscopy, JG Vaughn (ed.), Academic Press, 273-311.

Brooker BE (1987) The crystallization of calcium phosphate at the surface of mould-ripened cheeses. Food Microstruct. **6:** 25-33.

Brooker BE, Anderson M, Andrews AT (1986) The development of structure in whipped cream. Food Microstruct. **5:** 277-285.

Buchheim W (1982a) Aspects of sample preparation for freeze-fracture/freeze-etch studies of proteins and lipids in food systems. A review. Food Microstruct. **1:** 189-208.

Buchheim W (1982b) Electron microscopic localization of solvent-extractable fat in agglomerate spray-dried whole milk powder particles. Food Microstruct. **1:** 233-238.

Dobraszczyk BJ, Atkins AG, Jeronidis G, Purslow PP (1987) Fracture toughness of frozen meat. Meat Science **21:** 25-45.

Echlin P (1984) Procedures for low temperature scanning electron microscopy and x-ray microanalysis. In: Analysis of Organic and Biological Surfaces. Ed. Echlin P. Chemical analysis series Vol. **71:** 529-557.

Eveling DW (1987) Scanning electron microscopy of plant surfaces using low temperature dehydration prior to critical point drying. Micron Microsc. Acta **18:** 81-88.

Heathcock JF (1985) Characterisation of milk proteins in confectionery products. Food Microstruct. **4:** 17-27.

Heertje I, Leunis M, van Zeyl WJM, Berends E (1987) Product morphology of fatty products. Food Microstruct. **6:** 1-8.

Hicklin JD, Jewell GG, Heathcock JF (1985) Combining microscopy and physical techniques in the study of cocoa butter polymorphs and vegetable fat blends. Food Microstruct. **4:** 241-248.

Jewell GG (1972) Some observations on bloom on chocolate. Int. Chocolate Rev. **27:** 161-162.

Kalab M (1981) Electron microscopy of milk products: A review of techniques. Scanning Electron Microsc. 1981; III: 453-472.

Kalab M (1983) Electron microscopy of foods. In: Physical Properties of Foods. EB Bagley, M Peleg (eds.) AVI Publishing Co. Inc., Westport, Connecticut, 43-104.

Kalab M (1984) Artefacts in conventional scanning electron microscopy of some milk products. Food Microstruct. **3:** 95-111.

Kalab M, Modler HW (1985) Development of microstructure in a cream cheese based on Quesco Blanco cheese. Food Microstruct. **4:** 89-98.

Manning DM, Dimick PS (1985) Crystal morphology of cocoa butter. Food Microstruct. **4:** 249-265.

Marshall AT (1988) Progress in quantitative x-ray microanalysis of frozen-hydrated bulk biological samples. J. Electron Microsc. Technique **9:** 57-64.

McMeekin TA, McCall D, Thomas CJ (1986) Cryo-scanning electron microscopy of microorganisms in a liquid film on spoiled chicken skin. Food Microstruct. **5:** 77-82.

Pawley JB, Norton JT (1978) A chamber attached to the SEM for fracturing and coating frozen biological samples. J. Microsc. **112:** 126-141.

Robards AW, Crosby P (1979) A comprehensive freezing, fracturing and coating system for low-temperature scanning electron microscopy. Scanning Electron Microsc. 1979;II: 325-344.

Robards AW, Sleytr VB (1985) Low temperature methods in biological electron microscopy. Ed. Glauert AM. Elsevier, Amsterdam.

Roomans GM (1988a) Introduction to x-ray microanalysis in biology. J. Electron Microsc. Technique **9**: 3-17.

Roomans GM (1988b) Quantitative x-ray microanalysis of biological specimens. J Electron Microsc. Technique **9**: 19-43.

Saito Z (1985) Particle structure in spray dried whole milk and in instant skim milk powder as related to lactose crystallization. Food Microstruct. **4**: 333-340.

Saltmarch M, Labuza TP (1980) SEM investigation of the effect of lactose crystallization on the storage properties of spray dried whey. Scanning Electron Microsc. 1980; III: 659-665.

Sargent JA (1983) The preparation of leaf surfaces for scanning electron microscopy: a comparative study. J. Microsc. **129**: 103-110.

Sargent JA (1988a) Low temperature scanning electron microscopy: advantages and applications. Scanning Microsc. 2: 835-849.

Sargent JA (1988b) Cryo-stabilization of low melting-point materials for scanning electron microscopy. Proc. Roy. Microsc. Soc. 23: 275-281.

Schmidt DG (1982) Electron microscopy of milk and milk products: problems and possibilities. Food Microstruct. **1**: 151-161.

Wroblewski J, Wroblewski R, Roomans GM (1988) Low temperature techniques for x-ray microanalysis in pathology: alternatives to cryoultramicrotomy. J. Electron Microsc. Technique **9**: 83-98.

Discussion with Reviewers

D. Pechak: Have you seen evidence for the plaque-like bodies on oil droplets in mayonnaise in TEM sections?
Author: No, I have not examined this material in the TEM.

I. Heertje: You observed coalescence of water droplets in a low fat spread. Is this considered to have occurred in the original product or is it induced by shear during sample preparation?
Author: Although no special fracturing device, such as you have described, was used to avoid shearing during sample preparation, care was taken to minimize shear before freezing. In addition coalescence was commonly observed in all the samples examined.

I. Heertje: It is mentioned that the change in crystal modification in chocolate can be followed by morphological studies. Can this be based on morphological information alone?
Author: It is, of course, necessary to couple morphological observations on crystal form with studies of other physical properties. However, when those studies on polymorphic material have been made, as they have for cocoa butter, crystal morphology is a useful indicator of molecular state.

I. Heertje: The thin delicate walls of the meringue foam show a lot of perforations. Can this be caused by sample preparation or subsequent observation (vacuum) in the electron microscope?
Author: When these perforations were first observed it was natural to suspect that they were induced by pressure changes under vacuum in the microscope. However, light microscopy revealed the presence of at least the larger perforations before the material was prepared for the SEM. It seems certain that they occur during cooling of the cooked product. If the foam remained closed it would surely collapse totally during cooling.

J.F. Heathcock: How have you identified the droplet structures in the butter and spread as water? How do you think the network develops in the low fat spread?
Author: Water can be readily identified in samples such as this. On raising the stage temperature to -80°C water can be observed to sublime. Presumably the network develops by progressive coalescence of water droplets within a fairly viscous fat matrix.

J.F. Heathcock: Can you provide any further detail or interpretation of the plaque-like objects in the freeze-fracture preparation of mayonnaise?
Author: I have no further information concerning these structures.

FOOD MICROSTRUCTURE, Vol. 7 (1988), pp. 137-145
Scanning Microscopy International, Chicago (AMF O'Hare), IL 60666 USA

0730-5419/88$3.00+.00

ULTRASTRUCTURAL AND TEXTURAL PROPERTIES OF RESTRUCTURED BEEF TREATED WITH A BACTERIAL CULTURE AND SPLENIC PULP

E.A. Elkhalifa[1], N.G. Marriott[1]*, R.L. Grayson[2], P.P. Graham[1] and S.K. Perkins[2]

[1]Department of Food Science and Technology
and
[2]Electron Microscopy Laboratory
Virginia Polytechnic Institute and State University
Blacksburg, VA 24061

Abstract

Scanning electron microscopy (SEM), transmission electron microscopy (TEM) and Instron measurements were used to evaluate the effects of an Achromobacter iophagus culture (BC) and splenic pulp (SP) treatments on the structural and textural properties of flaked and restructured beef steaks. Both treatments improved the textural characteristics of the product when conditioned at 35°C. Electron microscopy studies revealed that the bacterial culture treatment caused a greater effect than SP on the connective tissue elements, with a degradation of the endomysial sheath and sarcolemma. Treatment with splenic pulp produced an overall excessive disruption at the Z-lines with little definition of the A-bands.

Initial paper received April 18, 1988
Manuscript received September 07, 1988
Direct inquiries to N.G. Marriott
Telephone number: 703 961 7640

Key Words: Bacterial culture, splenic pulp, restructured beef, Instron, electron microscopy, collagen, endomysium, sarcolemma, myofibrils.

*Person to contact: N.G. Marriott
Phone number 703 961-7640

Introduction

Tenderness is one of the most important characteristics that render restructured products acceptable to consumers. Collagen has been implicated in providing the so-called "background" toughness of meat (Bailey, 1972). Connective tissue fibers can be partially broken down by flake-cutting. This particle reduction procedure and accompanying restructuring technology enables the use of lower priced cuts of meat. However, the incorporation of different cuts of meat with varying amounts of connective tissue into the same product may reduce textural uniformity.

Collagenases selectively degrade connective tissue elements (Eino and Stanley, 1973). Postmortem injection of bacterial collagenases into muscle (Bernal and Stanley, 1986) or blending with a restructured beef product (Cronlund and Woychik, 1987) caused an increase in the collagen solubility and reduction in thermal stability. In a recent study*, Elkhalifa and Marriott (Submitted Manuscript, 1988) found similar results by injecting a bacterial culture into restructured beef steaks. Catheptic enzymes of bovine spleen have also been shown to degrade myofibrillar Z-bands and sarcolemma (Robbins and Cohen, 1976; Cohen et al., 1982) as well as collagen (Etherington, 1976; Elkhalifa and Marriott, submitted manuscript, 1988*) and they improved the textural uniformity of pre-cooked, freeze-dried meat (Cohen et al., 1979). The objectives of this study were to observe the effect of bacterial culture and splenic pulp treatments on the collagen of restructured beef as determined by the shear force and structural changes occurring within collagen and muscle fibers.

Materials and Methods

Sample preparation and treatment

Muscle samples were obtained from animals slaughtered at the Virginia Polytechnic Institute and State University Meat Science Laboratory. Postmortem muscle samples were removed from the longissimus dorsi (LD) to represent a low collagen (LC) control treatment and the extensor carpi radialis, flexor carpi radialis, flexor capri ulnaris, superficial digital flexor and deep digital flexor muscles to represent high collagen (HC) muscles of U.S. Choice steer carcasses that were stored at 2°C for 48 hr postmortem. Epimysium was not removed and samples were cut into 3.5 x 3.5 cm pieces which were frozen at -20°C and later tempered to -4°C before flaking. The

tempered samples were flaked with an Urschel Comitrol (Model 3600) using a head opening size of 6.1 x 17 mm. The flaked HC particles were formulated to contain 1.0% NaCl and 0.25% sodium tripolyphosphate (STP) through blending in a CSE Mixer (Model No. CDB 0615) for 10 min. Three portions were assigned to one of the following treatments: (a) HC-control; (b) HC-bacterial culture treated; (c) HC-3% (W/W) splenic pulp (SP). The SP samples were divided into two groups. One group was conditioned at 35°C for 3 h and stored at 4°C for 7 days. The other group was stored at 4°C for 7 days. Both treatments were wrapped and stored in waxed freezer paper. Splenic pulp was prepared by separating the connective tissue from bovine spleen. Samples from the LD products were flaked and formulated with 1.0% NaCl and 0.25% STP in a similar manner as the LC control.

The mixed meat samples from each treatment group were stuffed into 110 mm diameter casings. The stuffed 4.2 kg logs were frozen to -20°C and then tempered to -4°C over a 16 h period. The tempered meat logs were pressed in a Ross press (Superform 720) at a setting of 37 kg/cm^2 with 2 sec dwell time into the shape of a ribeye, and sliced with a Hobart (Model 512) slicer to produce 70 g, 12.5 mm thick steaks which were then wrapped in wax coated freezer paper and stored at -20°C until testing.

Bacterial growth and injection of restructured steaks

The collagenase producing strain of Achromobacter iophagus was purchased as a dried culture from the National Collections of Industrial and Marine Bacteria, Ltd., Aberdeen, Scotland and cultured by the technique of Keil-Dlouha et al. (1976) in 2.5% casamino acids in 0.1M Tris-HCl buffer (pH 7.6) plus 0.4 M NaCl and 2 mM $CaCl_2$. The procedure was to aerate the bacteria overnight in nutrient-broth, inoculate into the culture medium (1:10 v/v), and incubate in a water bath equipped with a shaker (250 rpm) at 30°C for 5 h to facilitate aeration. A final concentration of 2.5% peptic hydrolysate of collagen was added as a collagenase inducer to the growing culture. The insoluble collagen from bovine Achilles tendon (type 1, No. 9879) was obtained from Sigma Chemical Co. (St. Louis, MO). The growth was continued for an additional 6 h for a total overall growth period of 28 h to allow production of the collagenase enzyme.

The bacterial culture (BC) was injected with a single needle containing multiple openings for uniform distribution into HC-restructured beef samples at a level of 6.0% (v/w). Samples were divided into two groups. One group was conditioned at 35°C for 3 h, wrapped in waxed freezer paper, and then stored at 4°C for 7 days. The other group was not conditioned but was wrapped in waxed freezer paper and stored at 4°C for 7 days. HC control samples were injected with sterile buffer and then subjected to storage conditions similar to those for the experimental products.

Instrumental texture analysis

In this study, eighteen steaks were used per treatment. Steaks (12.5 mm thick) were placed into Ziplock plastic bags and cooked in a water bath to an internal temperature of 68°C. After the end-point temperature was achieved, the steaks were cooled to 25°C prior to cutting into samples for shear evaluation. Measurements of shear forces were made using the Instron Universal Testing Machine (Model 1123). Each steak was divided into 3.5 x 2.5 x 1.5 cm subsamples to give a total of 36 measurements/treatment. A crosshead speed of 100 mm/min and a chart speed of 200 mm/min were used. Peak force (newtons) and peak force per unit volume (newtons/cm^3) were determined from the recorded curve.

All data were subjected to analysis of variance (SAS User Guide, 1982). Tukey's HSD technique for multiple comparisions with the F-test at the 5% level of significance (Ott, 1984) was incorporated.

Isolation of connective tissue

Minced muscle samples (20 g) from restructured steaks were homogenized in a Brinkman Polytron and collagen was isolated according to the procedure of Fujii and Murota (1982). The collagen was washed briefly with 2% (w/v) sodium dodecyl sulfate (SDS) as described by Laurent et al. (1981) and used for electron microscopy studies.

Scanning electron microscopy (SEM)

Approximately 1 cm^3 particles of muscle and connective tissue were cut from each sample and fixed in 2% glutaraldehyde-paraformaldehyde in 0.1 M sodium cacodylate buffer (pH 7.2) overnight at 4°C. The fixed samples were reduced in size to 0.5 cm^3 and rinsed three times (15 min each) in sodium cacodylate buffer at a pH of 7.2. The samples were washed three times in distilled water (5 min each) and dehydrated in ethyl alcohol 15, 25, 40, 50, 60, 70, 80, 90, 100, 100, 100 series. Using acetone as the transition fluid, the samples were critical point dried using liquid CO_2 in a Ladd critical point drier. The dried samples were mounted on aluminum stubs with conductive silver paint, sputter coated with 20 nm gold- palladium in an Anatech Hummer X and examined in a Philips 505 Scanning Electron Microscope operated at 30 kV. Micrographs were recorded on Polaroid-Type 55 P/N film.

Transmission electron microscopy (TEM)

Samples of muscle and isolated connective tissue from each treatment were fixed in 2% glutaraldehyde-paraformaldehyde in 0.1 M sodium cacodylate buffer as described above. This procedure was followed by three (15 min each) rinses in cacodylate buffer, post fixation in 2% osmium tetroxide in 0.1 M cacodylate buffer (pH 7.2) for 1 h at 24°C, three buffer rinses (15 min each) and dehydration in a graded series of ethanol as previously described. After transition through acetone, samples were embedded in a low viscosity embedding medium (Spurr, 1969) and polymerized overnight at 70°C.

One micron sections were cut on a glass knife, mounted, stained with 0.5% toluidine blue and examined by light microscopy. Longitudinally-oriented areas were identified and the blocks were further trimmed and cut for electron microscopy. Thin sections were stained for 30 min with 2% uranyl acetate in 50% alcohol followed by 5 min in Reynolds lead citrate (Reynolds, 1963) with subsequent examination using a Zeiss EM-10C transmission electron microscope operated at 60 kV.

Results

Instrumental texture analysis

The instrumental shear measurements are presented in Table 1. The LC-control samples required less (P less than 0.05) shear force than the HC samples regardless of the treatment. Shear force values

of the HC-control samples at 4°C were not different (P greater than 0.05) from the bacteria and splenic pulp treated samples. The shear force value for the HC-control samples at 35°C was higher (P less than 0.05) than for the bacterial culture and spleen treated samples; however, there was no significant difference between the BC and SP treated samples. Both the BC and SP samples had lower standard errors than the control which suggests more uniformity among the treated samples.

Table 1. Mean shear force values for cooked control and texture-modified restructured beef steaks[1]

Samples	Shear Stress (Newtons/cm^3)			
	4°C[2]		35°C[2]	
	$\bar{X}$	SE	$\bar{X}$	SE
LC*-control	52.8	± 6.86^{Ca}	40.0	± 7.12^{Cb}
HC**-control	70.5	± 9.84^{ABb}	81.4	± 20.1^{Aa}
HC + A. iophagus culture[3]	74.7	± 10.06^{Aa}	69.9	± 13.06^{Ba}
HC + splenic pulp[4]	64.3	± 13.54^{Ba}	64.5	± 8.30^{Ba}

[1] N=18 steaks per treatment.

[2] Products were stored at 4°C for 7 days, or conditioned at 35°C for 3 h and then stored at 4°C for 7 days.

[3] 6% (V/W) bacterial culture injected into steaks.

[4] 3% splenic pulp added before forming steaks.

A,B,C Mean values in the same column with identical upper case superscripts are not different (P greater than 0.05).

a,b Mean values in the same row with identical lower case superscripts are not different (P greater than 0.05).

* LC=low collagen.

** HC=high collagen.

Scanning electron Microscopy (SEM)

Results and discussion are slightly abbreviated by discussion of only the SP samples that were stored at 4°C, since the data in Table 1 were not different (P greater than 0.05) between the two temperatures. Fig. 1 illustrates the SEM results of the muscle surface of untreated and treated restructured muscle samples. The LC-control (Fig. 1A) which possessed 4.7 mg/g tissue of collagen, contains few collagen fibers which allows the muscle fiber surface to be observed directly although the muscle fiber observed is a small part of the micrographic field shown. The HC-control (Fig. 1B) which had 20.2 mg/g tissue of collagen, is more heavily covered by collagen fibers than the other treatments. The structure of the HC-muscle tissue appeared to be looser and less compact than the LC-control. Representative HC-samples injected with the bacterial culture and conditioned at 35°C (Fig. 1C) showed major effects of this treatment by exhibiting aggregated and tight entanglements of randomly selected collagen fibers within the muscle tissue. In addition, Fig. 1C shows an area of muscle tissue where collagen fibers appear beaded on the surface and the sarcolemma has been degraded exposing the underlying myofibrils. These ultrastructural changes were not observed in the HC-samples treated with bacteria at 4°C (Fig. 1D), which showed structural characteristics similar to the HC-control. Samples treated with splenic pulp revealed some degradation of the sarcolemma exposing the underlying myofibrils (Fig. 1E). The muscle fibers appeared more degraded and disorganized than those of the HC-control. In addition, collagen fibers appeared somewhat fragmented and more loosely aggregated.

SEM was also used to study the morphology of isolated collagen fibers from the control and treated samples (Fig. 2). The LC-control samples (Fig. 2A) contained thin collagen fibers which appeared loosely aggregated and structurally disorganized. Collagen of the HC-control samples appeared as dense sheets of long unfragmented fibers (Fig. 2B). Because of their tight association, the collagen fibers appeared coarser than those of the LC-control. This is in striking contrast to the HC-treated with bacterial culture at 35°C which (Fig. 2C) appears to contain rather loose separated fibers and fiber bundles no longer in compact dense sheets. A similar arrangement of loose collagen fibers was also observed in the bacteria-treated HC at 4°C (Fig. 2D) and splenic pulp treated (Fig. 2E) samples. However, Fig. 2D does show some areas of loosely packed sheets of collagen and, like Fig. 2E, there is disorganization and loss of integrity of the fiber bundles. These observations support the differences in the Instron values of the LC- and HC-control samples.

Transmission electron microscopy (TEM)

Transmission electron micrographs representative of the control and treated restructured muscle samples are shown in Fig. 3. As seen in Fig. 3A and 3B, restructuring produced irregularities in the orientation of the myofibers. For the LC-control sample (Fig. 3A), the sarcolemma and the endomysium have some degradation. The endomysial sheath of the HC-control sample (Fig. 3B) appears to remain intact. However, the 35°C BC treated samples (Fig. 3C) reflect excessive degradation of the endomysium and sarcolemma. A slight degradation of the myofibrils occurred in certain areas. As illustrated in restructured samples treated with bacteria (Fig. 3D), some degradation occurred in the endomysium as well as the myofibrils. The SP samples (Fig. 3E) reflect considerable overall fiber disruption. The Z-lines and A and I bands are not well defined. Less degradation was evident in the endomysium and sarcolemma components than in the HC-controls (Fig. 3B).

The TEM micrographs of isolated collagen from control and treated samples are shown in Fig. 4. Collagen fibrils of LC-control samples have intact fibrils with separation of some fibrils into protofilaments (Fig. 4A). In Fig. 4B, collagen fibrils of HC-control samples are intact and tightly packed. The

Fig. 1. SEM Micrographs of: (A) A low collagen (LC-control) restructured control sample showing muscle tissue and associated collagen (C). Note the lack of individual collagen fibers over the surface of the muscle fiber (M). (B) A high collagen (HC-control) restructured sample. The surface of muscle fibers is thickly covered by collagen sheets. (C) A high collagen sample (HC-bacteria) treated with bacteria at 35°C. An area is shown in which the collagen fibers beaded on the surface (arrows) and underlying muscle fibers (M) are exposed. (D) A high collagen sample treated with bacteria at 4°C. Note the presence of collagen fibers (CF) on the surface of the tissue and the structural similarity to the control shown in Figure 2B. (E) A high collagen sample treated with splenic pulp and stored at 4°C. An area is shown in which the sarcolemma appears to have lost some of its integrity resulting in the exposure of what may be underlying myofibrils (arrow).

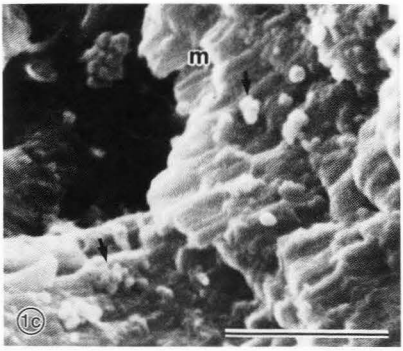

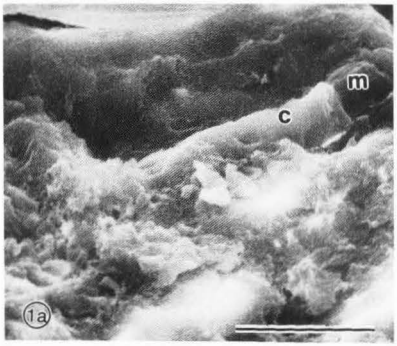

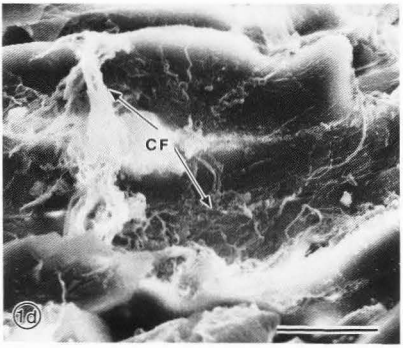

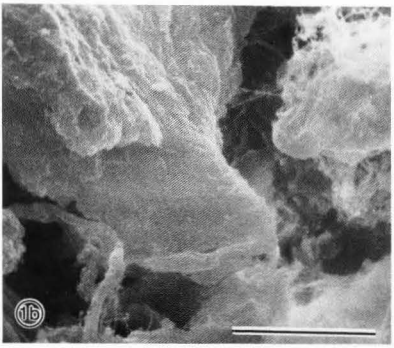

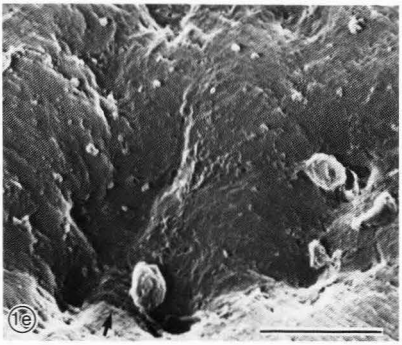

Bars = 50 μm (for A, D and E), 10 μm (for B) and 5 μm (for C).

Fig. 2. SEM micrographs of collagen fibers isolated from: (A) LC restructured control sample. The sample contains a high proportion of thin collagen fibers (arrows) which appear disorganized and loosely arranged. (B) HC restructured control sample. Collagen appears as dense sheets (C) composed of highly compacted fibers. (C) HC bacteria sample treated with bacteria at 35°C. Note the loose arrangement and separation of both thick and thin collagen fibers resulting from the degradative action. (D) HC sample treated at 4°C. Partial loosening of collagen fibers implies less bacterial degradation at 4°C than at 35°C (Figure 2C). (E) HC sample treated with splenic pulp and stored at 4°C. The loose arrangement of the collagen fibers appears similar to that seen in the samples treated with bacteria at 4°C (Figure 2D).

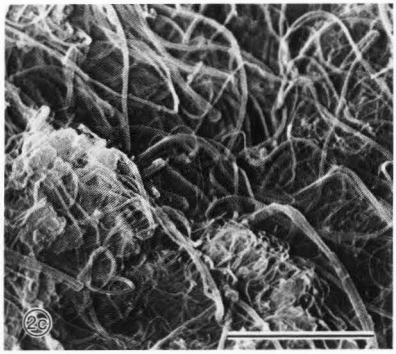

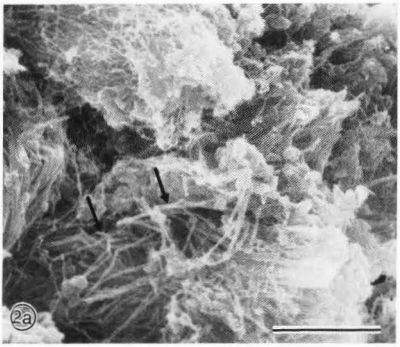

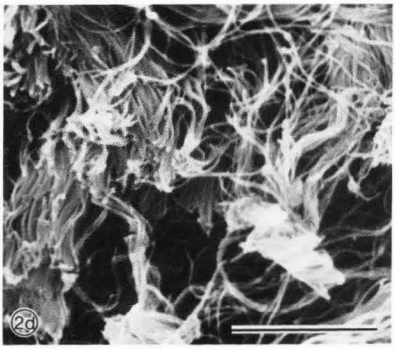

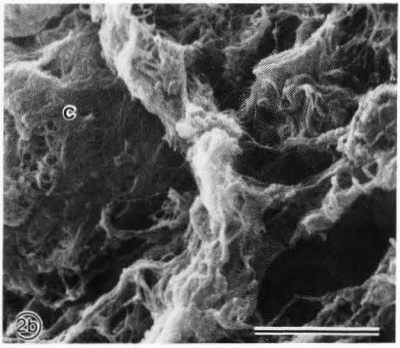

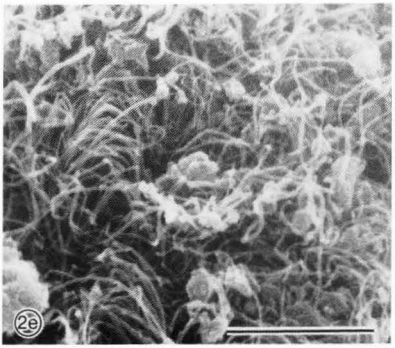

Bars = 10 μm (for A, B and E); = 5 μm (for C and D).

Fig. 3. TEM micrographs of: (A) Low collagen restructured control sample showing small remnants of the sarcolemma (S) and endomysium (E). There is some disruption of the structural organization of Z-lines and myofibrils due to the restructuring of tissue. (B) High collagen restructured control sample. In this oblique section, the endomysial sheath (E) appears to be intact. Structural disorganization of the myofibrils and associated components has resulted from restructuring or other forms of mechanical disruption of the muscle tissue. (C) High collagen restructured sample treated with bacteria at 35°C showing complete degradation of the endomysium, sarcolemma and Z-line (Z) configuration of the myofibrils. The space between the myofibers contains collagen remnants (small arrows). (D) High collagen restructured sample treated with bacteria at 4°C. Notice slightly less degradation of endomysium (E), myofibrils and Z-lines as compared to Fig. 3C. Cross-sections of collagen fibers occupy the space external to the endomysia. (E) High collagen restructured sample treated with splenic pulp and stored at 4°C. Z-lines and A and I bands are no longer apparent due to excessive disruption of the myofibrillar structure caused by the action of hydrolytic enzymes. Remnants of the endomysium (E) and sarcolemma (S) are present.

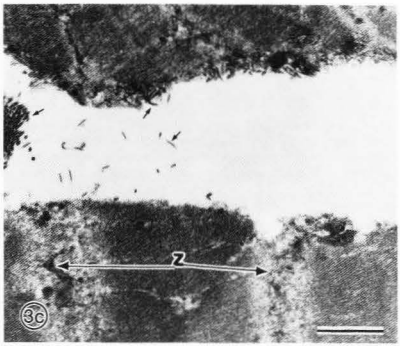

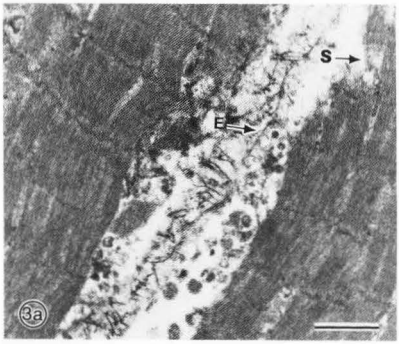

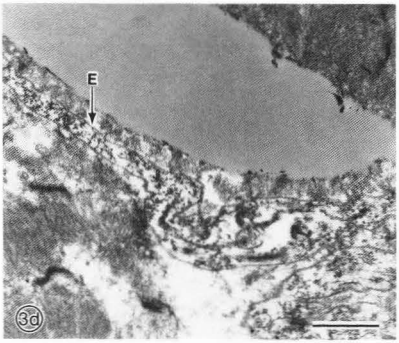

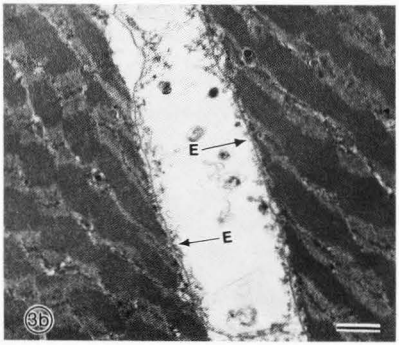

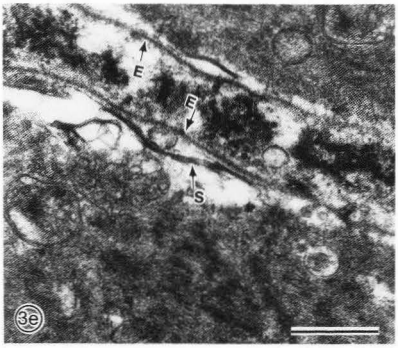

Bars = 1 μm (for A, B, C, and D) and 0.5 μm (for E).

Fig. 4. TEM micrographs of collagen fibrils isolated from: (A) A low collagen restructured control sample showing intact fibrils separated with some fibrils into protofilaments (arrows). (B) A high collagen restructured control sample. The collagen fibrils appear to be intact and tightly packed. (C) A high collagen restructured sample treated with a bacterial culture at 35°C. Amorphous regions can be seen within a single fibril (arrows). (D) A high collagen restructured sample treated with a bacterial culture at 4°C. Orientation of collagen fibrils has been disrupted as evidenced by numerous cross-sections relative to the control. This may have been caused by normal factors i.e., placement in block (4B). There is some separation of fibrils into protofilaments (arrow) similar to the low collagen control (4A). The diameter of the collagen fibrils is smaller than controls. Note bacteria (B). (E) A high collagen restructured sample treated with splenic pulp and stored at 4°C. This micrograph reveals that collagen fibril diameters are less than the controls. Cross-sections of collagen can be observed as being dispersed among longitudinal segments of banded collagen.

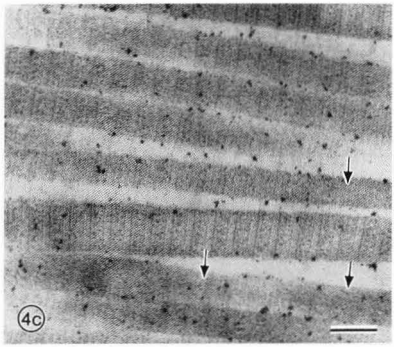

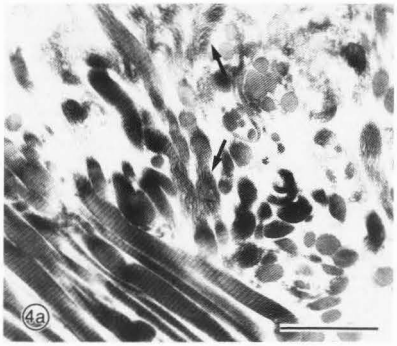

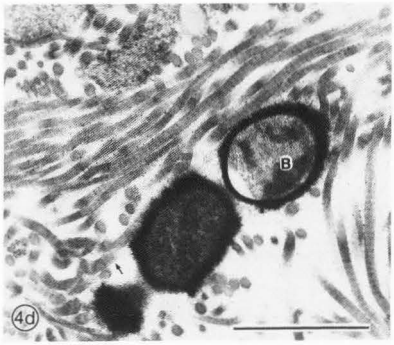

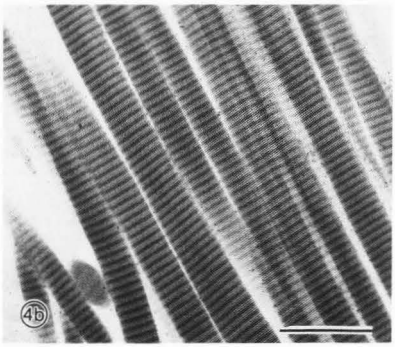

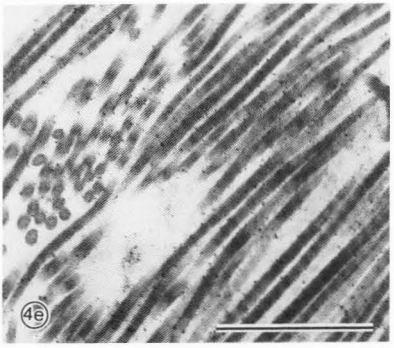

Bars = 1 μm (for A and D), 0.5 μm (for B and E), and 0.1 μm (for C)

BC treatment (35°C) resulted in amorphous regions along a single fibril (Fig. 4C). Figures 4D and 4E suggest that treatment with the bacterial culture at 4°C or splenic pulp (Figs. 4D and 4E) did not result in amorphous regions. These observations reveal that treated samples (Figs. 4C, 4D and 4E) have large proportions of relatively small diameter collagen fibers and predominantly short segments of normally banded collagen, suggesting effects of the BC and SP treatments.

Discussion

The reduction in shear force of the bacteria treated samples (35°C) is a reflection of the selective degradation of collagen (Figs. 3C and 4D) by a collagenase enzyme in the bacterial culture. Treatment with splenic pulp at either temperature resulted in excessive disruption of the myofibrillar structure as evidenced by the degradation of Z-lines and A and I bands (Fig. 3E) which was attributable to the lysosomal enzymes in spleen. In work on the effect of catheptic enzymes from spleen, Cohen et al. (1979) found that enzyme-treated samples were more tender and more uniform in texture.

As seen in the SEM micrographs, treatment with either the bacterial culture or splenic pulp gave rise to surface structural changes of the restructured samples. Using SEM, Eino and Stanley (1973) observed similar hydrolytic changes in the connective tissue and sarcolemma when rabbit psoas muscle was incubated with a bacterial collagenase. In a study on the muscle fiber surface of restructured beef, Cohen et al. (1982) demonstrated that catheptic enzymes from splenic pulp caused degradation of the sarcolemma and exposure of the myofibrils in restructured beef. Results from this investigation support what earlier researchers have reported and add to the knowledge base of the effects of these two treatments.

Ultrastructure of muscle and connective tissue of a restructured product have not been studied specifically by TEM. The structural differences between control and treated samples seen in the TEM micrographs (Figs. 3 and 4) are the degradation of the endomysial sheath, myofibrils and the sarcolemma. The degradation of sarcolemma and endomysium due to the bacterial culture treatment has important implications. Offer (1984) suggested a mechanism for water loss from muscle during cooking that involves shrinkage of actomyosin within muscle cells to leave free fluid which can then purge out. Since the structure of the endomysium is in intimate contact with such shrunken actomyosin components in samples cooked to 77°C, it may accelerate this passive process. Light et al. (1985) suggested that the endomysium may present a barrier to transverse fracture of muscle pieces which can develop a compressive force as shrinking constricts muscle cells, thus squeezing free water out of the cut ends of the muscle in an active process and thereby contributing to increased toughness. This hypothesis may be correct since the degradation of the endomysial sheath in BC samples at 35°C may contribute to the reduction in shear force. The improvement in tenderness of HC samples from the SP is evidence of the extensive degradation of the myofibrillar structure.

In view of the results presented here, there is no doubt that there was a greater effect on the connective tissue elements and sarcolemma by the 35°C bacteria treatment than by the SP treatment which produced microstructural changes within the myofibrils. It is reasonable to expect the technology of both treatments to be quite useful as exogeneous meat tenderizers to permit the use of less costly cuts of meat at significant monetary savings.

Acknowledgments

The authors thank Dr. K. C. Diehl for assistance with the instrumental texture analysis. Assistance from Mr. Steve Phelps is also acknowledged. The authors express their appreciation to the Virginia Cattle Industry Board and the Virginia Agricultural Council for financial support. Appreciation is extended to Ross Industries, Inc. for use of the Ross Superform 720 Press and to Urschel Laboratories, Inc. for loan of the Comitrol 3600.

References

Bailey AJ (1972). The basis of meat texture. J. Sci. Food Agric. 23, 995-1007.

Bernal VM, Stanley DW (1986). Proteolysis of intramuscular connective tissue during postmortem conditioning of beef muscle. In: Proc. 32nd Europ. Meeting of Meat Res. Workers. 32, 161-164. Ghent, Belgium.

Cohen SH, Kostick JA, Robbins FM, Segars RA, Walker JE (1979). Action of spleen extracts on stored pre-cooked freeze-dried beef. J. Food Sci. 44, 1118-1120.

Cohen SH, Segars RA, Cardello A, Smith J, Robbins FM (1982). Instrumental and sensory analysis of the action of catheptic enzymes on flaked and formed beef. Food Microstruc. 1, 99-105.

Cronlund AL, Woychik JH (1987). Solubilization of collagen in restructured beef with collagenases and α-amylases. J. Food Sci. 52, 857-860.

Eino MF, Stanley DW (1973). Surface ultrastructure and tensile properties of cathepsin and collagenase treated muscle fibers. J. Food Sci. 38, 51-55.

Etherington DJ (1976). Bovine spleen cathepsin B_1 and collagenolytic cathepsin: A comparative study of the properties of the two enzymes in the degradation of native collagen. Biochem. J. 153, 199-209.

Fujii K, Murota K (1982). Isolation of skeletal muscle collagen. Anal. Biochem. 127, 449-452.

Keil-Dlouha V, Mirashi R, Keil B (1976). The induction of collagenase and neutral proteinase by their high molecular weight substrates in Achromobacter iophagus. J. Mol. Biol. 107, 293-305.

Laurent GJ, Cockerill P, McAnulty RJ, Hasings JRB (1981). A simplified method for quantitation of the relative amounts of type I and type III collagen in small tissue samples. Anal. Biochem. 113, 301-312.

Light ND, Champion AE, Voyle C, Bailey AJ (1985). The role of epimysial, perimysial and endomysial collagen in determining texture in six bovine muscles. Meat Sci. 13, 137-149.

Offer G (1984). Progress in biochemistry, physiology and structure of meat. In: Proc. 30th Europ. Meeting of Meat Res. Workers. 30, 87-94. Bristol.

Ott, L (1984). An Introduction of Statistical Methods and Data Analysis, 2nd ed. PWS Publishers, Boston.

Reynolds ES (1963). The use of lead citrate at high pH as an electron-opaque stain in electron

microscopy. J. Cell Biol. 17, 208-212.

Robbins FM, Cohen SH (1976). Effects of cathepsic enzymes from spleen on the microstructure of bovine semimembranosus muscle. J. Texture Studies 7, 137-142.

SAS User Guide (1982). Statistics. Ray AA (Ed.). SAS Inst., Inc., Cary, NC.

Spurr, AR (1969). A low viscosity epoxy resin enbedding medium for electron microscopy. J. Ultrastruct. Res. 26, 31-43.

Discussion with Reviewers

Reviewer 1: Please describe the handling of the carcasses postmortem.
Authors: After the U.S. Choice steers were slaughtered, they were transferred from ambient temperature (25°C) to a chill cooler maintained at 2°C. After carcass storage for 48 h, the muscles were excised as described in the materials and methods of this paper.

Reviewer I: What is the reason for including the LC samples?
Authors: The low collagen (LC) samples were studied to compare their shear force values and ultrastructural characteristics with the other treatments. Our major objective for studying the LC samples was to determine how closely the samples treated with a bacterial culture or splenic pulp would resemble the LC controls.

Reviewer I: Where did you get or how do you prepare and store splenic pulp?
Authors: The splenic pulp was obtained from the spleens obtained during slaughter of these animals. Immediately before excising the muscles for this study, the connective tissue was separated from the bovine spleens and the resulting pulp was incorporated in the formulation.

Reviewer I: What was the concentration of bacteria in the inoculum used for injection of steaks? How old was the culture? What was the concentration of enzyme? Where do you inject it? Does any run out? Are the steaks wrapped for storage?
Authors: Concentration of the bacterial suspension was determined with the spectrophotometer. The concentration was 100 ml w/OD of 4.0-5.0 at 600 nm. The suspension was injected immediately after culture development. The concentration of the enzyme was unknown because living bacterial cells were used. Multi-injection was into the interior of the steaks with a single needle containing multiple openings for uniform distribution throughout the restructured product. Although we did not weigh the samples to determine moisture loss, no exudate was observed. This observation may be attributable to the STP in the formulation. The steaks were wrapped with waxed freezer paper prior to storage.

Reviewer I: What was the collagen content of the LC versus the HC samples?
Authors: The mean collagen content of the LC samples was 4.7 mg/g tissue. The HC samples had a mean collagen content of 20.2 mg/g tissue.

Reviewer I: Is one of your conclusions that more fibrous collagen occurs in the HC control?
Authors: This answer is based on our assumption that the reviewer meant more fibrous collagen occurs in the HC control than the LC control and HC samples treated with bacterial culture or splenic pulp. Yes, we concluded that more fibrous collagen occurs in the HC control. The LC samples had less collagen as evidenced by another study that has been submitted for publication separately.* The BC and SP samples had less fibrous collagen because of collagen degradation that occurred.

Reviewer I: Are the control microscopy samples randomly selected from your cuts? In samples such as these there must be considerable variation in the "terrain" to be viewed on a sample. How extensive was your microscopy? How many samples?
Authors: The samples were selected randomly. Fifteen samples per treatment were observed.

Reviewer I: How can you tell the difference between endomysium and sarcolemma in some of your TEM micrographs?
Authors: The endomysium is thicker since it surrounds the muscle fiber. The sarcolemma is thinner and is the innermost membrane. By the morphology location and measurement of the structures, we were able to distinguish between the endomysium and sarcolemma.

Reviewer IV: What are casamino acids? Are they available from a commercial supplier or must they be prepared in the laboratory?
Authors: Casamino acids is acid hydrolyzed casein recommended for use in microbial culture media which require a completely hydrolyzed protein as a nitrogen source. Casamino acids is well suited for the preparation of "synthetic" or chemically defined media. We incorporated this compound for the maintenance and growth of the A. iophagus culture used in this study. It is available commercially through Difco in Detroit, Michigan.

D.N. Holcomb: Please provide more details of the testing fixture used in measuring the shear forces with the Instron testing machine.
Authors: A cast aluminum alloy housing was incorporated with sample space size as follows: 67 mm between smooth walls, 66 mm between slotted walls and a depth of 62 mm. Ten blunt-ended, teflon-coated blades with a width of 3 mm and depth of 70 mm are guided into the slots, spaced at 3 mm apart, by a removable cover plate which rests on the top of the cell. The blades are suspended from an aluminum alloy housing which attaches to the load cell on the Instron testing machine.

---

*This companion paper has been submitted for publication. Preprints are available from N. G. Marriott, 103 Food Science Building, VPI & SU, Blacksburg, VA 24061.

FOOD MICROSTRUCTURE, Vol. 7 (1988), pp. 147-152
Scanning Microscopy International, Chicago (AMF O'Hare), IL 60666 USA

0730-5419/88$3.00+.00

CHARACTERIZATION OF HYPERCONTRACTED FIBERS IN SKELETAL MUSCLE OF DOMESTIC TURKEY (MELEAGRIS GALLOPAVO)

A. Sosnicki[1,2], R.G. Cassens[2,*], D.R. McIntyre[3], R.J. Vimini[3] and M.L. Greaser[2]

[1]Present address: Department of Biology, University of Pennsylvania, Philadelphia, PA 19104

[2]Muscle Biology Laboratory, College of Agricultural and Life Sciences, 1805 Linden Drive University of Wisconsin, Madison, WI 53706, and

[3]Oscar Mayer Foods Corporation, 910 Mayer Ave., Madison, WI 53707

Abstract

Several different muscles from a population of thirty Large White male turkeys were studied by histological and histochemical methods, and a high incidence of hypercontracted fibers was noted. The fibers were characterized in cross-section by an apparent swelling, a rounded rather than polygonal shape and a homogenous appearance. They were eosinophilic, positive to Gomori-trichrome and appeared to have an elevated lipid content. An unusual histochemical profile was noted. It was postulated that the hypercontracted fibers were real, not artifactual, and resulted from some change occurring in the muscle.

Initial paper received July 17, 1988
Manuscript received September 08, 1988
Direct inquiries to R.G. Cassens
Telephone number: 608 262 1792

Key words: Hypercontracted fibers, skeletal muscle, histopathology, domestic turkey

Person to contact:
*R.G. Cassens, Muscle Biology Laboratory,
1805 Linden Drive, University of Wisconsin,
Madison, WI 53706;
Telephone No. (608) 262-1792

Introduction

Hypercontraction is an excessive contraction of myofibrils and is reflected by abnormally short sarcomeres (Carpenter and Karpati, 1984). Hypercontracted fibers in cryostat cross sections appear enlarged and rounded ("giant" fibers). Because the normal myofibrillar and intermyofibrillar staining pattern is lost, the terms "hyaline", "waxy" or "opaque" have also been used to describe these fibers (Wohlfart, 1937; Schmalbruch, 1973; 1975; Cullen and Fulthorpe, 1975; Carpenter and Karpati, 1984; Uchino and Araki, 1986). Although the occurrence of hypercontracted fibers in muscle tissue in human and domestic mammals (pig, cattle, sheep) has been noted previously by many authors, the underlying causes of the phenomenon are controversial.

Carpenter and Karpati (1984) pointed out that hypercontraction of fibers seen in biopsies from Duchenne muscular dystrophy patients takes place during biopsy. On the other hand, Cullen and Fulthorpe (1975) and Schmalbruch (1973, 1975) have proposed that hypercontraction in human diseased muscle is a pathological reaction of muscle cells. In animals, "giant" fibers have been found in normal muscle of wild and domestic mammals in both pre-rigor and post-rigor conditions (Weatherspoon, 1969; Linke, 1972; Dutson et al., 1978; Schmidt and Dumont, 1981; Handel and Stickland, 1986; Sink et al., 1986; Salomon and Eastridge, 1987). Scheper (1979) and Schmidt and Dumont (1977) observed more of this type of fiber in muscle of cattle or sheep which exhibited gross enlargement or hypertrophy. Likewise, "giant" fibers were often found in pigs having the conditions of Porcine Stress Syndrome (PSS), Stress-myopathy or Pale, Soft and Exudative (PSE) meat (Cassens et al., 1969; Dutson et al., 1978; Sosnicki and Domanski, 1983; Sosnicki, 1987).

Description of the histochemical profile of hypercontracted fibers has also varied significantly. They were observed as myosin Ca^{++}-ATPase positive (Cassens et al., 1969) or negative (Fenichel, 1963); succinic dehydrogenase (SDH) positive (De Bruin, 1971; Handel and Stickland, 1986) or variable (Dutson et al., 1978, Sink et al., 1986, Sosnicki, 1987); lactic acid dehydrogenase (LDH) variable (Sosnicki, 1987) or positive (Hraste et al., 1980).

Klosowska et al. (1980) have noted the occurrence of "giant" fibers in muscle of chicken. Grey et al., (1986) and Seemann et al., (1986) observed what they termed "large rounded fibers" in a study of turkey breast muscle and thought they were

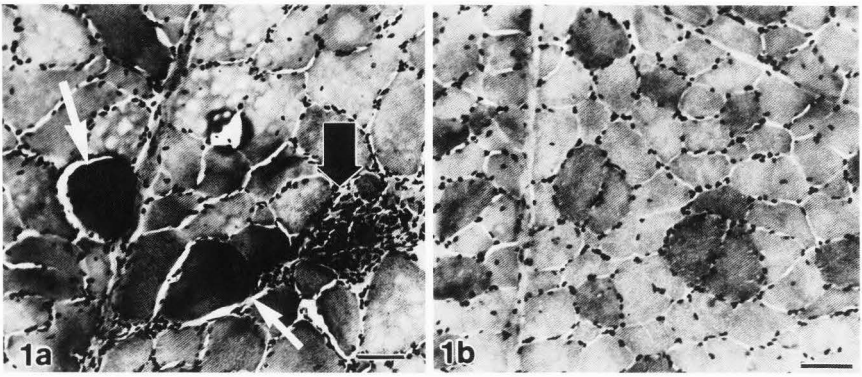

Figure 1 (a). Cross section showing muscle fiber undergoing necrosis (large arrow) and several hypercontracted fibers (small arrows). (b). Cross section showing normal appearing fibers. M. biceps femoris (Group A). H+E. Bar = 0.05 mm.

---

associated with toughness of the meat.

We have often observed hypercontracted fibers during the course of our histochemical studies of muscle of rapidly growing turkeys. The purpose of this work is to present frequency data about the hypercontracted fibers together with some possible explanation for their occurrence, and a description of histological and histochemical features is also provided.

Materials and Methods

Histological and histochemical studies of "giant" fibers were carried out on 30 Large White turkey males that were 14 (group A), 16 (group B) and 18 (group C) weeks of age (10 in each group). The birds were selected at random from commercial flocks which had been raised in light controlled houses and fed a standard corn/soybean meal poultry diet.

Samples for analysis were collected immediately post slaughter from 5 skeletal muscles: m. pectoralis thoracicus (superficialis), m. supracoracoideus (pectoralis deep), m. biceps femoris, m. semitendinosus and m. femorotibialis medius. To prevent trauma, muscle samples were held at rest length by forceps and then rapidly frozen in isopentane cooled with liquid nitrogen.

Serial cross and longitudinal sections 8 micrometers thick were obtained with a cryostat. In the analysis of histological traits, hematoxylin and eosin (H&E), modified Gomori-trichrome and Oil red O staining techniques were used. Histochemical reactions were conducted in order to show activity of myosin Ca^{++}-ATPase (Guth and Samaha, 1970), succinic dehydrogenase (SDH) (Barka and Anderson, 1963), alkaline and acid phosphatases and phosphorylases a and b (Chayen et al., 1973).

Results

While an exact quantification was not made, the muscle incidence was considered positive if hypercontracted fibers were present in a low power (25x) of cross-sectioned muscle (1.68 mm^2 area). A uniform pattern of incidence of the hypercontracted fibers in the particular birds was not seen nor were certain muscles more prone to fiber hypercontraction than others. They appeared to be distributed randomly throughout any given muscle bundle and were not located preferentially in either peripheral or central areas of the bundle. In some instances, only a few single, scattered hypercontracted fibers were seen, but, in other cases, they appeared in close proximity (being almost grouped) in numbers of three or more. In rare instances, up to twenty-five percent of the fibers in a small area appeared affected. In view of this distribution, we merely counted a bird positive if one or more hypercontracted fibers were present (see above for area viewed). From Table 1, it appears that the older birds had a higher incidence.

Typical hypercontracted and normal appearing muscle fibers are illustrated in Figures 1a and 1b respectively. In comparison to normal muscle cells, an apparent swelling of hypercontracted fibers was observed, and in cross-section they had a rounded rather than polygonal shape. They had a homogeneous appearance (described typically as "waxy" or "hyaline"), were eosinophilic and stained a uniform dark-red with the Gomori-trichrome procedure. The content of intracellular fat was also higher in comparison to that present in normal muscle cells (Figure 2). However, interpretation of this may be confused by a change of the histological staining appearance due to the contraction (an apparent stronger staining intensity may result from the denseness due to contraction). The hypercontracted fibers also had a characteristic appearance in longitudinal section (Figure 3). In some areas a strong contraction was obvious with associated tearing and separation of the contents of the fibers. Open areas were observed in many cases surrounding the hypercontracted fibers both in longitudinal (Figure 3) and cross

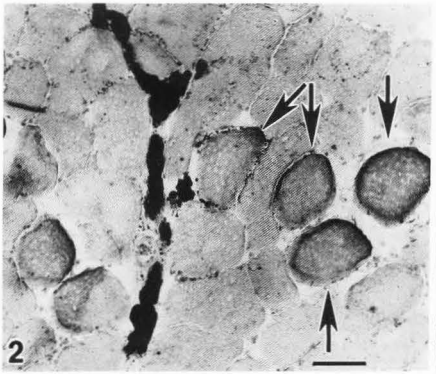

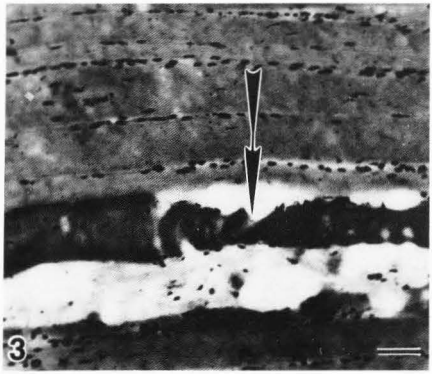

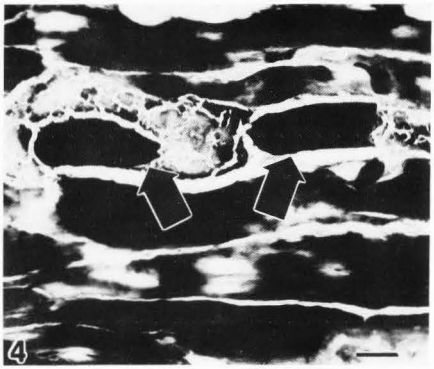

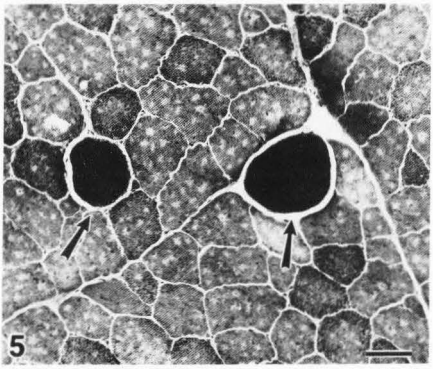

Figure 2. A higher content of intracellular fat in hypercontracted fibers (arrows) as shown with oil Red O staining. M. pectoralis thoracicus (Group A).

Figure 3. Longitudinal section showing a "compresse" appearance of hypercontracted fibers (arrow). M. pectoralis thoracicus (Group C). H+E.

Figure 4. Multifocal hypercontraction (arrows) within a fiber undergoing necrosis. M. supracoracoideus (Group C). Gomori-trichrome.

Figure 5. Hypercontracted fibers showing high SDH reaction (arrows); other muscle fibers show a weak activity. M. femorotibialis medius (Group B).

Figure 6. Ca^{++}-ATPase reaction (pH 4.60) showing a high activity in hypercontracted fibers (arrows). M. semitendinosus (Group B).

Bar (for all Figures) = 0.05 mm.

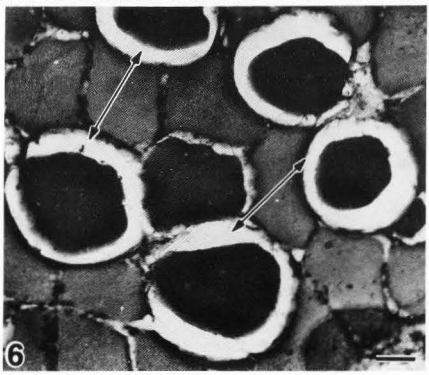

Table 1. Number of birds in which the hypercontraction of muscle fibers was recorded

Muscle	Groups[1]/Age in weeks A / 14	B / 16	C / 18
Pectoralis thoracicus	7	7	9
Supracoracoideus	8	7	10
Biceps femoris	7	7	9
Semitendinosus	7	7	9
Femorotibialis medius	7	6	9

[1] All groups contained 10 birds

sections (see also Figure 6). In other instances an apparent degeneration was observed in association with the hypercontracted fibers (Figure 4).

Because the reaction pattern of the hypercontracted fibers was not typical, the histochemical profile was somewhat confusing (Table 2). A strong positive SDH reaction was exhibited (Figure 5) and a positive reaction was found for myosin Ca^{++}-ATPase after either alkaline (pH 10.4) or acid preincubation (pH 4.6) (see Figure 6). For phosphorylase a and b, some cases of weak reaction were found but the majority of hypercontracted fibers possessed high activity. Therefore, a simple classification of the hypercontracted fibers as slow-oxidative (Type I), fast-glycolytic (Type IIb) or fast oxidative-glycolytic (Type IIa) was not possible. Positive, but diffuse, reactions for acid and alkaline phosphatase were observed.

Discussion

The question of artifact always deserves consideration, and hypercontracted fibers are a case in point - are they artifactual or reflective of an in vivo pathological reaction?

Carpenter and Karpati (1984) reported that hypercontracted fibers, seen in almost all biopsies from Duchenne dystrophic patients, did not show features of necrosis, rarely occurred in groups, and transitional stages between hypercontraction and true necrosis were not observed. Conversely, Cullen and Fulthorpe (1975) described the process of hypercontraction as resulting in the contractile filaments forming a homogenous mass (hyaline degeneration). The next step of degeneration was described as true necrosis of hypercontracted fibers (Cullen and Fulthorpe, 1975). Likewise, Schmalbruch (1975) reported some of the hypercontracted fibers contained phagocytes and macrophages, and they showed closely attached regenerating fibers with normal sarcomere spacing.

There is the question if the hypercontracted fibers we observed are an intermediate stage between normal fibers and those undergoing a necrotic change. We did not observe obvious regenerative changes. However, parts of a hypercontracted fiber in close proximity to a necrotic fiber and an area of mononuclear cell invasion were often seen. In addition, we noted a positive acid phosphatase activity in hypercontracted fibers which can be taken as evidence of necrosis. In the final step of breakdown of hypercontracted fibers fatty tissue replacement usually occurred (Cullen and Fulthorpe, 1975). Similar symptoms were observed in our study.

There may be a local inability of the sarcomeres to relax, which implies a defect of mitochondria or sarcoplasmic reticulum (Cullen and Fulthorpe, 1975). In other words, hypercontraction may be caused by an influx of extracellular calcium into the muscle fibers (Carpenter and Karpati, 1984). Indeed, the high enzyme reaction of hypercontracted fibers seen in the previous, and present study (see Table 2), may result from fragment breaks in the surface membrane in the vicinity of the observed hypercontraction (Carpenter and Karpati, 1984; Handel and Stickland, 1986, Levin et al., 1981, Sink et al., 1986). Furthermore, functional stressing of muscle fibers (i.e. a strong exercise) has been shown to affect calcium ion uptake and muscle relaxation, and consequently the fibers are thought to be more prone to post-mortem lysis (Salomons and Henriksson, 1981). On the other hand, evidence is also available to support the concept that the subcellular components of abnormal fibers (porcine PSE muscle) are more susceptible to the effects of freeze-thaw contraction (Cloke et al., 1981).

Finally, regarding an explanation for the basis of occurrence of hypercontracted fibers, we cannot make a definite conclusion. We favor the explanation that they are real and may be associated with actual changes occurring in the muscle. We conclude this because we did observe some areas of apparent degeneration and fatty tissue replacement in longitudinal sections of hypercontracted fibers. Moreover, the positive reaction for acid phosphatase in the hypercontracted fibers and an unusual histochemical profile support the idea that they are real and are associated with a developing or present muscle pathology.

Acknowledgements

This work was supported by the College of Agricultural and Life Sciences, University of Wisconsin, Madison and by Oscar Mayer Foods Corporation. Muscle Biology Laboratory Manuscript number 236.

References

Barka T, Anderson PJ (1963). Histochemistry. Theory, practice and bibliography. Harper and Row, Inc. New York. 312-318.

Carpenter S, Karpati G. (1984). Pathology of Skeletal Muscle. Churchill Livingstone, New York. 121-129.

Cassens R.G, Cooper CC, Briskey EJ. (1969). The occurrence and histochemical characterization of giant fibers in the muscle of growing and adult animals. Acta Neuropath. (Berl). 12,300-304.

Chayen J, Bitensky L, Butcher RG. (1973). Practical Histochemistry. John Wiley & Sons. London. 108-110; 112-115; 160-162.

Cloke JD, Davies EA, Gordone J, Hsieh SJ, Grider J, Addis PB, McGrath CJ (1981). Scanning and transmission electron microscopy of normal and PSE porcine muscle. Scanning Electron Microscopy,

Table 2. The characteristic staining and reaction pattern of normal and hypercontracted muscle fibers

Type of staining or reaction	Type of muscle fibers		
	I slow-oxidative	II fast-glycolytic	hypercontracted
H & E	positive (pink)	positive (pink)	eosinophilic (red)
Gomori-trichrome	positive (green)	positive (green)	positive (dark red)
Oil Red O	high	low	high
ATPase, pH 9.4	low	high	high
ATPase, pH 4.6	high	low	high
SDH	high	low	diffuse or high
Alkaline phosphatase	no activity	no activity	diffuse
Acid phosphatase	no activity	no activity	diffuse
Phosphorylases a, b	low	high	high

III: 435-446.

Cullen MJ, Fulthorpe JJ. (1975). Stages in fibre breakdown in Duchenne Muscular Dystrophy. An electron-microscopic study. J. Neurol. Sci. 24,179-200.

De Bruin A. (1971). Fiber characteristics and lactic acid level in porcine muscle. In Proc 2nd Int. Symp. on Condition and Meat Quality of Pigs. pp. 86-89 (Center for Agricultural Publishing and Documentation. Wageningen, The Netherlands).

Dutson TR, Merkel RA, Pearson AM, Gann GL. (1978). Structural characteristics of porcine skeletal muscle giant myofibers as observed by light and electron microscopy. J. Anim. Sci. 46,1212-1220.

Fenichel GM. (1963). The B fiber of human skeletal muscle. Neurology 13,219-226.

Grey TC, Griffiths NM, Jones JM, Robinson D. (1986). A study of some factors influencing the tenderness of turkey breast meat. Lebensm.-Wiss. u.-Technol. 19,412-414.

Guth L, Samaha FJ. (1970). Research note: procedure for the demonstration of actomyosin ATPase. Experimental Neurology 28,365-367.

Handel SE, Stickland NC. (1986). "Giant" muscle fibres in skeletal muscle of normal pigs. J. Comp. Path. 96,447-457.

Hraste A, Zobundzija M, Bego U. (1980). Appearance of giant fibers in the longissimus dorsi muscle of primitive breeds pigs. Vet. Arch. 50, 51-59.

Klosowska D, Niewiarowicz A, Klosowska B, Trojan M. (1980). Histochemische und histologische Untersuchungen an m. pectoralis superficialis mit beschleuniger, normaler und verzogerter Glykoserate in Broilern, Fleischwirtschaft 59:7-14.

Levin MA, Degennero P, Ross A, Serafin N, Steward J. (1981). A histochemical and electron microscopic study of the fast and slow-twitch muscle in genetically spastic mice. Tissue and Cell. 13:61-69.

Linke H. (1972). Histological investigation of pale watery pork. Fleischwirtschaft 52:493-496.

Salomons S, Henriksson J. (1981). The adaptive response of skeletal muscle to increased use. Muscle and Nerve 4, 94-105.

Salomon MB, Eastridge JE. (1987). Occurrence of giant fibers in muscles from wild pigs native to the United States. Meat Science 20:75-81.

Scheper J. (1979). Influence of environmental and genetic factors on meat quality. Acta Agricult. Scand. 21:20-29.

Schmalbruch H. (1973). Contracture knots in normal and diseased muscle fibers. Brain. 96:637-640.

Schmalbruch H. (1975). Segmental fibre breakdown and defects of the plasmalemma in diseased human muscles. Acta Neuropath. (Berl.) 33:129-141.

Schmidt O, Dumont BL. (1977). Distribution of giant fibers in muscle of meat animals. Proc. 25th Eur. Meet. Meat Res. Work. Budapest; Hungary. 219-224.

Schmidt O, Dumont BL. (1980). Detection of giant fibers and interpretation of their presence in pig muscle. in Porcine Stress and Meat Quality--Causes and Possible Solutions to the Problem. eds: T. Froystein, E. Slinde and N. Standil. Agr. Food Res. Sci. Norway. 53.

Seemann G, Jones JM, Griffiths NM, Grey TC. (1986). Der EinfluB von Lagerdauer und-temperatur auf die Qualitat von Putenbrustfleisch. Arch. Geflugelk. 50, 149-153.

Sink JD, Mann OM, Turgut H. (1986). Characterization of the giant myofibers in bovine skeletal muscle. Exp. Cell Biol. 54:1-7.

Sosnicki A, Domanski J. (1983). The relationship between the occurrence of giant fibers and PSE meat in the pig. Meat Economy (Poland) 2:17-21.

Sosnicki A. (1987). Histopathological observation of stress-myopathy in m. longissimus in the pig and the relationship with meat quality, fattening and slaughter traits. J. Anim. Sci. 65:584-596.

Uchino M, Araki S. (1986). The mechanism of muscle fiber breakdown in Duchenne Muscular Dystrophy - with particular reference to the significance of opaque fiber (Part 2) (Japanese). Clin. Neurol. 26:841-846.

Weatherspoon JR. (1969). The relationship of some anatomical and physiological characteristics of Sus domesticus to postmortem muscle properties. PhD Thesis. Michigan State University. East Lansing.

Wohlfart G. (1937). About the appearance of different kinds of muscle fibers in the skeletal musculature of human and some animals. Acta Psychiat. Neurol. Suppl. 12:1-119.

Discussion with Reviewers

Reviewer I: Was all the biopsied material frozen in isopentane cooled with liquid nitrogen? Although frozen tissue is necessary for histochemical studies and an H&E stain done on this material provides a "control" for histochemical studies, the basic morphology of the muscle seen by H&E stain might better be done on formalin fixed tissue.

Authors: All the muscle samples studied in this experiment were frozen in isopentane cooled with liquid nitrogen. We agree that a better morphology would undoubtedly have been seen if H&E staining had been done on formalin fixed tissue rather than on unfixed frozen tissue. However, formalin fixed muscle fibers usually have a more rounded shape in contrast to the more angular or polygonal shape of muscle fibers in frozen section. The rounded shape might have caused some confusion in interpretation of the hypercontracted fibers.

Reviewer II: Some experiments to be considered would be the effect of trauma at the time of slaughter where one might compare a lethal dose of Nembutol to exsanguination. Also, to answer the question of growth hypertrophy to the appearance of hypercontracted fibers, one might supplement the turkey's diet with steroids.

Authors: We did not study sacrifice by Nembutol injection or the effect of steroids in this experiment. Trauma during transport and slaughter is always a concern. The reasons for believing that the hypercontracted fibers are not artifactual are explained in the text.

Reviewer III: In regard to quantitation of hypercontracted fibers, how many fields per muscle per bird were counted and what was meant by "a slightly higher incidence of these fibers"?

Reviewer IV: How many hypercontracted fibers are found per bird and does the frequency increase with time?

Authors: We have not done a statistical quantification but merely reported that the hypercontracted fibers appeared quite frequently in the birds examined. Our work was directed more at an examination of the properties of the fibers in an attempt to determine if they were real or artifactual. One field under low power magnification (25x) is equal to about 1.65 mm^2, and the approximate area of our cryostat sections was 1 cm^2. Therefore, we usually evaluated about 60 fields for a given muscle and because the samples were collected from 5 different muscles, about 300 fields were evaluated per bird.

Reviewer III: If necrosis has occurred, would one expect to find regenerative changes?

Authors: Yes, the degeneration and regeneration processes usually occur together and we would expect to observe evidence of regeneration--but such was not the case. Necrosis is not always accompanied by regeneration, and, for example, is unlikely under ischemic conditions.

Reviewer III: What about the possibility of lysosomal proteases degrading the sarcolemma?

Authors: This is not an easy question because there is no direct evidence on the matter. One explanation for hypercontraction is an increase of available calcium in the fiber which could result from damage to the fiber during the preslaughter time or during collection and freezing of the sample. Our observations on acid phosphatase showed a positive but diffuse activity. We believe lysosomal proteases do not directly cause hypercontraction of fibers but may act in a secondary way.

Reviewer IV: Were the muscles restrained before removal from the carcass?

Authors: No. They were removed and then an attempt was made to adjust the sample to approximate rest length and restrain it with forceps during freezing.

FOOD MICROSTRUCTURE, Vol. 7 (1988), pp. 153-160
Scanning Microscopy International, Chicago (AMF O'Hare), IL 60666 USA

0730-5419/88$3.00+.00

POROSITY, SPECIFIC GRAVITY AND FAT DISPERSION IN BLUE CHEESES

K.M.K. Kebary and H.A. Morris

Department of Food Science and Nutrition
University of Minnesota
Saint Paul, Minnesota 55108

Abstract

Porosity was measured in Blue cheeses made from (i) homogenized butter oil-reconstituted nonfat dry milk (4% fat), (ii) homogenized butter oil-reconstituted nonfat dry milk (14% fat) standardized to 4% fat with reconstituted nonfat dry milk, (iii) homogenized raw cream (14% fat) standardized to 4% fat with raw skim milk, and (iv) homogenized pasteurized cream (14% fat) standardized to 4% fat with pasteurized skim milk. Cheeses made from (i) were the most porous and were significantly different from the other cheeses. In cheeses made from (i) and (ii), about 40% of the holes were less than 2 μm^2 in area, while in cheeses made from (iii) and (iv), 50% of the holes were less than 2 μm^2. Cheeses made from (iii) did not contain holes larger than 22 μm^2, whereas cheeses made from (iv), (ii) and (i) contained 0.76, 1.29, and 5.27%, respectively, of holes larger than 22 μm^2. Cheeses made from (i) had the lowest specific gravity and were significantly different from the others. Fat was well dispersed in cheese made from (i) with few small clusters. The other cheeses contained many large clusters of fat globules, and the fat distribution was less uniform than in cheeses made from (i).

Initial paper received June 09, 1988
Manuscript received August 16, 1988
Direct inquiries to H.A. Morris
Telephone number: 612-624-4293

Key words: Blue cheese, porosity, specific gravity, fat dispersion, homogenization, nonfat dry milk.

Introduction

There is interest in making Blue cheese from butter oil and reconstituted nonfat dry milk in such countries as Egypt. A first attempt was made by Omar and Ashour (1982), who made Blue cheese from unhomogenized cream standardized to 3.8% fat with reconstituted nonfat dry milk and also from reconstituted dry whole milk. However, these cheeses were inferior to those made from fresh cow's milk.

In the manufacture of Blue cheese in the United States, it is common practice to separate whole milk into 12-14% fat cream and skim milk. The cream is homogenized and then recombined with the skim milk. A less common practice is to simply homogenize whole milk. The use of these homogenized products results in the production of an open bodied, porous cheese structure that favors mold growth and sporulation (Morris, 1981). The resulting cheese is superior to that made from unhomogenized milks.

It is postulated that homogenization and incorporation of air in the milk up to the time of adding rennet increases porosity and results in a less dense, more porous cheese than when unhomogenized milks are used (Morris, 1981). But information is lacking about porosity per se and density of Blue cheese as influenced by the homogenization treatment.

Overall curd structure may be visualized as a para-casein sponge in which fat globules, bacteria (Kimber et al., 1974), whey (Green et al., 1981) and gases (Kalab et al., 1982; Lowrie et al., 1982) are held. Whether the fat globules exist singly or in clusters, and the amount of entrapped air, undoubtedly influence the structure and thus the physical parameters of cheese, such as porosity, size distribution of holes in cheese, and density.

Cheese porosity is defined, theoretically, as the ratio of the volume of the holes (pores) in cheese to the total volume of cheese (Noel et al., 1987). Our interest in porosity was inspired by the work of Green et al. (1981). They measured coarseness of the protein matrix in curds and cheeses. This was done by printing micrographs of the matrix on transparent paper. For cheese samples, the micrographs were placed on a 28 x 19 line rectangular grid (Green et al., 1981). "The black parts of the photograph (casein) made the grid invisible, but the grid lines could be seen through the clear parts of the photograph (fat, whey, or holes). We simply counted the number of bits of grid line visible, ignoring their length. The frequency of phase change was (count x

2) / total length of lines on the grid in mm. The coarseness was defined as the reciprocal of the frequency. Our prints were 72 x 48 mm and total length of lines on grid in mm" (Green, M.L. personal communication, 1987.).

To measure porosity accurately, all sections of cheese would need to be examined. Thus, in practice, the method for coarseness by Green et al. (1981), or similar approaches are feasible approximations to actual porosity.

Although pores have been noted in cheese structures and milk gels by Eino et al. (1976), Glaser et al. (1980), Green et al. (1978, 1981), Kalab and Emmons (1978), and by Kalab and Harwalkar (1973), porosity as such has not been measured.

Yiu (1985) studied fat distribution in commercial Blue cheese. She found large fat globules in the vicinity of the mold, while the fat globules away from the mold were smaller. It is not known whether or not the cheese was made from homogenized milks or homogenized creams.

Homogenization is essential to combine butter oil efficiently with reconstituted nonfat dry milk and to improve the quality of cheese over the use of unhomogenized mixtures. Comparability of resulting products with regular homogenized cream and milk in the manufacture of Blue cheese does not appear to have been investigated.

The literature on cheese density seems to be restricted primarily to work by Mayes and Radford (1983), who determined density in Cheddar cheese by determining the weight in air and the weight suspended in a liquid. They obtained values ranging from 1.073 to 1.078 g/mL at 20°C, and from 1.088 to 1.096 g/mL at 8°C.

In view of the aforementioned, the purpose of this work was to obtain information on porosity, density and fat distribution in Blue cheeses made from homogenized mixtures of butter oil and reconstituted nonfat dry milk.

Methods and Materials

Materials

The following materials were used (sources are indicated in parenthesis); butter oil (Level Valley Dairy Products, West Bend, WI); grade A low heat nonfat dry milk (NDM) (Mid-America Dairymen, Inc., St. Paul, MN); calf rennet (Pfizer, Inc., Milwaukee, WI); calcium chloride (Dairyland Food Laboratories, Inc., Waukesha, WI); Penicillium roqueforti powder (Dairyland Food Laboratories, Inc., Waukesha, WI); methylene blue and eosin (Hartman-Leddon Company, Philadelphia, PA); potassium hydroxide (Allied Chemical, General Chemical Division, Morristown, NJ); Sudan III dye (Sigma Chemical Company, St. Louis, MO); ethanol (Midwest Grain Products, Atchison, KS); acetone (Chemical MGF Corp., Gardena, CA); kerosene (Chemical Warehouse, University of Minnesota, Minneapolis, MN); monochlorobenzene and osmium tetroxide (Aldrich Chemical Company, Inc., Milwaukee, WI); formaldehyde (Hawkins Company, Minneapolis, MN); hematoxylin (E.M. Science, Cherry Hill, NJ); "hemo De" (a deparafinizing mixture of terpene, mineral oil, and butylated hydroxy-anisol) (PMP, Medical Industries, Los Angeles, CA); sodium phosphate dibasic, hydrochloric acid and glacial acetic acid (Mallinckrodt, Inc., Paris, KY); monobasic sodium phosphate (Columbus Chemical Industries, Inc., Columbus, WI); glycerin, aluminum ammonium sulfate, sodium iodate and Permount Mounting Medium (Fisher Scientific Company, Fair Lawn, NJ); and paraffin (Surgipath, Grayslake, IL).

Cheesemaking

Butter oil, sufficient to produce 4% or 14% fat blends with reconstituted (9% solids) NDM were prepared. NDM was thoroughly dispersed in water heated to 43.5°C. The appropriate amount of butter oil was then added to the milk. The mixture was heated to 54.5°C with agitation until all the butter oil was melted. Both 4% fat in reconstituted nonfat dry milk (4% RNDM) and 14% fat in reconstituted nonfat dry milk (14% RNDM) were homogenized at 13790 + 3448 kPa (2000 + 500 psi) and 54.5°C. All products used in the manufacture of cheese were double stage homogenized at 13790 + 3448 kPa and 54.5°C in a Gaulin Model 125/ 83MF12A, 384L/H (Manton Gaulin Company, Inc., Everett, MA). After homogenization the 14% fat RNDM was standardized with reconstituted NDM to 4% fat (14-4% RNDM). Both mixtures were held overnight at 4-5°C. Two 454 kg portions of normal raw whole milk (3.8% fat) were used to make the control cheese. One portion was separated to get 14% fat cream and skim milk. The cream was homogenized, then recombined with the skim milk to make 4% fat milk (14-4% R). The other portion of normal raw milk was separated and both 14% fat cream and skim milk were pasteurized, then 14% fat pasteurized cream was homogenized and added back to the pasteurized skim milk to make 4% fat milk (14-4% P). Blue cheeses were made from 182 kg of reconstituted nonfat dry milks and 454 kg of 14-4% R and 14-4% P using the method described by Morris (1981), except that calcium chloride was added to 4% RNDM, 14-4% RNDM and the 14-4% P milks. Cheese-making trials were done in triplicate.

Table 1 describes the sample designations used in the rest of the paper.

Table 1. Sample designations.

Designation	Blue cheese made from
4% RNDM	Homogenized 4% fat in reconstituted nonfat dry milk
14-4% RNDM	Homogenized 14% fat in reconstituted nonfat dry milk standardized to 4% fat with reconstituted nonfat dry milk
14-4% P	Homogenized 14% fat pasteurized cream standardized to 4% fat with pasteurized skim milk
14-4% R	Homogenized 14% fat raw cream standardized to 4% fat with raw skim milk

Cheese porosity

Blue cheese samples were taken before salting, prepared and stained using the method of Hansson et al. (1966) with the following modification: sections were 4 µm thick prepared by using a cryogenic micrometer (Model CTD-International-Harris Cryostat

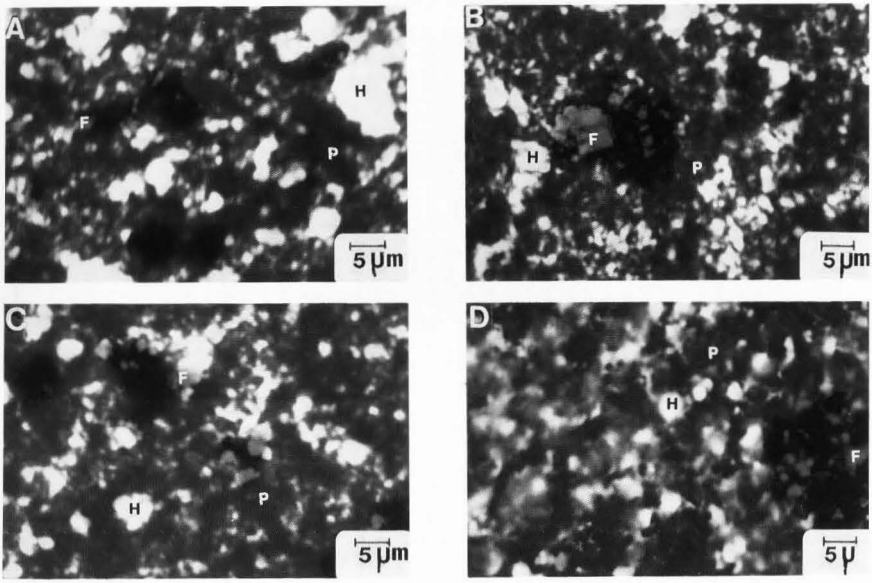

International Equipment Company, Needham Heights, MA). Two photomicrographs of each cheese were obtained using a camera (Nikon M-35S, 35 mm, Nikon, Tokyo, Japan) attached to a light microscope (Olympus BH, Olympus Optical Company Limited, Tokyo, Japan). A transparent micrograph was made for each photomicrograph obtained. Transparent micrographs were used to measure the area of the holes (pores) using a Hipad digitizer (Houston Instrumental, Austin, TX) attached to an Apple II computer (Apple Computer, Inc., Cupertino, CA). The area of each hole on the micrograph was recorded in cm^2 and the total area of the photomicrograph was calculated in cm^2. The ratio of the area of the holes to the area of photomicrograph was calculated and called porosity. Actual dimensions in μm^2 were used in the display of frequency distributions and in statistical calculations. This experiment was duplicated.

Table 2. The porosity of Blue cheeses. (Porosity = the total area of holes / the total area of the photograph.)

Cheese samples	Porosity[a] Trial 1	Trial 2	Porosity[b]	SE
4% RNDM	0.1259	0.0988	0.1124**	0.0136
14-4% RNDM	0.0716	0.0680	0.0698*	0.0018
14-4% P	0.0625	0.0598	0.0612*	0.0014
14-4% R	0.0530	0.0479	0.0514*	0.0017

a = mean of two photographs;
b = mean of the two trials;
SE = standard error for the two trials;
* = not significantly different;
** = significantly different.

Figure 1. Light photomicrographs of sections of Blue cheeses:
A - 4% RNDM; B - 14-4% RNDM; C - 14-4% P; and D - 14-4% R.
F = fat; P = protein matrix; H = holes

Specific gravity of cheese

Cheese samples were cut into 1 cm cubes. Four cubes were used for each type of cheese. The method described by Stoll (1966) to measure the specific gravity of curd using different solutions of kerosene and monochlorobenzene was used to measure specific gravity. The experiment was triplicated.

Distribution of fat in cheese

Cheese pieces (1 x 1 x 0.3 cm) were fixed in 10% buffered formalin solution (Hansson et al., 1966) and postfixed in 1.5% osmium tetroxide to stabilize the fat and stain it black. Routine Harris hematoxylin and eosin method (Luna, 1968) was used for

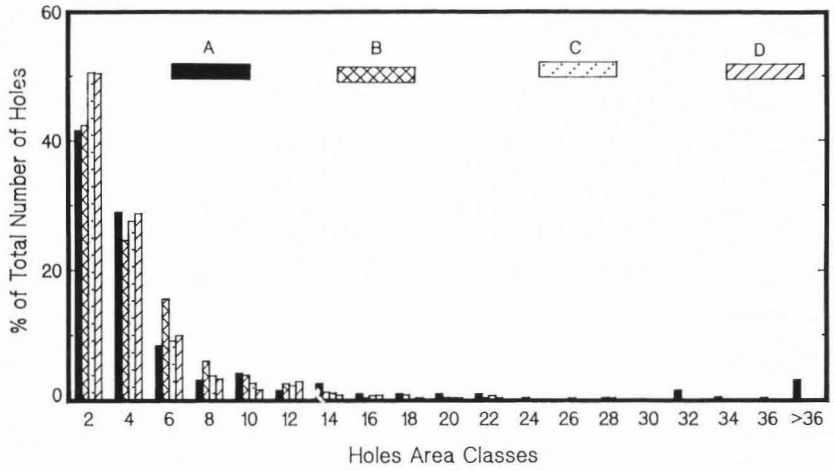

Figure 2. Size frequency distribution of holes (area in μm^2) in blue cheeses: A - 4% RNDM; B - 14-4% RNDM; C - 14-4% P; D - 14-4% R. The number (% of total number) is given per 2 μm^2 class widths.

staining and preparing the cheese on the slides except that the sections were not dipped in ammonia or lithium and hemo De was substituted for xylene. The distribution of fat in cheese was studied using two slides from each of the four cheese types and photomicrographs were obtained using a Nikon camera attached to a light microscope. This experiment was duplicated. Therefore, four slides were evaluated for each type of cheese by counting the number of clusters in 8 fields for each slide.

Results and Discussion

Porosity of cheese was calculated by the ratio of total area of holes and the area of cheese observed. Holes as measured in this study contained whey or gases. Cheese made from 4% RNDM had the most porous structure and was significantly (P less than 0.05) different from other cheeses (Table 2 and Figure 1).

The frequency distribution of holes in the Blue cheeses is shown in Figure 2. About 50% of the total holes were less than 2 $\mu m2$ in Blue cheeses made from 14-4% R and 14-4% P, while cheeses made from 14-4% RNDM and 4% RNDM had only about 40% of the total holes less than 2 μm^2. Cheese made from 14-4% R did not have any holes larger than 22 μm^2, while cheeses made from 14-4% P, 14-4% RNDM and 4% RNDM had 0.76, 1.29 and 5.27% of the total holes larger than 22 μm^2, respectively. Cheeses made from 4% RNDM were the only ones that had holes larger than 36 μm^2 (3.16%).

Specific gravity of cheese

The mean specific gravities for each of the three trials along with the overall means are shown in Table 3. Cheeses made from 4% RNDM had the lowest specific gravity and were significantly different (P less than 0.05) from the other cheeses.

Specific gravity values varied from 1.0339 to 1.0520 at 32°C. According to Mayes and Radford (1983), Cheddar cheese varies in density from 1.073 to 1.078 g/ml at 20°C and from 1.088 to 1.096 g/ml at 8°C. Thus, Blue cheese is much lighter than Cheddar cheese. Not surprising, the most porous cheese had the lowest specific gravity (cheese made from 4% RNDM) and the cheese that had the least porous structure had the highest specific gravity (cheese made from 14-4% R). This suggests that many of the holes contained gases and not whey.

Distribution of fat in cheese

The distribution pattern of fat globules was studied in Blue cheeses made from the homogenized mixtures of 4% RNDM, 14-4% RNDM, 14-4% R and 14-4% P. The terminology to be used concerning the association of two or more fat globules is that of Mulder and Walstra (1974), whose plate 3 clearly shows the difference between flocs and homogenization clusters. The distribution of fat in Blue cheeses made from 14-4% RNDM, 14-4% R and 14-4% P was not uniform and existed mostly as clusters (Figs. 3B, C and D). The non-uniformity of distribution is similar to other cheeses (Hall and Creamer, 1972; Taranto et al., 1979). In contrast, fat in cheese

Figures 3 and 4 (on the opposite page). Light photomicrographs of sections of Blue cheeses showing: Figure 3: examples of overall distribution of fat; and Figure 4: examples of cluster formation. A - 4% RNDM; B - 14-4% RNDM; C - 14-4% R; and D - 14-4% P. The black particles are fat.

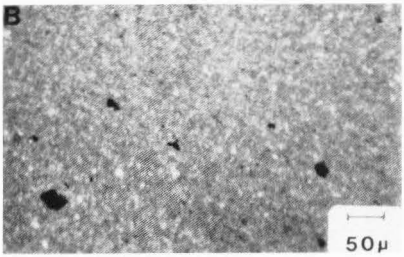

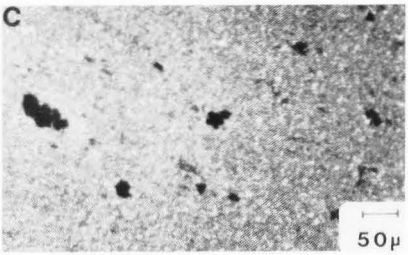

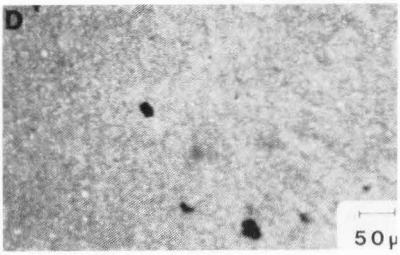

Bars = 50 μm (for all figures in Fig. 3).

Bars = 5 μm (for all figures in Fig. 4).

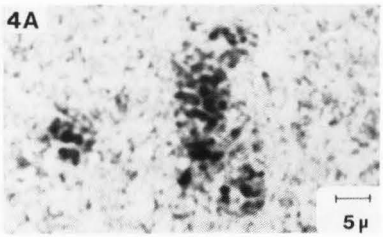

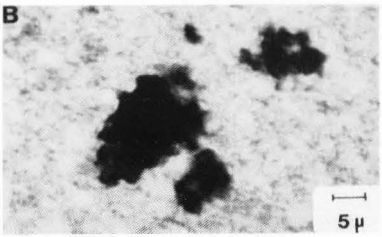

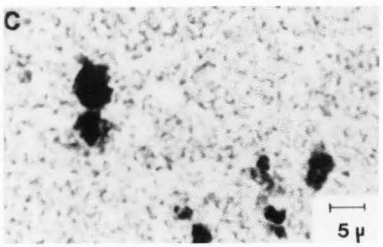

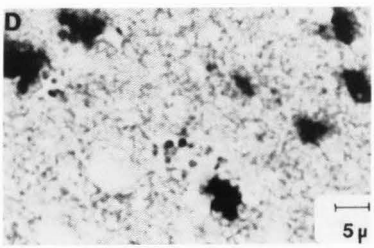

Table 3. The specific gravity of cheeses.

Cheese samples:	Specific Gravity[a]			Specific Gravity[b]	SE
	Trial 1	Trial 2	Trial 3		
4% RNDM	1.0347	1.0358	1.0347	1.0351**	0.0006
14-4% RNDM	1.0449	1.0460	1.0430	1.0446*	0.0012
14-4% P	1.0453	1.0471	1.0453	1.0459*	0.0006
14-4% R	1.0483	1.0498	1.0471	1.0484*	0.0006

[a] = mean of four samples of cheese for trial; [b] = mean of the three trials; SE = standard error of the three trials; * = not significantly different; ** = significantly different.

Table 4. Fat distribution (clusters) in Blue cheeses.

Cheese	Number of clusters[a]		Number of clusters[b]	SE
	Trial 1	Trial 2		
4% RNDM	2.0	2.0	2.0**	0.00
14% RNDM	5.0	5.0	5.0*	0.00
14-4% P	4.0	4.0	4.0*	0.00
14-4% R	5.0	4.0	5.0*	0.5

[a] = mean of the number of clusters in 16 fields for each trial; [b] = mean of the number of clusters in 32 fields in the two trials; SE = standard error of the two trials; * = not significantly different; ** = significantly different.

made from 4% RNDM was distributed more uniformly in the form of single globules (Fig. 3A) or as floccules (Fig. 4A), although a few clusters were present. Cheeses made from 14-4% RNDM, 14-4% R and 14-4% P had many clusters of fat entrapped in casein matrix (Figs. 4B, C and D). The number of clusters was significantly different from cheese made from 4% RNDM (P less than 0.05) as shown in Table 4. These results would be predicted from the work of Ogden et al. (1976), who found that homogenization of cream induced the clustering of fat globules due to sharing of fat globules by casein micelles. Clusters formed by homogenizing 14% fat mixtures were not dispersed by the second stage homogenization or by standardizing to a 4% fat mixture (unpublished data, Kebary, K.M.K.). Similarly, Knoop and Peters (1972) found in Camembert cheese made from partly homogenized milk that fat clusters were embedded in the casein matrix. As noted, cheese made from 4% RNDM had a few small clusters and floccules. In preliminary work on changes in the distribution pattern of fat globules in homogenized raw milk, homogenized pasteurized milk and in the homogenized 4% RNDM mixture left for 48h at 10°C, there was a slight increase in the number of floccules. This observation does not account for the relatively greater number of floccules observed in the cheese. Perhaps agitation of the milk, or other factors during manufacture results in more aggregation of this type. Also, aggregation of fat globules was observed in Cheddar cheese (Taranto et al., 1979).

In conclusion, cheese made from 4% RNDM had the highest porosity and lowest specific gravity and was significantly different from cheeses made from 14-4% RNDM, 14-4% R and 14-4% P. Fat distribution was more uniform in cheese made from 4% RNDM than cheese made from 14-4% RNDM, 14-4% R and 14-4% P. Many clusters were noted in cheeses made from the 14-4% products.

Acknowledgements

Published as paper no. 16,064 of the scientific journal series of the Minnesota Agricultural Experiment Station on research conducted under Minnesota Agricultural Experiment Station Project No. 18-79 supported by Hatch Funds and funds from Amideast-Peace Fellowship Program for Egypt and the Cultural and Educational Bureau, Embassy of the Arab Republic of Egypt.

The authors wish to thank Mr. Ray Miller and Ms. Krisann Thompson for their help in cheese-making.

References

Eino MF, Biggs DA, Irvine DE, Stanley DW. (1976). Microstructure of Cheddar cheese: Sample preparation and scanning electron microscopy. J. Dairy Res. 43, 109-111.

Glaser J, Carroad PA, Dunkley WL. (1980). Electron microscopic studies of casein micelles and curd microstructure on cottage cheese. J. Dairy Sci. 63, 37-48.

Green ML, Hobbs DG, Morant SV, Hill VA. (1978). Intermicellar relationship in rennet-treated separated milk. II Process of gel assembly. J. Dairy Res. 45, 413-422.

Green ML, Turvey A, Hobbs DG. (1981). Development of structure and texture in Cheddar cheese. J. Dairy Res. 48, 343-353.

Hall DM, Creamer LK. (1972). A study of the sub-microscopic structure of Cheddar, Cheshire and Gouda cheese by electron microscopy. New Zealand J. Dairy Sci. and Tech. 7, 95-102.

Hansson E, Olsson H, Sjostrom G. (1966).

Microphotography of cheese structure. Milchwissenschaft 21, 331-334.

Kalab M, Emmons DB. (1978). Milk gel structure 9. Microstructure of cheddared curd. Milchwissenschaft 33, 670-673.

Kalab M, Harwalkar VR. (1973). Milk gel structure 1. Application of scanning electron microscopy to milk and other food gels. J. Dairy Sci. 56, 835-842.

Kalab M, Lowrie RJ, Nichols D. (1982). Detection of curd granule and milled curd junction in Cheddar cheese. J. Dairy Sci. 65, 1117-1121.

Kimber AM, Brooker BE, Hobbs DG, Prentice BE. (1974). Electron microscope studies of the development of structure in Cheddar cheese. J. Dairy Res. 41, 389-396.

Knoop AM, Peters K-H. (1972). Dependence of the submicroscopical structure of rennet coagulum and young Camembert cheese mass on the conditions of manufacture. Milchwissenschaft 27, 153-159.

Lowrie RJ, Kalab M, Nichols D. (1982). Curd granule and milled curd junction patterns in Cheddar cheese made by traditional and mechanized processes. J. Dairy Sci. 65, 1122-1129.

Luna LG. (1968). Manual of Histologic Staining Methods of the Armed Forces Institute of Pathology. 3rd edition. Pages 38-39. The Blakiston Division, McGraw Hill Book Company, New York.

Mayes JJ, Radford DR. (1983). Density of Cheddar cheese. Australian J. Dairy Tech. 38, 34.

Morris HA. (1981). Blue Veined Cheeses. Pages 13-27. Pfizer, Inc., New York.

Mulder H, Walstra P. (1974). The milk fat globule-emulsion science as applied to milk products and comparable foods. Plate 3 between pages 96 and 97, and page 103. Commonwealth Agricultural Bureaux, Farnham Royal, Bucks, England.

Noel Y, Ramat JP, Gervais A, Lablee J, Cerf O. (1987). Physical properties of the coagulum. In: Cheesemaking Science and Technology. Pages 13-17. A. Eck (ed.). Lavoisier Publishing, Inc., New York.

Ogden LV, Walstra P, Morris HA. (1976). Homogenization-induced clustering of fat globules in cream and model system. J. Dairy Sci. 59, 1727-1737.

Omar MM, Ashour MM. (1982). Blue-like cheese from dried milk. Die Nahrung. 26, 863-867.

Stoll WF. (1966). Synersis of rennet-formed milk gels. Ph.D. Thesis. Univ. of Minnesota, St. Paul, MN.

Taranto MV, Wan PJ, Chen SL, Rhee KC. (1979). Morphological, ultrastructural and rheological characterization of Cheddar and Mozzarella cheese. Scanning Electron Microsc. 1979; III: 273-278.

Yiu SH. (1985). A fluorescence microscopic study of cheese. Food Microstructure. 4, 99-106.

Discussion with Reviewers

M.L. Green: It should be possible to deduce the density of the contents of the holes from between-cheese comparisons of the proportions of holes and densities. This should help to identify hole contents. What does such an analysis reveal?

Authors: Your question led us to plot the means for porosity against the means for specific gravity to determine the regression equation and the correlation coefficient as shown in Figure 5. As would be expected, on average, as specific gravity increases, porosity decreases. It would appear to be possible to calculate the weight of air from the specific gravity if the composition of the cheese is also known. The formula is:

$$S = \frac{\%F + \%N + \%W + \%air}{(\%F / SF)+(\%N / SN)+(\%W / 1)+(\%air / S\ air)}$$

where S = specific gravity, F = fat, N = solids not fat and W = water. Using the S determined by experimentation, S of F = 0.93, S of N of 1.6007, S of air is 0.001205 (at 20°C and atmospheric pressure for dry air), and the cheese composition at the time the S was determined, the amount of air can be calculated by solving for % air. Unfortunately, we measured specific gravity of the cheeses before the cheeses were salted and before mold grew in them and determined cheese composition after salting, thus we do not have the needed information. We plan to do this experiment.

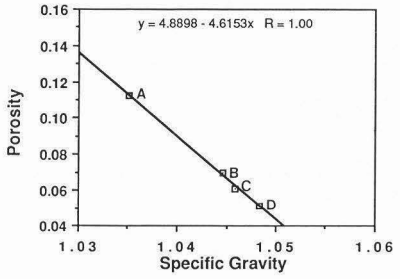

Figure 5. The relationship between porosity and specific gravity for the four cheeses used in these experiments:
A - 4% RNDM, B - 14-4% RNDM,
C - 14-4% P, and D - 14-4% R.

L.K. Creamer: Could porosity have been measured by weighing the cheese, weighing the cheese submerged in oil and then evacuating the cheese while submerged and weighing the degassed cheese?

Authors: Such an approach might be feasible if the pores contained only gases. But if some contain gas (air, carbon dioxide or ammonia) and others contain whey, the problem becomes more complicated. How well gases might be evacuated from the cheese matrix while immersed in oil would need to be explored.

L.K. Creamer: Why was porosity measured on only two sets of cheese?

M.L. Green: In Table 2, why only results of two trials when experiment was done in triplicate?

Authors: The overall project was concerned with the manufacture of Blue cheese from nonfat dry milk and butter oil. Three cheese-making trials were planned using the preparations indicated in this paper. Initially we planned on following acid development, sensory evaluation of the curds during manufacture, chemical composition of the cheeses, specific gravity

of the cheeses, extent and distribution of mold growth, and chemical changes during ripening along with sensory evaluations. Trials were scheduled for the spring, summer, and winter. After the first trial we included porosity and fat distribution in the cheese to the parameters to be determined. To avoid possible complications of variations in salt content and mold growth in the cheeses, specific gravity, porosity and fat distribution were all determined on the cheeses just prior to dry salting. Cheeses from the first trial had been salted, punched, and mold had grown in them before we had decided to determine porosity and fat distribution. That is why specific gravity was run on the cheeses in the three trials and porosity and fat distribution were run only on the last two trials.

M.L. Green: In the absence of evidence that the fat globules are clustered in the milks at the start of cheesemaking, can the authors suggest why clustering should occur. Could the mode of aggregation of the casein have any influence?
Authors: We do have evidence that fat globules were clustered in the milks at the start of cheesemaking. This is a part of the unpublished work referred to in the text. The same is true in commercial manufacture as shown in Fig. 6. The creation of homogenization induced clusters is explained in the Ogden et al. (1976), and in the Mulder and Walstra (1974) references in the text. Since homogenization clusters are only redispersible with considerable energy, they are not broken up when the homogenized 14% fat mixtures are standardized to 4%. Ogden et al. (1976) also showed that the clusters stay intact after dilution. They also explain the effects of fat content, shareable surfactant (casein micelles) content, homogenization pressure, and surfactant particle size on the extent of clustering.

L.V. Ogden: Does the more open cheese that results from homogenization of 4% milk actually result in better mold growth and more acceptable product?
Authors: All of the cheeses made were very acceptable. Mold did grow more abundantly in the cheese made from the 4% fat containing butter oil-reconstituted nonfat dry milk blend than in the others. We did not use 4% homogenized normal milk but would expect similar results.

L.K. Creamer: On the basis of the present results would you recommend any particular manufacturing protocol?
Authors: For the manufacture of Blue cheese from mixtures of butter oil and reconstituted nonfat dry milk, i.e., 14-4% RNDM vs. 4% RNDM, based on porosity, specific gravity and mold growth, the 4% fat mixture would be preferred. But results from a consumer acceptance panel showed that there was no significant difference between the cheeses at four months of age, but at eight months the 14-4% RNDM cheeses were preferred. Since the cheeses were relatively comparable from a consumer viewpoint, the economics of homogenizing a lower volume of 14% fat product compared to homogenizing the 4% mixture would favor the manufacture from the 14-4% RNDM mixture using conventional methods.

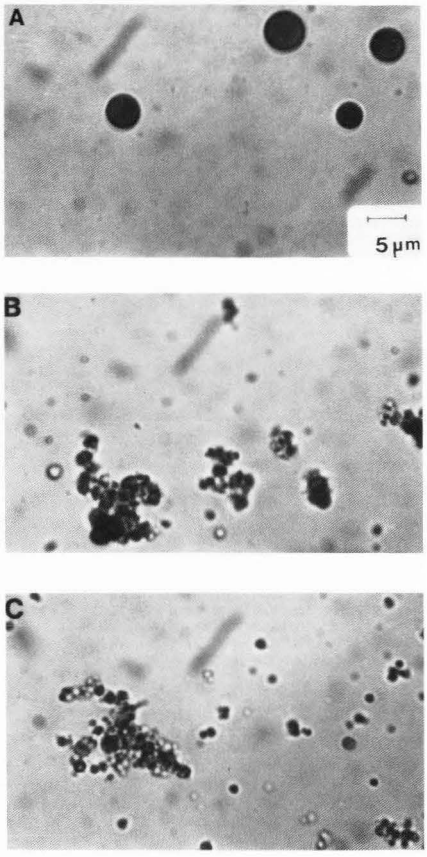

Figure 6. Effect of fat content on clustering and sizes of fat globules of normal milk (commercial samples) homogenized at 13790 + 3448 kPa. A - unhomogenized cream (14% fat); B - homogenized 14% fat cream; C - homogenized 14% cream diluted back to 3.4% fat with skim milk. The magnification is same in the three micrographs.

FOOD MICROSTRUCTURE, Vol. 7 (1988), pp. 161-172
Scanning Microscopy International, Chicago (AMF O'Hare), IL 60666 USA

0730-5419/88$3.00+.00

APPLICATION OF SCANNING ELECTRON MICROSCOPY AND X-RAY MICROANALYSIS TO INVESTIGATE CORROSION PROBLEMS IN PLAIN TINPLATE FOOD CANS AND EXAMINE GLASS AND GLASS-LIKE PARTICLES FOUND IN CANNED FOOD

James E. Charbonneau

National Food Processors Association
1401 New York Avenue, NW
Washington, D.C. 20005

Abstract

Scanning Electron Microscopy (SEM) and X-ray Microanalysis (EDS) have been used to investigate product container interaction problems in plain tinplate metal food containers and to examine glass and glass-like particles that were found in canned food.

Through the use of SEM-EDS, it was determined that: sulfate containing particles from the cannery cooling water reacted with exposed iron or tin-iron alloy on the tinplate surface causing an external rusting problem; sulfur dioxide was responsible for a container discoloration and a pitting corrosion problem in canned fruit nectar; hydrogen sulfide produced from the SO_2-tinplate reaction was the cause of an associated off-odor problem; copper, possibly from a side seam welding operation, excessive headspace oxygen and a beading defect on the container body wall helped explain a detinning and pitting corrosion problem in canned fried apples.

A quantitative SEM-EDS method was used to measure the composition of glass particles in two alleged product tampering cases involving canned food. Glass-like particles from a tomato powder and canned peas were also examined.

Initial paper received July 05, 1988
Manuscript received November 25, 1988
Direct inquiries to J.E. Charbonneau
Telephone number: 202 639 5972

Key Words: Scanning Electron Microscopy, X-ray Microanalysis, Tinplate Food Cans, External Rusting, Internal Can Corrosion, Glass, Glass-like Particles, Product Tampering.

Introduction

The food industry is committed to providing consumers with a safe and quality product. The industry is primarily concerned that the product not be adversely affected by the corrosion reactions between product and package, nor the quality affected by the presence of extraneous materials. By ensuring package and product integrity, manufacturers are then able to produce a product with extended shelf life. Industry's record for achieving success is reflected by the hundreds of safe products produced each day.

Occasionally, container corrosion occurs or foreign materials are found in a product. Food producers need to find explanations for these events so they can take steps to prevent their recurrence. In this paper, scanning electron microscopy and X-ray microanalysis were used to investigate three typical corrosion problems found in plain tinplate cans to examine glass and glass-like particles that were found in canned foods.

Materials and Methods

Materials

Tinplate, glass and glass-like particles are the materials studied.

Tinplate. Tinplate, tin free steel, nickel plated steel and aluminum are the materials used to manufacture metal food cans. Metal can-making technology (types of cans, trends and selection factors) have been reviewed (Kopetz, 1978). In this paper only corrosion processes that occur in three piece welded cans fabricated from plain tinplate are considered. Plain refers to tinplate with no internal enamel coating.

Tinplate defined. (Beese and Ludwigsen, 1974; AISI, 1979) The tin can is made from a special grade of low carbon, cold rolled steel which is generally referred to as a tin mill product. The base steel is cleaned electrolytically and plated with tin. It is then passed through a melting tower to melt and reflow the tin to form a shiny tin surface and tin-iron alloy layer. The plate is then chemically treated to prevent oxide growth and lubricated with a thin layer of a Food and Drug Administration (FDA)-approved synthetic oil.

In specialized k plate, a nearly continuous tin-iron alloy layer improves the corrosion resistance of tinplate for mildly acid products.

The tin coatings on tinplate can be purchased in thicknesses ranging from 0.39 to about 1.54 μm. Differentially coated tinplate with the heavier coating on the food contact surface is also available. Tin coating weights are expressed in pounds per base box and represent the total of tin coating on both sides with the exception of the coating weight on differentially coated tinplate. In this later product, the coating weights expressed represent the equivalent of double the coating for each side.

Tinplate can be purchased in a wide range of tempers and thicknesses. Thicknesses ranging from 0.1 to about 0.3 mm are commercially available. The chemistry of the base steel is carefully regulated to control physical properties and corrosion resistance.

Glass and Glass-Like Particles. The food industry has an excellent record for supplying a safe and quality product to the consumer. There have been, however, a few incidences of alleged product tampering in which extraneous materials have been deliberately added to the food product. Particles that are glass or look like glass have been found by our laboratory in canned food products. Product tampering is not the main source of glass in the product. More commonly glass could accidentally be present in food resulting from a deviation from good manufacturing practices or even incidental contamination.

Methods

SEM–EDS Analysis. An Amray 1600 T SEM and a Kevex 8000 X-ray Microanalysis system equipped with a Kevex Extra detector were used to examine corroded specimens, glass and glass-like particles.

Qualitative Analysis of Corroded Specimens, Glass and Glass-Like Particles. Areas of tinplate with rust deposits or the outside of cans were cut from the cans and examined with no additional preparation. Areas of tinplate with corrosion deposits on the inside of cans were cut from the cans, washed with distilled water to remove adhering food material, air dried and examined by SEM–EDS without additional surface preparation.

Glass particles found in canned meat and glass-like particles found in tomato powder and canned peas were washed with distilled water and air dried. Prior to analysis the materials were sputter coated with carbon using a Polaron Sputter Coater Model E5100.

Quantitative Analysis of Glass Particles. Glass particles found in canned beets and canned tuna were quantitatively analyzed for elemental composition using SEM–EDS. The

Table 1. Approximate Element Composition Typical of Some Types of Glass.

Mfg. Code[1], Glass & Description	% Composition									
	SiO_2	Al_2O_3	B_2O_3	Na_2O	K_2O	MgO	CaO	Fe_2O_3	SO_3	Other
LOF, Window, Soda-Lime	72.6	1.1		13.3	0.1	3.8	8.6	0.1	0.3	
LOF, Architectural, Soda-Lime	72.2	0.1		13.9		2.1	11.2	0.1	0.4	
Container, Soda-Lime	72.1	2.1		14.0	0.5	0.6	10.4	0.1	0.2	0.04 BaO; 0.02 SrO
CGW-0081, Lamp, Soda-Lime	73.4	1.4		16.2	0.4	3.4	5.0	0.05	0.1	
CGW-7251, Auto Headlamp, Soda-Borosilicate	78.1	2.0	14.9	4.9					0.1	
CGW-0088, Tubing, Soda-Lime	70.5	2.0	2.6	12.2	5.3	3.0	4.2		0.2	
CGW-7740, Lab, process, Soda-Borosilicate	80.3	2.3	13.3	4.0						
CGW-7913, Lab, gauge, 96% Silica	96.5	0.5	3.0							
CGW-7331, Ignition Tube, Lime-Magnesia Alumino Silicate	60.7	17.3	5.0	1.0	0.2	7.4	8.6			0.5 As_2O_3
CGW-7570, Solder Glass, Lead Borosilicate	3.7	10.7	11.2	3.8						74.4 PbO
CGW-7720, W, Sealing, Soda-Lead Borosilicate	73.5	1.6	14.4	3.8						0.9 As_2O_3, 5.7 PbO, 12.4 ZnO

[1] LOF = Libbey Owens Ford, CGW = Corning Glass Works

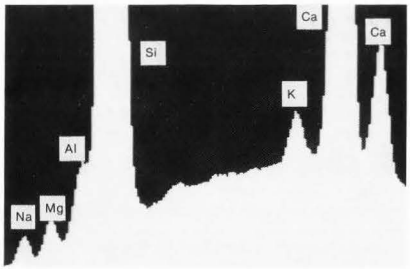

Figure 1. EDS spectrum of container glass.

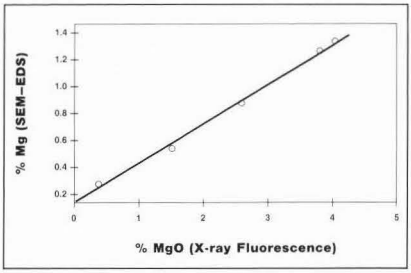

Figure 2. Typical standard curve for the analysis of magnesium in glass.

SEM–EDS is particularly useful for examining glass because the analysis is non-destructive, thus preserving evidence. Also extremely small particles (5–100 μg) can be analyzed using this technique (Winstanley, 1986).

Table 1 lists the approximate composition of 11 different types of glass (ACS, 1986; Tooley, 1984). The compositions are rough averages. Subtle differences in composition may exist within each type and there may be some overlaps between types.

Occasionally it is possible to distinguish glass particles by qualitative X-ray microanalysis. For example, the major elements of container glass (Figure 1) are sodium, magnesium, aluminum, silicon and potassium. This glass is readily distinguishable from Pyrex on the basis of calcium content. Pyrex is a borosilicate glass containing 3–5% alkali.

In general, it is difficult to qualitatively distinguish one glass from another. However, with careful quantitative analysis of the major components and, in some instances, the minor components, glass types can be distinguished from one another using SEM–EDS.

SEM–EDS Method For Glass Analysis

Sample Preparation

The unknown sample and glass standards were mounted in a metallurgical mount, and polished (180, 320 and 600 grit silicon carbide). Mounting of very small glass particles may not be feasible. In such cases, the analysis can be performed on a fracture surface after washing the particles with nitric acid and distilled water to remove extraneous surface residue.

The polished samples were sputter coated with carbon.

Standards. The standards were commercial glasses that had a range of composition for the major elements, *i.e.*, sodium, magnesium, aluminum, potassium and calcium. The composition of the standards was determined by X-ray Fluorescence.

Quantitation

An EDS spectrum was acquired for the unknown sample and each of the standards under identical conditions of specimen tilt (34°), working distance (12 mm), emission current (150 μa), and acceleration voltage (20kV). The count rate was held at 3,000 cps to avoid the 2× Si sum peak (Winstanley, 1986). The Kevex X-ray detector was operated in the Beryllium window mode.

For the sample and each standard, the peak intensity of the K alpha peak minus background was measured for each element and the concentration of each element was expressed as the percentage of the total X-ray counts collected in 300 seconds.

A standard curve was constructed for each element plotting percentage of the total X-ray counts versus the quoted percentage composition of each standard.

Table 2. Linear Regression Analysis of Calibration Data For a Typical Glass Analysis.

Regression equation	Standard Error of Estimate	Coefficient of Determination
$Na = -0.820 + 0.154\ Na_2O$	0.014	0.998
$Mg = 0.089 + 0.296\ MgO$	0.024	0.998
$Al = 0.076 + 1.109\ Al_2O_3$	0.142	0.977
$S = 0.092 + 1.403\ SO_3$	0.048	0.853
$K = 0.010 + 1.932\ K_2O$	0.056	0.992
$Ca = 1.575 + 1.533\ CaO$	0.536	0.983
$Fe = 0.004 + 0.643\ Fe_2O_3$	0.037	0.949

In the above linear regression equation, $y = a + bx$, a is the y-intercept, b is the slope of the calibration line, y is the element concentration determined by SEM–EDS and x is the element oxide concentration determined by X-ray Fluorescence.

Table 3. NBS SRM 1831, Soda-Lime Sheet Glass.

	%							
	Na_2O	MgO	Al_2O_3	K_2O	CaO	SO_3	Fe_2O_3	SiO_2[1]
Certified	13.3	3.5	1.2	0.3	8.2	0.25	0.087	73.1
SEM–EDS	14.0	3.5	1.2	0.5	8.0	Trace	Trace	72.8

[1] SiO_2 by difference

The concentration of the unknown was determined from the standard curve.

Figure 2 shows a typical standard curve for magnesium. The standard curve has good linearity. Linear regression equations, standard errors of estimate and coefficients of determination for a typical analysis are presented in Table 2. The standard curves for the major elements are considered to be good. Linearity tends to be significantly worse for the minor elements, *i.e.*, iron and sulfur.

Minor constituents of glass can be useful in distinguishing one glass from another. Strontium and rubidium have been used to characterize glass-making plants in the U.K. (Hickman, 1984) Barium and iron can also be used to distinguish container glasses. The detection limit for BaO and Fe_2O_3 by SEM–EDS is approximately 0.03%.

In Table 3 the elemental analysis of glass obtained by SEM–EDS is compared to the certified composition of a National Bureau of Standards (NBS) glass standard reference material (SRM). Certified values are the average composition of the glass obtained by several independent methods. The SRM is No. 1831, soda lime sheet glass. The SEM–EDS value is in close agreement to the NBS value for the major elements.

X-ray Fluorescence

The chemical composition of soda–lime–silicon glasses was determined using a Philips PW1400 sequential X-ray fluorescence spectrometer. This is a crystal spectrometer that utilizes rhodium primary X-rays and pentaerythritol-tetrakis (hydroxymethyl)-methane (PET), lithium fluoride LiF (200) and thallium hydrogen phthalate (TLAP) analyzing crystals (Bertin, 1978). The unit was operated in a vacuum at a constant 2,500 watts of power, *i.e.*, 50 kV and 50 mA.

A set of 80 glasses was used to establish a calibration of the instrument. These include the available NBS glasses. The remaining glass standards were carefully characterized in triplicate using atomic absorption, and the results were used in the X-ray calibration.

Background corrections and line overlap corrections were made where necessary and inter-element effects were accounted for using a Rasberry–Heinrich calculation model (Bertin, 1978).

Samples and standards were all 3.2 cm in diameter, and an intensity ratio technique was utilized to minimize effects of long term drift on the calibration.

X-ray Diffraction (XD)—(Cullity, 1956). A Siemens D500 X-ray diffraction system was used to analyze glass-like particles found in canned peas. The compounds identified represented the best match to standards in the Joint Committee on Powder Diffraction Standards (JCPDS) diffraction file data base.

XD Operating Conditions. Cu k alpha target X-ray Tube; 1.54051 Lambda; 40 kV; 30 mA; Scintillator Detector.

Chemical Analysis

Sulfate, Chloride, Ammonia

A Dionex Ion Chromatograph, Model 2010i, (Dionex Corp. Sunnyvale, CA) equipped with a conductivity detector was used to analyze the chloride and sulfate content of cooling water and the ammonia content of particles found in canned peas.

Sample Preparation. The cooling water was filtered through a 0.45 μm filter before analysis. The particles were solubilized in 6M hydrochloric acid prior to analysis.

Analysis Conditions

Chloride and Sulfate.
Column: Dionex AS4A analytical column and AG4A Guard Column
Eluant: 0.77 mM $NaHCO_3$ and 1.00 mM Na_2CO_3
Suppressant: 0.025 N H_2SO_4
Flow Rate: 2.5 mL/min
Operating Pressure: approximately 1,000 psi (6.9×10^6 Pa)

Ammonia.
Column: Dionex CS1 analytical column and CG1 guard column
Eluant: 5 mM HCl
Suppressant: Packed Bed Cation Suppressor
Flow Rate: 2.5 mL/min
Operating Pressure: approximately 500 psi (3.4×10^6 Pa)

Sulfur Dioxide. The sulfur dioxide content of canned fruit nectar and canned fried apples was determined using the Monier-Williams procedure (with modifications) for sulfites in foods (FDA, 1986). This is the Association of Official Analytical Chemists (AOAC) official final action method for sulfites.

Hydrogen Sulfide. Hydrogen sulfide in canned fruit nectar and canned fried apples was qualitatively determined by its characteristic "rotten egg" odor and by the brown-black stain, *i.e.*, PbS, which formed on a piece of lead acetate-treated filter paper when the paper was held above an acidified sample of the product.

Trace Metals. The trace metal content of canned fried apples was determined using Inductively Coupled Plasma Spectrometry (ICP). The ICP used was an Instrumentation Laboratories Plasma 200 sequential unit with an air path and vacuum monochromator allowing operation over the range of 160–800 nm. Sample flow rate was 1.0 mL/min (peristaltic pump) into a cross-flow nebulizer.

Results and Discussion

Part I. Corrosion Investigations

Normal Corrosion Process. Internal can corrosion is basically electrochemical in nature (FAO, 1986). Inside food cans in a solution of fruit acids, tin forms the anode whereas steel forms the cathode. This is either due to the high hydrogen overpotential of tin or the formation of stable stanno complex anions.

The normal corrosion process inside tin cans is slow, even detinning of the tinplate surface. Tin reacts with the product to produce stannous ions and electrons. Electrons combine with hydrogen ions from the product producing hydrogen gas. Hydrogen either accumulates in the can headspace or diffuses through the container walls. When the cans eventually fail after many years of storage, it is either due to a hydrogen swell or a perforation. A hydrogen swell occurs when hydrogen generated by corrosion causes swelling of the ends. Perforations are pin holes through the container metal caused by localized corrosion of iron.

The outside of the tin can should retain its shiny appearance throughout the shelf life of the canned product.

Case History No. 1—External Rusting

Each year, the industry experiences a few external rusting problems. Outside corrosion of cans may cause the entire lot of canned food to be unmarketable. There are technical services available

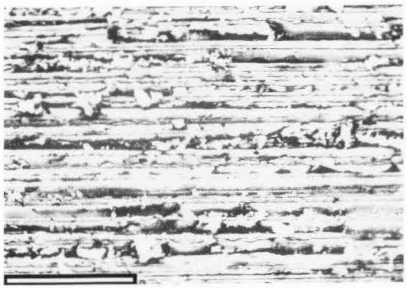

Figure 3. Backscattered electron image of the tinplate from a can that rusted. (Acceleration voltage=20kV, Bar=100 μm)

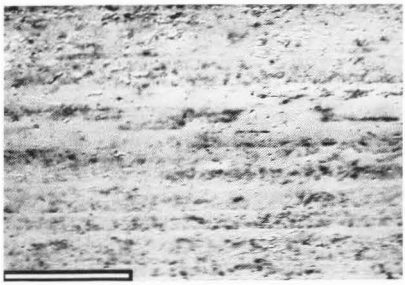

Figure 4. Backscattered electron image of the tinplate surface from a can that did not rust.
(Acceleration voltage=20kV, Bar=100 μm)

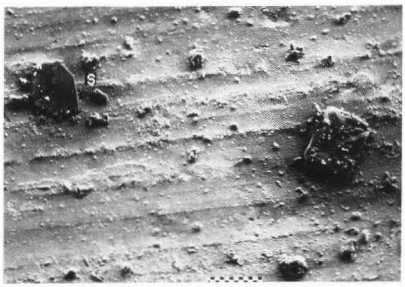

Figure 5. Approximately 30 μm particles found in and around rusted areas on tinplate containers.
(Acceleration voltage=10kV, Bar=30 μm)

to remove external rust from canned goods. The worth of using these services depends largely on the quantity of cans that are rusted. External rusting is normally a cosmetic problem and not a food quality problem. However, in severe cases of rusting, the can may perforate from the outside causing the product to spoil. External rusting of tinplate cans may be caused by a number of factors (FAO,1986):

1. Hard wiping of side seams at the time of can manufacture.
2. Scratches on the tin coating.
3. Use of rusty retort baskets.
4. Product residue on the cans.
5. Product residue from leaking cans.
6. Excessive chlorine or salts in cooling water.
7. Salt content of label paper.
8. Salt content of boxboard.
9. Moisture from labels and boxes.
10. Poor storage conditions.
11. Location of storage.
12. Storage in a corrosive atmosphere.

In Case History No. 1, discontinuities of tin on the external surface of the tinplate in combination with salts dissolved in the cooling water help explain an external rusting problem.

Description of Problem. An external rusting problem developed in an entire pack of tomato sauce. Varying degrees of brown rust deposits formed on the approximately 0.5 million cans in the pack. The pack was produced over the 1986 canning season. Rusted cans and control samples that did not rust were submitted for analysis. The control samples were produced over the same time period as the rusted samples, and would have been subjected to the same commercial canning process as the rusted samples (filling, closing, thermal sterilization, cooling in cooling water treated with a bactericide, rinsing, drying and warehouse storage). Both the control and the rusted cans had an outside tin coating weight of 0.25 pounds per basis box (5.6 g/m^2 of tinplate). This is the usual tin coating weight used on the outside of tinplate food cans. The cans that rusted were supplied by one can supplier, while the control cans were supplied by another can supplier. The cans used for the pack were made from at least two but probably several different batches of tinplate.

Tin Discontinuity

Backscattered electron images representative of the tinplate surface of a rusted and control sample are presented in Figures 3 and 4. The surface of the tinplate that rusted is rougher and the tin coating is more discontinuous than the surface of the control tinplate. The dark areas in the figures are either exposed tin–iron alloy, $FeSn_2$, or exposed base steel. Steel exposure is needed for rusting to occur, and it appears that the plate that rusted should have a higher tendency to rust because it has more exposed steel. The difference in appearance of the two surfaces is probably due to a difference in the surface finish imparted to the plates at the time of manufacture. Tinplate is available in a variety of surface finishes which depend on the texture or roughness of the steel base and on whether the tin coating is flow-melted. The surface roughness of the steel base is obtained by the use of work rolls of controlled surface texture during the final stages of temper-rolling the steel (AISI, 1979; Britton, 1975). The end use of the plate determines the type of surface finish required.

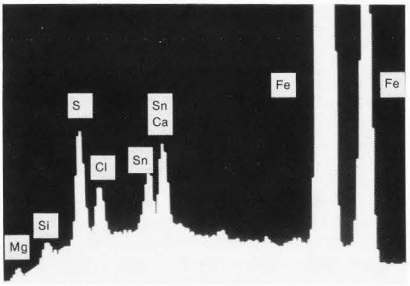

Figure 6. EDS spectrum of a typical rusted area.

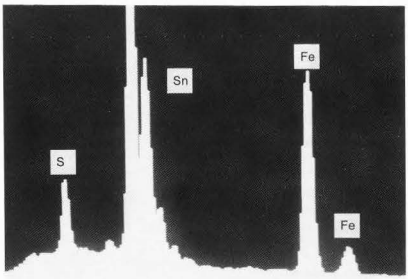

Figure 7. EDS spectrum of a black stained area in the headspace area of the body wall of a 12-ounce (355 mL) can that contained fruit nectar.

Dissolved Salts in the Cooling Water

The outside surfaces of the rusted and control samples were examined using light microscopy. At 200–1,000× under normal reflected light many particles were present on both types of samples. No differences between the samples were evident. Under polarized light bright particles were visible on the black background of the tin surface of both samples. The particles were particularly noticeable in the rusted areas. The particles were also present in some of the grooves or voids on the rusted plate where the tin coating was discontinuous. Several rusted cans had this same pattern of particle distribution.

The particles were examined by SEM–EDS. Two types of particles were present. Particles about 30 μm in diameter (Figure 5) contained mainly sulfur. Smaller particles about 10 μm in diameter contained sulfur and chlorine. Figure 6 shows an EDS spectrum of a typical rusted area. It contains both sulfur and chlorine in addition to magnesium, silicon, calcium, tin and iron. It appears that the particles on the surface are in the rust.

A sample of water that was used to cool the cans after thermal processing was analyzed for anions using ion chromatography. The chloride concentration found, *i.e.*, 77 ppm, was within acceptable limits, but the sulfate concentration of 366 ppm was quite high.

Corrosive neutral salts are often present in waters supplied for processing and cooling. The most objectionable of these are chlorides and sulfates which frequently cause external rusting of cans when their concentration approaches 150 ppm. Under some conditions neutral salts have caused rust at levels of under 100 ppm (Murray, 1951). The levels of chloride and sulfate cited in this reference are not an industry standard but are based on one can supplier's investigations of many external can rusting problems. The level of sulfate in the cooling water, 366 ppm, is excessive and could promote external rusting.

What appears to have happened in this external rusting problem is that cooling water adhering to the cans evaporated leaving chloride and sulfate salts deposited on the surfaces of the cans. The salts are probably hygroscopic, drawing and retaining moisture from the air during storage. The moist salts reacted with the exposed steel on the plate where discontinuities in the tin coating were numerous, thus causing rust. The control cans had significantly less exposed base steel and no rust developed.

Case History No. 2—Sulfur Related Discoloration and Pitting Corrosion of Cans Containing Fruit Nectar

Corrosion problems sometimes occur inside tin cans which result in an a unsightly black, brown or purple discoloration of the food contact surface. Headspace detinning (Board and Steele, 1975), tin sulfide staining, iron discoloration problems (Britton, 1975), milk plate staining and asparagus staining (Carter and Helwig, 1969 and Laubscher, 1963) are typical examples of container discoloration problems. These problems are cosmetic and do not normally lead to early pack failure. They are costly because they often lead to consumer complaints.

In Case History No. 2 the presence of sulfur dioxide (SO_2) in canned fruit nectar appears to explain a container discoloration problem. Hydrogen sulfide produced from the SO_2-tinplate reaction helps to explain an associated off-odor problem. Unlike the usual cosmetic problem, Case History No. 2 resulted in a pack failure because of the off-odor that was produced.

Description of Problem. A black discoloration developed in the can headspace areas of 12-ounce (355 mL) cans that contained a fruit nectar drink. Forty-six-ounce (1,360 mL) samples produced at about the same time as the 12-ounce (355 mL) samples were free of the problem. The black deposits loosely adhered to the surface of the tinplate unlike a tin sulfide stain that tightly adheres to the tin crystal grains. The 12-ounce (355 mL) samples had a distinct rotten egg off-odor.

The tinplate under the black deposits had undergone substantial pitting corrosion, *i.e.*, localized corrosion attack of the base steel. Pitting corrosion was also observed on the can body in contact with the product particularly at the beads. A can which is re-enforced by having ring indentations (beads) around the can body is called a beaded can. Additional strength is built into a can by the use of a beaded construction. The pits on the can body below the can headspace areas were not as deep as the pits in the can headspace areas.

The problem developed in the 1985 packing season. Both the 12 and 46 ounce (355 and 1360 mL) samples had an identical tin coating weight, 0.75 pounds per basis box (16.8g/m^2 of

tinplate) on the inside body of the cans. The food contact surface of the can ends was lacquered and was free of corrosion.

The black stain covered an area of approximately 1.6 cm^2. A section of the plate covered with approximately 0.8 cm^2 of black deposit was examined using SEM–EDS. Figure 7 shows an EDS spectrum of a representative stained area. Sulfur is a major component of the discolored area. The product was analyzed for sulfur compounds. The problem sample contained 22 ppm SO_2 and tested positive for H_2S. Neither of these two compounds was detected in the 46-ounce (1,360 mL) sample.

The source of the SO_2 is probably the corn syrup added to the packing media. SO_2 is used as a clarification agent during the refining process of corn syrup (NCA, 1975). Levels of 20–30 ppm SO_2 in corn syrups are sometimes encountered.

Levels of SO_2 need to be carefully monitored because SO_2 is known to be a corrosion accelerator of plain tinplate cans packed with acid fruits (NCA, 1975). It promotes both rapid detinning and pitting corrosion.

Effects of SO_2 on Tinplate

In acid products, SO_2 accelerates detinning by functioning as an oxidizing agent and an acid (McKay and Worthington, 1936). As an oxidizing agent, SO_2 reacts with nascent hydrogen to produce water and H_2S. At the same time the sulfurous acid produced by the combination of SO_2 with water liberates a considerable quantity of hydrogen ion.

The other type of corrosion that SO_2 promotes in acid fruits is pitting corrosion or iron solution with no detinning (Cheftel and Monvoisin, 1954). According to these authors, SO_2 reacts with the tinned surface forming a brown or purple tin sulfide stain, SnS, (Mantell, 1970) and reduces the surface area of anodic tin. Once the tin surface becomes passivated by this film formation its action as a sacrificial anode, protecting the steel base, disappears and rapid iron solution occurs. The presence of 10–20 ppm SO_2 in the product is reportedly sufficient to initiate rapid dissolution of iron, formation of ferrous sulfide and blackening of the product.

In Case History No. 2 a pitting corrosion mechanism leading to the formation of a black iron sulfide deposit appears to be the major corrosion mechanism. Iron sulfide deposits would not be stable in acid products at pH 3–4 (Britton, 1975), explaining why no deposits were present on the can surfaces in contact with the product. The iron sulfide would most likely decompose in the product to produce the observed H_2S which in turn would cause the observed off-odor. However, in the can headspace the pH of condensed volatile matter may be above pH 6 and this would allow the observed iron sulfide deposits to form (Britton, 1975).

Case History No. 3—Pitting Corrosion of Cans Containing Fried Apples

Most acid foods packed in plain tinplate cans corrode them by dissolving tin with little attack on the base steel. Instances sometimes occur where the tin fails to protect the steel, the steel base develops corrosion pits, and there is either little or no attack of the tin. Such packs fail early as a result of hydrogen swells or perforations.

Kamm and Willey (1961) recognized two types of pitting corrosion of tinplate: (1) partial detinning accompanied by moderate pitting; and (2) pitting with no detinning. Corrosion by partial detinning and pitting usually occurs in cases of an abnormal product or an inferior base steel. The authors indicate that certain types of base steel are susceptible to this type of corrosion in an abnormally corrosive pear nectar packed in plain tinplate cans. Severe pitting with no visible detinning has been observed by these authors in strawberry carbonated beverages formulated with phosphoric acid packed in enamelled tinplate cans.

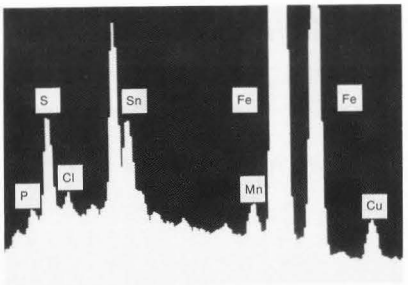

Figure 8. EDS spectrum of a corrosion pit on the inside body wall of a swollen can that contained fried apples.

Case History No. 3 is an example of an internal can corrosion problem involving a pack failure by a partial detinning and pitting corrosion mechanism. Copper, oxygen and a container beading defect help to explain the cause of the problem.

Description of Problem. Sixteen ounce (454 g) canned fried apples developed hydrogen swells within eight months after packing in either November 1985 or January 1986. At a minimum, six packing dates were affected by early corrosion. The cans were made from plain tinplate bodies and lacquered tin-free steel ends.

The cans were made from double reduced tinplate and had a tin coating weight of 0.75 pounds per basis box (16.8g/m^2 of tinplate) on the food contact surface. Severe detinning and pitting corrosion was present on the body beads of the swollen cans. Pitting was also evident in the steel away from these major pitted areas. The can ends were free of corrosion.

Control canned samples that were packed around the same time as the problem canned samples and that were stored similar to the problem canned samples were obtained. One significant difference was that the control cans were manufactured by a different can supplier than the cans that swelled. The control cans had an internal organic liquid stripe over the welded side seam. The cans that swelled did not. No corrosion problem developed in the 1984 pack. Containers from the two can suppliers were also used to produce this pack. Fried apples from the 1984 pack that had been packed in cans from the two can suppliers were obtained for comparison.

Copper

Sections of the can body cut from the area of the beads and the weld were examined using SEM–EDS.

Figure 8 shows an EDS spectrum of a representative corrosion pit. Sulfur, chloride, phosphorus and manganese were

found in the pitted areas. Sulfur could have come from the product. No sulfur dioxide or hydrogen sulfide was found in the product. Chloride and phosphorus probably came from the product. The source of the manganese is probably the base steel. The maximum level of manganese permitted in tinplate is 0.6% (AISI, 1979). At this level it is difficult to detect manganese by EDS. The corrosion pit appeared to be enriched in manganese. A possible source of the manganese is manganese sulfide inclusions.

Traces of copper were detected in and around some of the pitted areas. These trace levels could not be X-ray mapped.

Copper is known to promote internal can corrosion (Hartwell, 1951; Lueck, 1974).

Copper has a higher electropositive potential than either steel or tin and if the copper is not bound by complexing agents it will displace these elements from a tin can into the food product, *i.e.*:

$$Cu^{+2} + 2e \longrightarrow Cu^{0}$$

$$Fe^{0} \longrightarrow Fe^{+2} + 2e$$

or

$$Sn^{0} \longrightarrow Sn^{+2} + 2e$$

These displacement reactions are also the basis of a test to check for metal exposure through lacquered coatings on tinplate (Britton, 1975).

The product and the containers were further examined in an attempt to locate the source of this potentially corrosion-promoting element.

Copper may enter the product through horticultural or prodct handling practices (Britton, 1975). Copper salts are ingredients in agricultural sprays, and copper may be found in various metal surfaces, *e.g.*, brass fittings and copper tubing.

Fried apples from swollen and control cans were analyzed for trace metal content using inductively coupled plasma spectrometry (ICP). The results are listed in Table 4. The manganese, iron and tin levels in the swollen sample are significantly higher than in the control sample. The difference is probably due to internal can corrosion. No copper was detected in the product, but the product cannot be entirely eliminated as the source of the copper. It may have been that

Table 4. Trace Metals in Fried Apples by I.C.P.

	Parts Per Million	
Element	**Swell**	**Control**
Potassium	705	607
Iron	262	20
Tin	202	63
Sodium	163	111
Phosphorus	89	65
Magnesium	26	28
Calcium	24	27
Strontium	0.9	0.9
Manganese	0.80	0.24
Chromium	0.24	0.10
Nickel	0.06	0.03
Copper	0.0	0.0

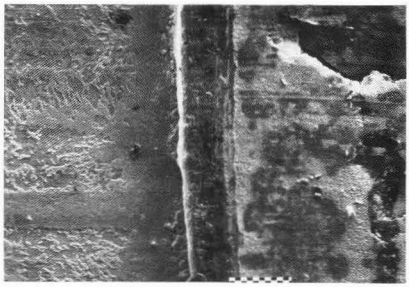

Figure 9. The welded side seam from a can that contained fried apples. Copper particulates and corrosion pits are present on the right side of this figure.
(Acceleration voltage = 20kV, Bar = 128 μm)

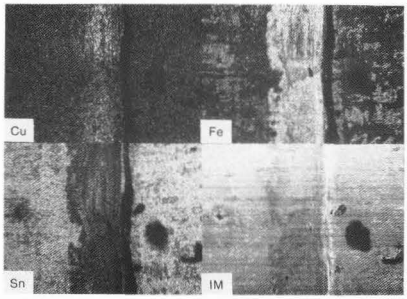

Figure 10. X-ray maps for copper, iron, tin and the image (IM) at a typical welded area.

Table 5. Glass in Canned Beets.

	%							
Sample	**Na_2O**	**MgO**	**Al_2O_3**	**K_2O**	**CaO**	**SO_3**	**Fe_2O_3**	**SiO_2[1]**
Denver	13.8	3.7	1.5	0.4	4.7	Trace	Trace	75.9[1]
Danville	10.5	3.3	1.5	0.4	5.4	Trace	Trace	78.9[1]
Light Bulb	16.2	3.4	1.4	0.4	5.0	0.1	0.05	73.4

[1] SiO_2 by difference

by the time the samples were analyzed, copper from the product may have already completely plated out on the walls of the can.

Tinplate contains traces of copper (AISI, 1979). No copper was detected in the tinplate away from the pitted areas.

Copper was found at both corroded and uncorroded areas next to the welded side seam using SEM–EDS. Figure 9 shows a section of a welded side seam. Copper particles were found on the raised side of the weld on the right in the Figure. The particles were about 1 micron in diameter. The depressions on the right in the Figure are corrosion pits.

Figure 10 shows X-ray maps for tin, copper and iron at a typical area along a welded side seam. The white areas in the maps show the distribution of tin, copper and iron. The dark areas in the iron map show the location of free tin on the tinplate surface. Copper is located on the raised area of the weld in the center of the copper X-ray map. The cans were welded with a copper wire electrode. The copper deposits are most likely residues from the wire welding operation. Although the control cans had copper deposits at the weld copper was not available for reaction with the product because the organic liquid stripe over the weld fully covered the side seam including the copper deposits. The previous year's pack used unstriped cans with exposed copper at the weld. These cans did not manifest significant pitting corrosion. It appears that the presence of exposed copper at the weld does not by itself result in pitting corrosion. The source of copper in the corrosion pits and its role in this and similar pitting corrosion problems in industry are under investigation.

Headspace Volume. Headspace volume is the volume of the air space between the product and the can end. Headspace volume is closely related to the amount of residual air in the can at the time of closing. Headspace volume varied between 17–40 mL for all samples. An average commercial headspace for this size can would be close to 20 mL so that headspace volume and therefore air content is excessive overall. Air is a corrosion accelerator for canned foods in general (Hartwell, 1951). Kohman (1923) reported that oxygen caused perforations in enamelled cans containing apples. The excessive air content of the fried apples most likely contributed to the corrosion problem.

Beading Defect. Visual inspection of the outside of the swollen cans revealed the presence of many depressions in the plate in the valleys of each of the six beads on the body of the cans. Examination of these indented areas using SEM showed that many of them were actually fractures in the can wall about 1mm in length. Severe pitting corrosion was present on the inside of the can at these fractures. The indented areas in the plate may be the result of a beading defect which occurred when the cans were fabricated. The control cans did not have this defect.

It appears that the cause of the pitting is not related to any one factor but is likely due to a combination of factors, *i.e.*, copper, excessive oxygen and a beading defect.

Part II—Glass Particles

Glass particles found in three different canned food items were submitted by the food packers to the NFPA for analysis using SEM–EDS. The packers were concerned that product tampering, *i.e.*, intentional contamination of the food, was the source of the glass. The details of the investigations by the food companies are confidential. It may have turned out that the source of the glass was accidental contamination rather than product tampering.

The first incident involved glass fragments in canned beets. Staff at two hospitals, *i.e.*, in Denver, Colorado, and Danville, Illinois discovered the glass fragments in canned beets and immediately notified the food packer. The largest fragment was approximately 25.4 mm × 19.1 mm in area and approximately 1 mm thick. The chemical composition of the two fragments are in close agreement (Table 5). The fragments would appear to have come from a singular source. The fragments were curved and they looked as if they came from a light bulb. A typical composition of a light bulb is given in the Table for comparison (ACS, 1986). The composition of all three samples is similar and the results suggest that the fragments may be from a light bulb. Glass fragments were found in unopened cans. This would suggest that the contamination occurred at the food packing plant.

The second incident occurred in canned tuna. The particles were approximately 5 mm × 4 mm × 2 mm in size. The particles closely agree in chemical composition (Table 6). Possible sources are window glass (ACS, 1986) and tableware glass (Tooley, 1984). In initial testimony the claimant said that the glass particles were from two cans of tuna with different lot codes. When the claimant learned of the SEM–EDS results he changed his story. The case was dismissed.

The glass particle in Figure 11 was found in a can of meat. This is the third product contamination incident. The particle is about 3 mm wide. The center of the particle appeared to be a white ceramic material. This is a backscattered electron image of the particle. The white outer section of the particle is highest in atomic number. The gray material in the center is next highest in atomic number. The substance inside the black circle is lowest in atomic number.

Figure 12 shows the EDS spectrum for the particle. The particle was analyzed with the X-ray detector in the ultra thin window mode. The particle contains oxygen, sodium, aluminum, silicon, lead, chlorine, potassium and zinc.

Figure 13 shows X-ray maps for some of the elements. The outer parts of the particle contain lead. Silicon is located throughout the matrix except in the dark circular area. The circular area is where the chlorine is located. The center wedge in the particle contains zinc.

Glass-like Particles. Particles have been examined that look like glass but in fact are not glass.

Table 6. Glass in Canned Tuna.

	%							
	Na_2O	MgO	Al_2O_3	K_2O	CaO	SO_3	Fe_2O_3	SiO_2[1]
Particle 1	13.2	3.9	1.5	0.9	6.2	Trace	Trace	74.3[1]
Particle 2	14.8	4.2	1.3	1.0	6.8	Trace	Trace	71.9[1]
Window	12.8	3.8	1.4	0.7	8.2	0.3	0.1	72.7
Tableware	14.6	3.8	1.2	0.3	5.3	0.2	0.04	74.6

[1] SiO_2 by difference

The particle in Figure 14 was found in a tomato powder. It's about 3 mm in diameter. The particle was analyzed with the detector in the Beryllium window mode. Silicon is the sole constituent of the EDS spectrum. The particle was insoluble in nitric acid. Silicon dioxide was added to the tomato powder as an anticaking agent. It seems likely that the particle is silicon dioxide but this needs to be confirmed.

The particle in Figure 15 is from a crop of particles that was found in a can of peas. The particles are approximately 0.5 mm long and 0.2 mm wide. The particles dissolved in hydrochloric acid. They are not glass.

Figure 16 shows the EDS spectrum for the particle. The X-ray dectector was used in the ultra thin window mode. The particle contains oxygen, magnesium, phosphorus and potassium. The particles were analyzed by ion chromatography and found to contain substantial quantities of ammonia. X-ray mapping showed that the elements are uniformly distributed in the particle and not localized in any given area.

Particles from a separate incident in canned peas were found to contain calcium in addition to the above elements. The particles were analyzed by X-ray diffraction (XD). XD analysis indicated the presence of several phases. The best fit of the data indicated the presence of:

(1) $K_5P_3O_{10}$.$2H_2O$;
(2) $(NH_4)2MgP_2O_7$.$4H_2O$;
(3) $Mg_3(PO_4)_2.4H_2O$;
(4) Ca $Mg(CO_3)_2$; and
(5) K_2CO_3 .$1\frac{1}{2}$ H_2O.

From peak intensity measurements it appears that compounds 1 and 2 are present in the highest concentrations.

Glass-like crystals have been reported in canned seafood (NFPA, 1982). They have been identified as struvite, *i.e.*, NH_4MgPO_4 .$6H_2O$. The XD data for the particles from canned peas are not a good fit for struvite. The product was given a process to retain its natural green color. The process uses magnesium hydroxide, magnesium oxide, and magnesium carbonate (FDA, 1983). The details of the process are proprietary. The product was at the end of its shelf life and the occurrence of these crystals in canned peas is an unusual occurrence.

Concluding Remarks

Scanning electron microscopy and X-ray microanalysis in combination with food chemistry analytical methods provides a powerful tool to investigate the causes of food product/metal container interaction problems like external rusting, sulfide discoloration, detinning and pitting corrosion. SEM–EDS is also a useful technique to examine extraneous materials in food like glass that may come from product tampering or glass-like particles that may arise from chemical and physical changes in the food product.

Acknowledgement

The author would like to thank E. W. Shaffer, Brockway Inc, for supplying the standard glass samples and for his helpful suggestions on the SEM–EDS method to analyze glasses. The author would also like to thank the reviewers for their helpful suggestions in preparing the paper.

References

ACS (American Ceramic Society, Inc). (1986). Ceramic Source Book '86. Annual Source Book. Smothers, W J. (Ed.) **1**, p.p. 303-306.

AISI (American Iron and Steel Institute). (1979). Steel Products Manual (Tin Mill Products) Washington, D.C. p.p. 23, 21, 14.

Beese, R E, Ludwigsen R J. (1974). 1. Trends in the Design of Food Containers. Gould, R F. (Ed.). Advances in Chemistry Series 135, American Chemical Society. Washington, D.C. p.p. 1-7.

Bertin E P. (1978). Principles and Practices of X-ray Spectrometric Analysis. Plenum Press, New York-London. p.p. 689-690, 982-999.

Board P W, Steele R J. (1975). Diagnosis of Corrosion Problems in Tinplate Food Cans. Division of Food Research Technical Paper No. 41. Commonwealth Scientific and Industrial Research Organization, Australia. p. 8.

Britton S C. (1975). Tin Versus Corrosion. International Tin Research Institute Publication No. 55. p.p. 62, 40-44, 37, 95.

Carter P R, Helwig E J. (1969). Custom Chemical Treatment of Tinplate for Specific End Uses. Metal Finishing p. 55.

Cheftel H, Monvoisin J. (1954). La Corrosion des Boites de Fer-Blanc dans l'Industrie des Conserves. Etabl, J. J. Carnaud et Forges de Basse—Indre Laboratorie de Recherches, Bull. No. 12. Paris. p.p. 66-67.

Cullity B D. (1956). Elements of X-ray Diffraction. Addison Wesley Publishers. Reading, Mass.

FAO (Food and Agriculture Organization of the United Nations). (1986). Guidelines for Can Manufacturers and Food Canners. Rome. Food and Nutrition Paper 36. p.p. 43-44.

FDA (Food and Drug Administration). (1983). 21 CFR Part 155. Canned Peas and Canned Dry Peas; Standards of Identity. Fed. Register **48** (69) p. 15241.

FDA (Food and Drug Administration). (1986). Appendix A for Part 101. Monier-Williams Procedure (with Modifications) for Sulfites in Food. Fed. Register **51** (131) p.p. 25012-25020.

Hartwell R R. (1951). Internal Corrosion in Tinplate Containers. VIII. Trace Elements 2. Copper. In Advances in Food Research. Mrak E M, Stewart G F. (Eds). Academic Press Inc. New York. Vol III, p. 355.

Hickman D A. (1984). Linking Criminals to the Scene of the Crime. Anal. Chem. **56(7)**, 844A-852A.

Kamm G G, Willey A R. (1961) The Electrochemistry of Tinplate Corrosion and Techniques for Evaluating Resistance to Corrosion by Acid Foods. First Intern. Cong. on Metallic Corrosion. Buttersworth, London. p.p. 493-503.

Kohman E F. (1923). Oxygen and Perforations in Canned Fruits. Ind. Eng. Chem, **22** (5) p.p. 527-558.

Kopetz A A. (1978). Metal Cans: Types, Trends and Selection factors. In Modern Packaging Encyclopedia and Buyers Guide, Morgan-Grampian Publishing Co. (Available from American–National Can Company, Barrington, IL)

Kreidl N J. (1984). Optical Properties. In Handbook of Glass Manufacture. Tooley F V. (Ed) Ashlee Co. Inc. New York. Vol. 2, p. 970.

Laubscher A N. (1963). In Consideration of Tinplate. Modern Packaging. p. 144.

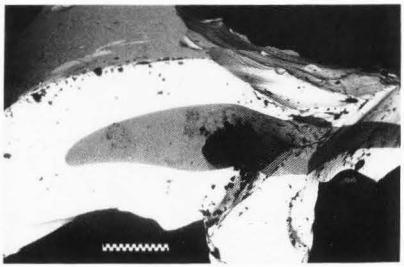

Figure 11. Backscattered electron image of a piece of glass tha was found in a can of meat. White areas contain lead. Gray areas contain zinc. The black area in the center contains chlorine. (Acceleration voltage=20kV, Bar=510 μm)

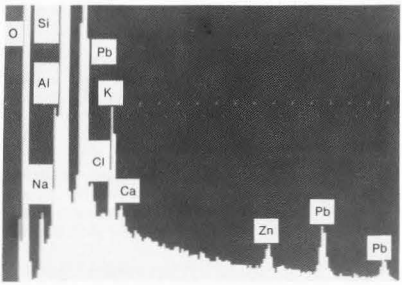

Figure 12. EDS spectrum of glass found in a can of meat.

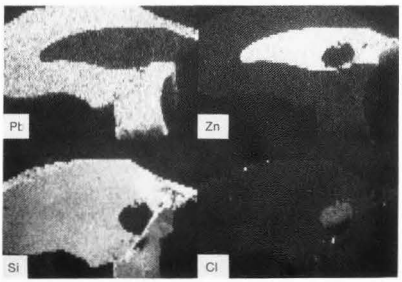

Figure 13. X-ray maps showing the distribution of lead, zinc, silicon and chlorine in a piece of glass found in a can of meat.

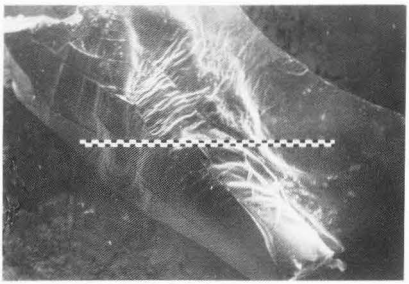

Figure 14. Particle found in tomato powder. (Acceleration voltage=24kV, Bar=2,450 μm)

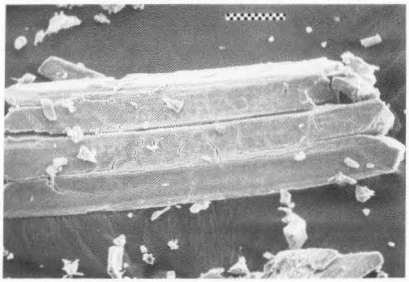

Figure 15. Particle found in a can of peas. (Acceleration voltage=20kV, Bar=102 μm)

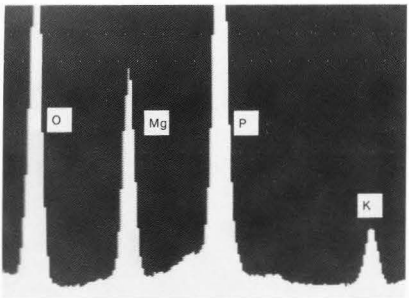

Figure 16. EDS spectrum of the particle found in a can of peas.

Lueck R H. (1974). Factors Controlling the Corrosion of Tinplate. Fifty Year Search for the Abominable Snow Man. Ind. Eng. Chem. Prod. Res. Develop. **13** (1) p.p.18-29.

Mantell, C L. (1970). Tin: Its Mining, Production, Technology and Applications. Hanover Publishing Co. New York. p. 476.

McKay, R J, Worthington R. (1936). Corrosion Resistance of Metals and Alloys. International Textbook Press. Scranton, PA. p.p. 76-77.

Murray R V. (1951). Water For Canning. Continental Can Company Inc. Res. Bulletin No. 22. p. 20.

NCA (National Canners Association). (1975). Sulfur Dioxide: Corrosion Accelerator of Plain Tinplate Containers Packed with Acid Fruits. National Food Processors Association. Washington, D.C. p.p. 1-7.

NFPA (National Food Processors Association). (1982). Crystals in Canned Seafoods. Bulletin 18-L. Washington, D.C.

Tooley F V, Knight M A, Lyle A K, Swicker V C. (1984). The Glass Preparation Process. In the Handbook of Glass Manufacture. Tooley F V. (Ed) Ashlee Co. Inc. New York. Vol. 1. p. 558.

Tooley F V. (1984). Glass Composition Design and Development (Update). In The Handbook of Glass Manufacture. Tooley F V. (Ed) Ashlee Co. Inc New York. Vol.1. p.p. 18 (1-8).

Winstanley R. (1986). The Quantitative Analysis of Very Small Fragments By X-ray Fluorescence Spectrometry. Glass International. p. 55.

Additional Reading on Corrosion

Charbonneau J E. (1978). Sulfide Black in Canned Foods. National Food Processors Association. Washington, D.C.

Farrow R P, Charbonneau J E, Lao N T, Collaborators from Seven Universities. (1969). The Tinplate Producers—CMI—NCA Research Program on Internal Can Corrosion. National Food Processors Association. Washington, D.C.

The Food Processors Institute. (1982). The A to Z of Container Corrosion. Another Path to Productivity. Washington, D.C. The proceedings contain many references on internal can corrosion.

Additional Reading on Glass and Glass-Like Particles

McCrone W C, Brown J A, Stewart J M. (1980) The Particle Atlas Vol. VI. Electron Optical Atlas and Techniques. McCrone W C. (Ed). Ann Arbor Science Publ. Inc. Ann Arbor, Michigan.

McCrone W C, Delly J G, Palenik S J. (1979). The Particle Atlas Vol. V. Light Microscopy Atlas and Techniques. Ann Arbor Science Publ. Inc. Ann Arbor, Michigan.

Discussion with Reviewers

D. N. Holcomb: What services does the National Food Processors Association offer to its members?
Author: NFPA is a scientifically based trade organization representing over 600 food processing companies and suppliers to the industry. NFPA maintains three fully staffed and equipped food science research laboratories with eight scientific research divisions: chemistry, processing, packaging, microbiology, microanalytical, sanitation, environmental and engineering. The association coordinates industry-wide research committees and serves as a liaison to the government agencies. NFPA investigates consumer claims against member companies and defends against unwarranted claims.

D. N. Holcomb: Does NFPA have an electron microscopy discussion group for its members?
Author: Yes. The mission of the group is to provide a forum to discuss non-proprietary information on microscopy methods in general to examine packaging materials, food products and related materials. Methods to troubleshoot product container interaction and product tampering problems which are described in this paper are examples of topics that are discussed.

K. Kiss: The chemical composition of the sulfur-containing deposit could be determined by a laser Raman microprobe (LRM). Did the author recommend this technique to his sponsors?
Author: No. I agree that LRM would have been a good technique to shed more light on the problem. I did recommend that my sponsor monitor the sulfate and chloride levels in his water supply and take steps to reduce high levels either by using ion exchange resins or switching to a different source of water.

K. Kiss: Did the author investigate the particles in tomato powder with a polarizing optical microscope?
Author: No. I agree that refractive index and/or crystallographic analysis could have substantiated the identification.

E.W. Shaffer: Have you used or do you feel that identification of glass particles would be aided by other types of analyses? How might thermal history or strain energy mask the usefulness of density or refractive index measurements?
Author: Besides elemental composition refractive index and density are glass properties that are helpful in distinguishing among glass types. Both properties are dependent on the thermal history of the glass. If a glass is quenched from a temperature at which it was in equilibrium a refractive index and a density characteristic of such a temperature can be frozen in and persist at room temperature. This temperature has been termed the fictive temperature (Kreidl, 1984). Values for both the refractive index and the density are lower for higher fictive temperature because there was less opportunity for the atomic arrangement to approach the low temperature state. Index differences resulting from different heat treatments of the same glass can, under practical conditions, be of the order of 0.001 or even more (Kreidl, 1984). The effects of thermal history may be removed by giving the glass a constant heat treatment before it is evaluated. Any heat treatment is satisfactory providing it is sufficiently reproducible and relatively simple and rapid (Tooley *et al.*, 1984).

FOOD MICROSTRUCTURE, Vol. 7 (1988), pp. 173-179
Scanning Microscopy International, Chicago (AMF O'Hare), IL 60666 USA

0730-5419/88$3.00+.00

THE ROLE OF β-LACTOGLOBULIN IN THE DEVELOPMENT OF THE CORE-AND-LINING STRUCTURE OF CASEIN PARTICLES IN ACID-HEAT-INDUCED MILK GELS

V. R. Harwalkar and Miloslav Kaláb

Food Research Centre, Research Branch, Agriculture Canada
Ottawa, Ontario, Canada K1A OC6

Abstract

Acid-heat-induced gels were obtained by coagulating casein micelle dispersions at 90°C using glucono-δ-lactone. The casein micelles used were isolated from raw skim milk by centrifugation, washed free of whey proteins and soluble salts, and dispersed in water or a milk dialyzate. The pH values of the gels varied from 4.7 to 6.3. A core-and-lining ultrastructure developed in casein particles coagulated at pH 5.2 to 5.5 from casein micelle dispersions in the milk dialyzate provided that β-lactoglobulin or whey proteins (10 mg/mL) were added to them prior to coagulation. Addition of β-lactoglobulin to aqueous casein micelle dispersions led to the development of a considerably less distinct core-and-lining ultrastructure of the resulting gels. Coagulated casein particles obtained from casein micelle dispersions in water or in the milk dialyzate to which neither β-lactoglobulin nor whey proteins were added, did not show the core-and-lining ultrastructure but contained void spaces inside and were covered with loosely aggregated protein on the surface.

It was concluded that both β-lactoglobulin or whey proteins and the milk salt system are essential for the formation of the core-and-lining ultrastructure in the casein micelle dispersions gelled by heating at 90°C at pH 5.2 to 5.5.

Initial paper received April 02, 1988
Manuscript received August 15, 1988
Direct inquiries to V.R. Harwalkar
Telephone number: 613 995 3722

Key Words: Acid-heat-induced milk gels, Casein micelles, Core-and-lining structure, Electron microscopy, Gelation, Glucono-δ-lactone, β-Lactoglobulin, Milk.

Introduction

Variations in the ultrastructure of casein micelles have been observed in gels obtained by coagulating milk using various acidulants. A unique 'core-and-lining' structure was observed in gels obtained by coagulating milk heated to 90°C at pH 5.5 [3, 4, 6]. This structure, observed in gels produced with many acidulants used in the study (*i.e.*, glucono-δ-lactone and citric, hydrochloric, and oxalic acids) is characterized by an outer membrane-like lining surrounding a solid core which is separated from the lining by an annular space, 50 to 80 nm wide. The core-and-lining structure is characteristic of some acid-heat milk gels, such as the Latin-American White cheese (Queso Blanco) [9] and Indian paneer [8]. It is very stable and has been observed in process cheese which contained White cheese as an ingredient [1]. The existence of this structure was demonstrated using various electron microscopy techniques such as thin-sectioning of samples embedded in a resin, replication of frozen hydrated samples, and replication of dried samples [6]. The findings were confirmed by others [M. A. Christman, personal communication].

The mechanism of the formation of the core-and-lining structure is not fully understood. However, it was observed to develop only at temperatures exceeding 70°C [4], *i.e.*, at temperatures at which the formation of a complex composed of β-lactoglobulin and κ-casein is promoted.

The objective of this study is to examine the role of protein interactions in the development of the core-and-lining structure. For this purpose, model systems involving isolated casein micelles, β-lactoglobulin, and milk dialyzate were studied.

Materials and Methods

Casein micelle dispersions

Fresh skim milk used in this study was prepared by separating cream from pooled milk obtained from the herd of dairy cows at the Central Experimental Farm of Agriculture Canada in Ottawa.

Casein micelles were prepared from the skim milk by centrifugation at 8×10^4 *g* in a Beckman Model L4 ultracentrifuge operated at 4°C for 2 h. The whey and residual fat layers were removed by suction using a Pasteur pipet. The casein micelle pellet was washed twice by dispersing it in

glass-distilled water or in a milk dialyzate at the original volume of the milk and recentrifuging it under the same conditions as mentioned above. The washed casein micelles were finally dispersed in distilled water or in a milk dialyzate for use in this study.

Milk dialyzate was obtained by dialyzing sterile distilled water closed in dialyzing tubing, 20 mm in diameter, that was suspended in a bulk milk tank at 4° to 6°C for 24 h.

Whey proteins were prepared by thoroughly dialyzing acid whey against distilled water and by freeze-drying the dialyzate. β-Lactoglobulin was of commercial origin as '3x crystallized β-lactoglobulin' (Sigma Co., St. Louis, MO, USA).

Gelation

Washed casein micelles were dispersed in distilled water or in a milk dialyzate to obtain 2% solutions. Aliquots (3 mL) of these dispersions were used either plain or following the addition of crystalline β-lactoglobulin or whey proteins (10 mg/mL). The dispersions were placed in small test tubes, heated at 90°C in a water bath, and solid glucono-δ-lactone (GDL, 7 to 30 mg) was added to them to form 0.25% to 1.0% solutions. The mixtures were stirred and held at 90°C until the protein formed gels as the result of acidulation by gluconic acid developing from hydrolysis of GDL. The protein gels were then rapidly cooled to 22°C using cold water and sampled for electron microscopy.

Electron microscopy

Small cubes (approximately 1 mm^3) of the gels under study were fixed at 22°C in an aqueous 2.8% glutaraldehyde solution for 2 h and were postfixed under similar conditions in a buffered (0.05 M veronal-acetate buffer, pH 6.75) 2% osmium tetroxide solution. Then the samples were washed with the veronal-acetate buffer, dehydrated in a graded (20%, 40%, 60%, 80%, 96%, and 100%) ethanol series, and embedded in Spurr's low-viscosity resin (J. B. EM Service, Inc., Pointe-Claire, Dorval, Quebec). Sections, 90 nm thin, were stained with uranyl acetate and lead citrate solutions and examined in a Philips EM-300 electron microscope operated at 60 kV [9].

Results and Discussion

Addition of solid GDL (0.25 to 1.0%) to casein micelle dispersions heated at 90°C produced gels having pH values between 5.0 and 6.3 and varying in characteristics (Table 1).

Plain casein micelle gels

The microstructures of the acid-heat-induced protein gels obtained from casein micelle dispersions in distilled water are shown in Figs. 1 - 3 and gels obtained from casein micelle dispersions in a milk dialyzate are presented in Figs. 4 - 6. All these figures show large, loosely aggregated-to-fused particles of casein. In some samples, there are large pores or void spaces which presumably result from the solubilization of colloidal calcium phosphate at low pH [11]. In the absence of colloidal calcium phosphate, the submicellar structures of the casein micelles collapse and fuse by hydrophobic interaction which is promoted by low pH and high temperature. However, the typical core-and-lining structures were not evident in any of these gels obtained solely from washed casein micelles (Figs. 1 to 6). Although the gels made at pH 5.5 using casein micelles dispersed in the milk dialyzate showed a compact layer at the surface of the aggregated casein particles (Fig. 5), there was no annular space that would separate the core from the lining. The formation of the compact protein layer at the casein particle

Table 1. Characterization of casein micelle gels

Dispersion in:	Protein added:	pH:	C-&-L*:	Fig.:	Note on structure:
Water	None	6.3	No	1	Corpuscular
Water	None	5.6	No	2	Void spaces
Water	None	5.3	No	3	Void spaces
Dial.**	None	6.3	No	4	Void spaces
Dial.	None	5.5	No	5	Void spaces
Dial.	None	5.0	No	6	Void spaces
Dial.	β-LG†	4.7	No	7	Like yoghurt
Dial.	β-LG	5.5	Yes	8	-------
Dial.	β-LG	5.3	Yes	9	-------
Water	β-LG	5.5	Weak	10	Corpuscular
Water	β-LG	5.3	Weak	11	Corpuscular
Dial.	WP††	5.3	Strong	12	Like in milk gels

* Core-and-lining ultrastructure
** Milk dialyzate
† β-Lactoglobulin, 10 mg/mL
†† Whey proteins, 10 mg/mL

Figs. 1 - 3. Heat-induced gels obtained from aqueous dispersions of casein micelles at 90°C at pH 6.3 (Fig. 1), pH 5.6 (Fig. 2), and pH 5.3 (Fig. 3). Casein micelle entities have vanished in all gels. Corpuscular ultrastructure composed of particles varying in dimensions (pairs of small light arrows in Fig. 1) was observed in all 3 gels. Large pores or void spaces (large light arrows) developed as pH was decreased (Figs. 2 and 3). Minute dark particles in Fig. 2 (small dark arrows) are an artefact (probably a glutaraldehyde-osmium tetroxide complex [10]).

Figs. 4 - 6. Heat-induced gels obtained from dispersions of casein micelles in a milk dialyzate at pH 6.3 (Fig. 4), pH 5.5 (Fig. 5), and pH 5.0 (Fig. 6). Large void spaces (light arrows) in compact casein particles are filled with loosely aggregated protein. Similar protein may be observed on the particle surface (small dark arrows). Casein gels obtained at pH 5.5 (Fig. 5) have a compact protein layer (large dark arrows) at their surface. Corpuscular ultrastructure composed of particles smaller than 0.1 μm in diameter is particularly evident in gels made at pH 5.0 (pairs of small light arrows in Fig. 6).

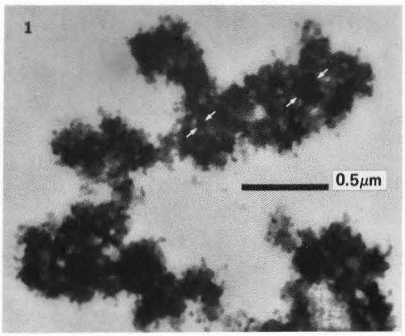
1
0.5μm

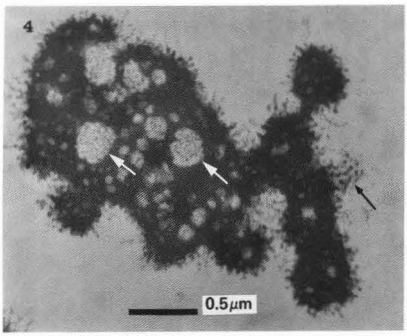
4
0.5μm

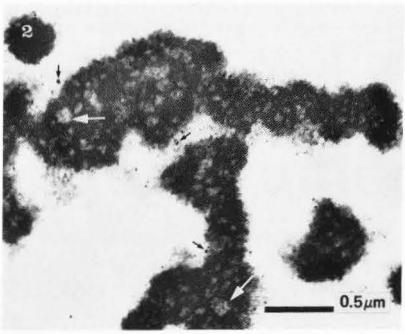
2
0.5μm

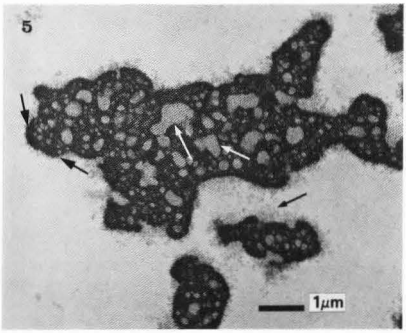
5
1μm

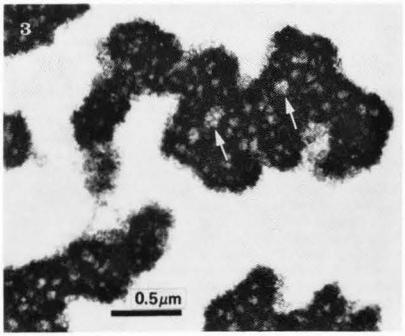
3
0.5μm

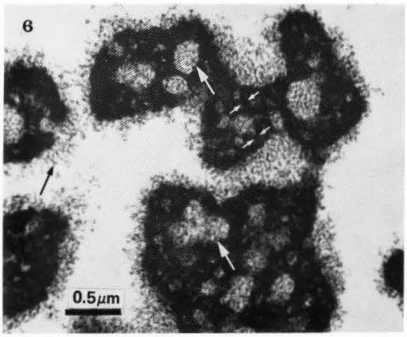
6
0.5μm

surface may be linked to the dissociation and reassociation of casein micelles observed by Heertje et al. [5]. As pH is further lowered to 5.5, β-casein is released from the micelles [13]. An increase in non-sedimentable caseins and a decrease in colloidal calcium phosphate are also observed at pH 5.5 [11].

Changes in the mineral balance caused by heating may also contribute to the deposition of casein on the surfaces of the altered casein micelles. As the temperature is increased, soluble calcium phosphate precipitates. This precipitation lowers pH possibly to the point of minimum Zeta-potential of β-casein to approximately pH 5.2 and causes the precipitation of β-casein on the periphery of the caseinate particles. The membrane-like lining is less evident in aqueous dispersions than in the milk dialyzate dispersions. There is very little soluble calcium phosphate in the aqueous dispersions and pH changes due to heating are presumably less extensive.

Casein micelle gels containing β-lactoglobulin or whey proteins

The microstructures of gels obtained by heating dispersions of casein micelles to which 1% of β-lactoglobulin was added, are shown in Figs. 7 to 11. Gels obtained from casein micelles dispersed in milk dialyzate are featured in Figs. 7 to 9 and gels obtained from casein micelles dispersed in distilled water are shown in Figs. 10 and 11. The microstructure varied depending on the final pH value of the gels after heating and on the medium in which the casein micelles had been dispersed. At pH 4.7, the gel network of fused casein micelles is similar to that of skim milk gels heated at that pH as observed earlier. At pH 5.2 or 5.5, the typical core-and-lining structure is evident (Figs. 8 and 9) though not as clearly as in the skim milk gels [3, 4]. The typical core-and-lining structure was also evident when the dispersions of casein micelles in milk dialyzate were heated in the presence of whey proteins at pH 5.3. Fig. 12 shows the structure to be well developed. However, micrographs of gels obtained by heating aqueous dispersions of casein micelles with β-lactoglobulin at pH 5.3 and 5.5 (Figs. 10 and 11) showed the core-and-lining structure to be developed less distinctly. It may be assumed, therefore, that the presence of either β-lactoglobulin or whey proteins in conjunction with the milk salt system is essential for the development of the typical core-and-lining structure. It was observed that heating of casein micelle dispersions with the milk salt system in the absence of β-lactoglobulin or whey proteins did not lead to the development of the core-and-lining structure (Figs. 4 to 6).

Earlier work [4] has shown that the heating of skim milk, which contained β-lactoglobulin and the milk salt system, at pH 5.5 and at temperatures higher than 70°C was essential for the formation of the core-and-lining structure to take place. It is well known that heating at temperatures above 70°C promotes the formation of a complex between β-lactoglobulin and κ-casein. The formation of the core-and-lining structure is thus associated with the existence of that complex and the presence of the milk salt system.

Since pH of 5.2 to 5.5 is critical to the development of the core-and-lining structure, it may be assumed that the properties of casein micelles at this pH are very important. In this pH range, casein micelles have the optimal voluminosity or hydrodynamic volume, high percentage of non-sedimentable casein, and a reduced concentration of colloidal calcium phosphate. These phenomena have been linked to the removal of the colloidal calcium phosphate and some casein and swelling of the residual micelles [11]. The heat-induced interaction between β-lactoglobulin and κ-casein results in the development of filamentous appendages [2, 7]. Calcium ions enhance this interaction [12] which partly explains the importance of the milk salt system for the formation of the core-and-lining structure. The caseins, particularly β-casein, dissociated from the micelle during the heat treatment precipitate on the protruding filamentous appendages to form a lining and leave an annular space between the casein core and the lining formed. These considerations based on the data presented in this paper are consistent with the model proposed earlier [4] to illustrate the mechanism of the formation of the core-and-lining structure. The hypothesis that the core-and-lining structure may be the result of differences in contraction of the different proteinaceous materials during redeposition of dissociated caseins [5] cannot be supported by the present work. The micrographs in Figs. 1 to 6 produced in the absence of β-lactoglobulin do not show the contraction behaviour mentioned above to result in the formation of the core-and-lining structure.

Acknowledgments

Skillful technical assistance provided by Mrs. Paula Allan-Wojtas and Mrs. Bernadette Boutin-Muma is acknowledged. The authors thank Dr. H. Wayne Modler for useful suggestions. Electron Microscope Unit, Research Branch, Agriculture Canada in Ottawa provided facilities. Contribution 772 from the Food Research Centre.

Figs. 7 - 9. Heat-induced gels obtained from casein micelle dispersions in a milk dialyzate in the presence of added β-lactoglobulin (10 mg/mL) at pH 4.7 (Fig. 7), pH 5.5 (Fig. 8), and pH 5.3 (Fig. 9). At pH 4.7, the protein network resembles that of yoghurt [2, 7, 10]. The core-and-lining ultrastructure developed in gels made at pH 5.5 and 5.3 (arrows).

Figs. 10 and 11. Heat-induced gels obtained from aqueous casein micelle dispersions containing β-lactoglobulin (10 mg/mL) at pH 5.5 (Fig. 10) and pH 5.3 (Fig. 11). The core-and-lining structure developed at pH 5.3 is less distinct than at pH 5.5 (large dark arrows). Compact particles approximately 0.1 μm in diameter (pairs of small light arrows) are connected with each other by loosely aggregated protein (small dark arrows).

Fig. 12. Heat-induced gel obtained at pH 5.3 from casein micelles dispersed in a milk dialyzate which contained whey proteins. The core-and-lining ultrastructure (arrows) is well developed and similar to that found in milk gels [3, 4].

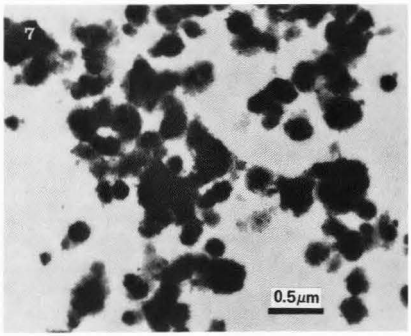
7
0.5μm

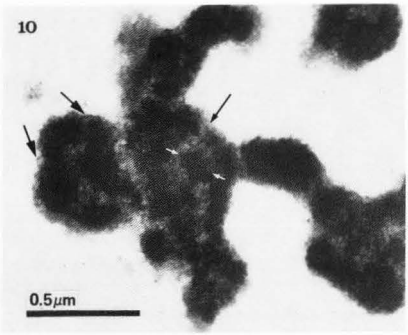
10
0.5μm

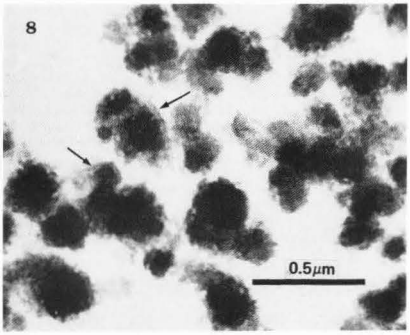
8
0.5μm

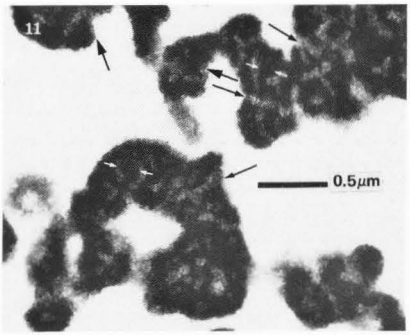
11
0.5μm

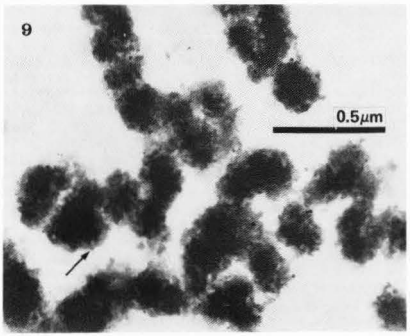
9
0.5μm

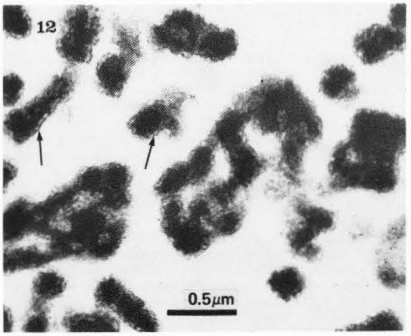
12
0.5μm

References

1. Carić M, Kaláb M. (1987). Processed cheese products. In: Cheese: Chemistry, Physics and Microbiology. Vol. 2. PF Fox (ed.), Elsevier Applied Science Publishers Ltd., New York, NY, USA, 339-383.
2. Davies FL, Shankar PA, Brooker BE, Hobbs DB. (1978). A heat-induced change in the ultrastructure of milk and its effect on gel formation in yoghurt. J. Dairy Res. 45, 53-58.
3. Harwalkar VR, Kaláb M. (1980). Milk gel structure. XI. Electron microscopy of glucono-δ-lactone-induced skimmilk gels. J. Texture Stud. 11, 35-49.
4. Harwalkar VR, Kaláb M. (1981). Effect of acidulants and temperature on microstructure, firmness and susceptibility to syneresis of skim milk gels. Scanning Electron Microsc. 1981; III:503-513.
5. Heertje I, Visser S, Smits P. (1985). Structure formation in acid milk gels. Food Microstruc. 4(2), 255-267.
6. Kaláb M. (1980). Milk gel structure. XII. Replication of freeze-fractured and dried specimens for electron microscopy. Milchwissenschaft 35(11), 657-662.
7. Kaláb M, Emmons DB, Sargant AG. (1976). Milk gel structure. V. Microstructure of yoghurt as related to heating of milk. Milchwissenschaft 31(7), 402-408.
8. Kaláb M, Gupta SK, Desai HK, Patil GR. (1988). Development of microstructure in raw, fried, and fried and cooked paneer made from buffalo, cow, and mixed milks. Food Microstruc. 7(1), 83-91.
9. Kaláb M, Modler HW. (1985). Development of microstructure in a Cream cheese based on Queso Blanco cheese. Food Microstruc. 4(1), 89-98.
10. Parnell-Clunies EM, Kakuda Y, Humphrey R. (1986). Electron-dense granules in yoghurt: Characterization by x-ray microanalysis. Food Microstruc. 5(2), 295-302.
11. Roefs SPF, Walstra P, Dalgleish DG, Horne DS. (1985). Preliminary note on the changes in casein micelles caused by acidification. Neth. Milk Dairy J. 39, 119-122.
12. Smits P, Van Brouwershaven JH. (1980). Heat-induced association of β-lactoglobulin and casein micelles. J. Dairy Res. 47, 313-325.
13. Snoeren THM, Klok HJ, Van Hooydonk ACM, Damman AJ. (1984). The voluminosity of casein micelles. Milchwissenschaft 39, 461-463.

Discussion with Reviewers

Y. Kakuda and D. G. Schmidt: Were the mixtures heated at 90°C for any appreciable time prior to the addition of glucono-δ-lactone?
Authors: It took approximately 3 to 5 min to reach that temperature and there was no holding before glucono-δ-lactone was added.

Y. Kakuda: Were the initial pH values different for the distilled water samples compared to the dialyzates?
Authors: The initial pH values were nearly the same within 0.02 unit with the micelles suspended in water or the milk dialyzate.

Y. Kakuda: Were the final pH values determined at 90°C or after cooling to 22°C?
Authors: The final pH values were determined after cooling the milk gels to 22°C.

D. G. Schmidt: How much time was required to reach the desired pH?
Authors: We did not determine the time required to reach the final pH. However, it is known that glucono-δ-lactone hydrolyzes very rapidly in water at 90°C. The time required for gelation to take place at 90°C was usually 1 to 2 min at pH values lower than 5.7 and about 3 to 5 min at pH between 5.7 and 6.3. Heating at a higher pH required a longer time to gel the milk although the final pH value may have been reached earlier.

R. Cartwright: Did you assume that β-lactoglobulin and the whey proteins used were totally undenatured prior to gelation? If so, what effects would you expect to see if the β-lactoglobulin or whey proteins had been partially denatured prior to gelation?
Authors: Undenatured β-lactoglobulin or whey proteins were added to the micelle suspension but the heat treatment before the addition of glucono-δ-lactone denatured a considerable portion of these proteins. We have shown previously [4] that the heat treatment insufficient to denature the protein does not give rise to the core-and-lining structure. We have not added previously denatured proteins to the casein micelle suspensions because the solubility would be a problem. It would be interesting to learn how previously denatured proteins will interact with the casein micelles and whether, indeed, they would contribute to the core-and-lining structure.

D. G. Schmidt: At 4°C, a large part of β-casein dissociates from the micelles and the micelles obtained after the second washing, therefore, will have a composition differing from that of the original ones. Dispersing the micelles in distilled water will result in their disintegration, particularly if it takes much time. Will you comment, please?
Authors: We agree that the washing procedure used, particularly using distilled water, may have an effect on the composition of the washed casein micelles. The disintegration of the micelles was not expected in our work since the micelles were not stored for long periods. Prolonged storage of dilute casein micelles is known to cause their dissociation [14]. Despite this limitation, the results obtained by heating aqueous micelle suspensions at various pH values and in the presence or absence of β-lactoglobulin are valid in that they emphasize the need of β-lactoglobulin for the core-and-lining structure to develop.

Y. Kakuda: The model requires conditions where β-casein dissociates into the serum phase and, at the same time, precipitates on the appendages. Does this require a drop in pH from 5.5 (dissociation of β-casein) to 5.2 (minimum charge) or does this signify two different types of interactions

for β-casein - one interaction with the micelle and the other with the appendages?
Authors: It should be remembered that the pH of 5.5 was measured after rapidly cooling the heated samples. During heating, we envisage that the pH at the high temperature may have dropped further to possibly 5.2, *i.e.*, to a point of the minimum charge. This could be the result of the combined effect of high temperature and the precipitation of calcium phosphate. The precipitation of the caseins that dissociated from the micelles as the pH was lowered would take place irrespective of the presence or absence of the appendages on the casein micelle surfaces.

Y. Kakuda: The addition of whey proteins (and skim milk in previous studies) produced a more distinct core-and-lining structure. Does this imply some role for α-lactalbumin?
Authors: The possible contribution of whey proteins other than β-lactoglobulin to the development of the core-and-lining structure was not examined in this report. It may be worthwhile to do so.

B. E. Brooker: How could voids in the casein particles arise by solubilization of calcium phosphate? How would calcium phosphate associate into such large structures in the first place?
Authors: The cause of the void spaces in the casein particles is speculative. These voids presumably result from a number of different effects. As the pH is lowered, colloidal calcium phosphate and some caseins are removed and swelling is observed [11]. The casein particles are closer to their isoelectric point. During the gelation of these particles by heat at the lower pH, aggregation may take place through hydrophobic interactions. Steric hindrance during aggregation by fusion may also play a role.

B. E. Brooker: Why is there greater aggregation of micelles in the heat-induced gels in Figs. 10 and 11 compared with those in Figs. 8 and 9?
Authors: We have no answer for this difference. Possibly, the lack of minerals in aqueous suspensions contributes to a more extensive fusion of the casein particles during heating.

D. G. Schmidt: I have noticed that the 12 micrographs presented have been obtained at 5 various magnifications, which makes their comparison difficult. Is there any reason for such differences in magnification or would it be better to show all the micrographs on the same scale?
Authors: Our intention was to show the casein aggregates as well as the detail of the structures developed. Thus, although the images shown in Figs. 5 and 6 are similar, Fig. 5 shows the entire cluster and Fig. 6 shows the detail of void spaces and submicellar structures. In order to show the development of the core-and-lining structure in some gels (Figs. 8 to 10), a higher magnification had to be used.

D. P. Dylewski: Would the application of scanning electron microscopy (SEM) in conjunction with TEM provide additional information to help interpret the structure of core-and-lining in casein particles, or is this unnecessary?
Authors: TEM is best suited to show the core-and-lining structure, be it by staining thin sections of embedded samples or replication of freeze-fractured samples with platinum and carbon. The need to examine the interior of the casein particles in order to reveal the void annular space around the core and the small dimensions of that void space make it more difficult to study this structure by SEM.

Additional Reference

14. McGann TCJ, Donnelly WJ, Kearney RD, Buchheim W. (1980). Composition and size distribution of bovine casein micelles. Biochim. Biophys. Acta 630, 261-270.

FOOD MICROSTRUCTURE, Vol. 7 (1988), pp. 181-188
Scanning Microscopy International, Chicago (AMF O'Hare), IL 60666 USA

0730-5419/88$3.00+.00

MICROSTRUCTURE OF SHORTENINGS, MARGARINE AND BUTTER - A REVIEW

A.C. Juriaanse and I. Heertje

Unilever Research Laboratorium
P.O. Box 114
3130 AC Vlaardingen, The Netherlands

Abstract

Fat spreads are composed of liquid oil, fat crystals and water. The fat crystals in these products give the product the required consistency and stabilize the water droplets. Shortenings are water-free products, the rheology of which depends on the solid fat content and interactions between fat crystals. Size and interaction between crystals is influenced by both composition and processing. Crystals form a three-dimensional network. Recrystallization phenomena, especially formation of large beta-crystals, can create product defects like sandiness. Margarines and halvarines are water-in-oil emulsions and have a relatively simple product structure. Because of the wettability of fat crystals, part of the solids are present in the water/oil interface, and influence the stability of the emulsion. Depending on the type of application, tropical margarines, table margarines, halvarines, puff-pastry, creaming margarines, etc., the ratio of solid/liquid and water content can be varied. No essential differences exist in the microstructure of products for different applications. Butter differs in its microstructure from margarines because of different processing and raw materials. Butter still contains a number of fat globules (derived from the cream) in its final product structure. These globules are dispersed in a matrix of fat crystals and oil descending from fat globules that were broken during churning. Also the moisture is present in different forms ranging from droplets to "free moisture". Differences in microstructure can be introduced by different processing regimes.

Initial paper received September 20, 1988
Manuscript received November 30, 1988
Direct inquiries to I. Heertje
Telephone number: 31 10 4605513

Key words: Fat spreads, shortening, butter, fat crystals, crystal network, fat globule, water droplet, air, microstructure, electron microscopy

Introduction

Microstructural studies in the area of fats and fat-based spreads are becoming increasingly important. Both the dairy and margarine industries are realizing the importance of these studies, since with the knowledge of the product microstructure, a better understanding of the product properties and ways to influence these can be obtained. Initial research focussed on properties like crystal modification and overall product properties, such as product rheology. More recently, the use of new techniques such as electron microscopy (EM) in combination with well established knowledge of margarines and butter has led to a significant improved understanding of structures and their effect on product properties.

From a microstructural point of view, essentially three different structure-types can be distinguished: shortenings (100% fat), margarines and halvarines (80 and 60% fat respectively), and butter (80% fat). Both composition and processing can be used to influence the product microstructure. Margarine and shortenings not only can be composed of a relatively wide range of triacylglycerols but also the aqueous phase may contain different ingredients. The composition of butter is much less subject to change: the only compositional changes result from changes in the milk composition due to, e.g., barn / pasture feeding, level of underfeeding, stage of lactation, breed of cattle, etc. Consequently differences in butter microstructure often result from changes in processing. For margarines and shortenings the many degrees of freedom has led to a diversification of products of 100 to 40% fat, from soft high polyunsaturated fatty acids to hard puff-pastry products.

The present paper reviews the literature on the microstructure of fat spreads. Micrographs used to illustrate the microstructure of fat spreads have been obtained from the investigations by the authors.

Structural elements

Fat crystals

The formation of texture in spreads is the result of crystallization of triacylglycerols with high melting points. The crystals do not behave as single crystals, but show different types of aggregation with formation of a three-dimensional fat crystal network. The strength of this network is influenced by many compositional and processing parameters (6).

Triacylglycerols crystallize in four different modifications: sub-α, α, β' and β (8). The first two

modifications, sub-α and α, are unstable and therefore do not exist in spreads. The β' modification is stable but its crystal lattice is less well ordered than the β modification. Of all modifications the β modification has the highest ordering and consequently the highest melting point. In most spreads different raw materials are blended to arrive at the desired overall crystallization and melting behaviour. As a consequence the triacylglycerol composition of the blends is rather complicated. This implies that in spreads the β modification does not occur very often; the β' modification is the predominant one. Fat crystals can be either needles (Fig. 1) or platelets. The β modification is frequently correlated with structural defects: large β crystals are perceived as sandiness (1) (Fig. 2).

Fat globules

Fat globules as found in butter (Fig. 3) (14) originate from the cream. Prior to the churning process, the cream is physically ripened (i.e., the cream is cooled to such an extent that fat crystallization in the oil droplets occurs). Depending on their strength these fat globules will survive the churning process (19).

The fat globule in cream is covered with a fat globule membrane, whereas in butter parts of the membrane may be removed as a result of churning. The outside of this membrane is a hydrophilic, proteinaceous layer of complex composition (14) (Fig. 4). The periphery of the globule is formed by an approximately 0.1 - 0.5 μm thick crystalline shell (15). Different opinions exist about whether this crystalline shell is composed of high melting β crystals (15, 18), which concentrate in the oil/water (O/W) interface as a result of ripening conditions and crystallization at the interface (2). Alternatively a shell would result crystals that are formed randomly in the oil droplet during ripening and subsequently transported to the O/W interface as a result of deformation during churning (24). The average diameter of globules in butter is 3 μm.

Networks

Fat Spreads derive their consistency from interactions between fat crystals which form a three dimensional network (Fig. 5a and 5b). The nature of the interactions between the fat crystals determines the type of network structure and the rheology of the product. Quite a number of publications deal with rheological properties of fat spreads (for a review see reference 3).

Many aspects are related to the amount and the nature of the interaction between fat crystals (6):

- the hardness of a spread depends on the amount of fat crystals;
- blend composition will influence the molecular arrangement in crystals and thus the strength of interactions between crystals;
- slowly crystallizing blends will continue to crystallize after packaging, which favors the formation of a strong network;
- high crystallization speeds give rise to soft and overworked products.

Two types of bonds are assumed for crystal-crystal interactions (5):

- primary bonds, which result from crystals growing together at some points. These bonds are "irreversible", i.e., do not re-form after rupture;
- secondary bonds, which are (weak) London-Van der Walls forces, which are "reversible", i.e., do re-form after rupture.

Primary bonds are considered to be responsible for the hardness of products, whereas secondary bonds contribute little to consistency.

In other works (21) such a distinction between primary and secondary bonds is considered to be arbitrary and it is suggested that a true characterization should be based on the concept of a spectrum of bond strengths. In margarine, weak bonds form only a minor proportion of the bond strength spectrum, strong bonds form the major part. Butter on the other hand contains a small proportion of strong bonds.

Microstructural observations of network structures substantiate such a concept (7, this work).

Water droplets

Margarines and butter roughly contain 16 - 20% water, which is present in the structure as finely dispersed droplets. An impression of the status of the water droplets in spreads can be obtained by using freeze-fracture as the sample preparation technique for EM observation.

Fig. 6 shows the result of this technique for a fat spread, indicating that the sample fractures either over the surface of the water droplets, or that cross fracture of the droplet occurs. Because of their wettability fat crystals can be found in the O/W interface, which stabilizes the water droplets (17). This stabilizing action of the fat crystals strongly depends on the presence of surface-active ingredients like monoacylglycerols, phospholipids and proteins (9).

Emulsifying systems applied in spreads usually are based on monoacylglycerols and lecithins (11). Only in products for other (e.g. bakery) applications sometimes other surfactants are used. Milk protein (O/W emulsifiers), as present in the aqueous phase of spreads, tend to destabilize the emulsion. Water droplets in spreads should be kept small (preferably < 5 μm) to reduce microbiological risks (22, 23). Small droplets induce a greasy taste (see ref. 8, page 221).

Air

In some products (shortenings and margarines) air is introduced to influence either consistency (4, 12) or appearance. Air usually is entrapped in the liquid oil phase of a spread. Small crystals have been described to orientate tangentially to the surface (1). It is not clear whether these fat crystals have a stabilizing effect on the air bubbles. After churning, a similar type of arrangement is observed in fat globules of butter (14). Under polarized light a birefringent layer is observed, also ascribed to tangentially oriented fat crystals in the outer layers

---

Fig. 1. Typical example of fat crystals (freeze-fracture).
Fig. 2. Spherulites in β-crystal modification, isolated from a fat spread, inducing sandiness.
Fig. 3. Examples of a fat globule as present in butter. The open crystalline shell structure is induced by removing the oil from the inside of the globule during the preparation procedure (reference 7).
Fig. 4. Example of a cross-fractured butter globule. Orientation of fat crystals parallel to the droplet surface (arrow 1); traces of remaining water around the droplet (arrow 2).
Fig. 5. Three dimensional networks of fat crystals in a shortening at (a) low and (b) high magnification.

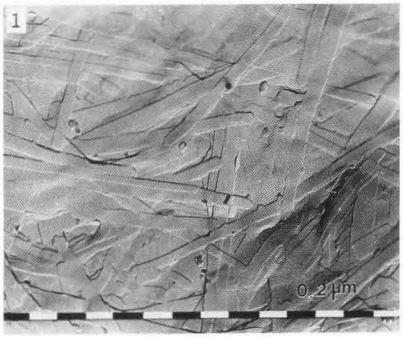
1
0,2 µm

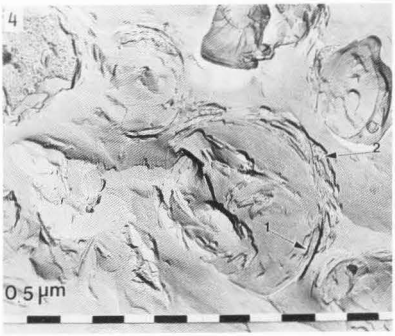
4
2
1
0,5 µm

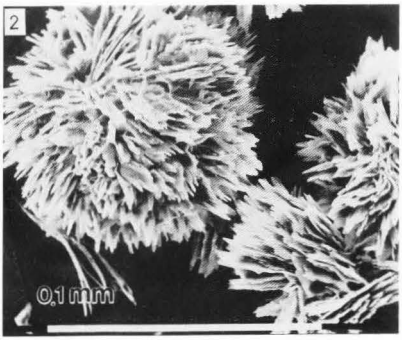
2
0,1 mm

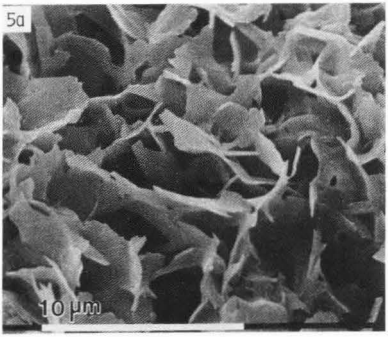
5a
10 µm

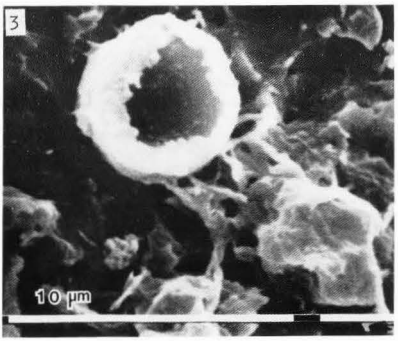
3
10 µm

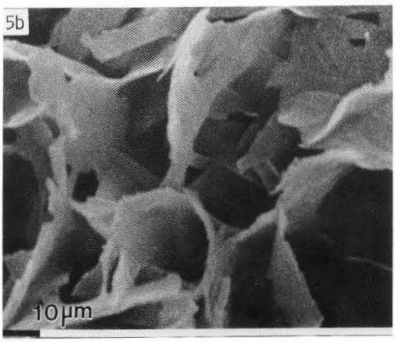
5b
10 µm

of the fat globules and induced by pressure exerted by air during churning.

Air is present in products in all shapes (Fig. 7), from round bubbles to strongly deformed areas, depending on the way it has been introduced into the product. Smooth round air bubbles are found when introduction is done at low solids levels, e.g., during whipping of margarines or shortenings in cake preparation. Strongly deformed air bubbles are found when high solid contents are present at the moment of air introduction, e.g., during processing or churning. In butter some air (approximately 5 %) is still present as a result of the churning process (14) (Fig. 8).

Product structure

Shortenings

Due to their composition shortenings have the simplest product structure of all fat spreads. These products are composed of liquid oil and fat crystals only. Blending different oils offers a wide range of solid/liquid ratios. Fat crystals usually take the shape of needles or platelets.

The existence of a three-dimensional network of fat crystals has been postulated for many years (5), but only recently sample preparation techniques have developed (7) that could demonstrate the existence of such a network. The nature of the network structure will depend on both composition and processing conditions. In particular, the extent to which individual crystals aggregate, determines the character of the observed network. As an example of this, Fig. 9 shows the microstructure of two shortenings of the same composition. The only difference is found in the processing condition.

For some applications air-containing shortenings are produced. The presence of air does not principally affect the crystal-crystal interactions in the crystal network but it does reduce the number of crystals per unit of volume. The product hardness (g/cm^2) decreases with increasing air contents (5). At higher levels of air, brittleness may occur (4).

Tempering, i.e., storage above ambient for a few days (5) is sometimes applied for shortenings. During this process recrystallization takes place in which mixed crystals (as formed during fast crystallization in a votator) "demix" and form other more stable crystals. This generally leads to larger crystals and a slightly softer products.

Margarine

Like shortening, margarine derives its consistency from a fat crystal network. No essential differences in fat crystal network are found on comparing these two types of products. The most striking difference in structure is the presence of water droplets in margarine. Water droplets of a few μm are formed during intensive mixing of fat and water phase during processing. In this process crystals can orientate at the water droplet surface.

In margarines "shells" of fat crystals can be found (7) (Fig. 10) that surround the water droplets. These "shells" seem to be interconnected with the three-dimensional fat crystal network.

The water droplet size distribution can be influenced by processing: intensive shear during processing results in a finer emulsion (Fig. 11). The main difference in microstructure found in all 80% fat products is the nature of the fat crystalline network, e.g., the size, shape, and aggregation of fat crystals. Depending on the type of product, more or less solids are applied. Over the last two decades the fats industry has diversified the margarine area into products aimed at specific applications such as margarine for tropical countries, halvarines, and products for bakery applications like creaming, cake-making and puff-pastry products.

In halvarines essentially the same microstructure is found as in margarines: only the ratio water droplets/fat/oil is different. In puff-pastry a finer crystal structure is preferred to a coarse crystal structure (10, 11). The finer crystal structure was found to give a better performance in pastry preparation while the pastry margarine itself showed less work softening.

Butter

In butter a limited number of milk fat globules are still present in the final product. The number of fat globules that survive processing strongly depends on the ripening procedure of the cream (19,20) and on the working conditions during and after processing (20): Cold-warm-cold (CWC) ripening procedures give stable globules with thick surface crystal layers of high melting triacylglycerols, while the interior of the globule contains crystal aggregates and liquid oil. A large number of these globules survive processing in contrast to globules formed during "cold-ripening" (19) which are less stable and break during processing (Fig. 12).

Intensive working destroys fat globules resulting in a more crystalline interglobular phase and consequently a harder consistency. A combination of "C-ripening" and intensive working is applied in the production of summer butter. Winter butter is produced by applying a CWC-ripening (20).

The interglobular phase in butter is a mixture of liquid oil, crystal aggregates and membrane residues. In fresh butter the crystals are slightly curved and sometimes arrange in groups with parallel orientation. The liquid phase often contains ordered structures which are not as distinctly differentiated from amorphous areas as real crystals. Possibly they represent liquid crystals (16). After 10 days storage of fresh butter an increase of uncurved newly formed crystals is observed. This phenomenon is thought to be related to the setting and hardening of butter (16).

Fig. 6. Water droplets in fat spreads. The freeze fracture technique gives rise to two different images of water droplets depending on whether the sample breaks (S) over the surface of the droplet or (C) whether cross-fracture occurs "through" the droplet.

Fig. 7. Example of air cells in a shortening. Air dosed during votator processing.

Fig. 8. Air cell in a churned product. (g) fat globule; (w) water. The air interface is covered with fat globules.

Fig. 9. Partial crystallization in rest shows a structure of interconnected crystal clusters (a), whereas complete crystallization in a votatorline shows a structure of connected plate-like crystals (b).

Fig. 10. Fat crystalline network (f) and water droplet structure (w) showing a crystalline shell, in a margarine.


6
s
s
1 µm

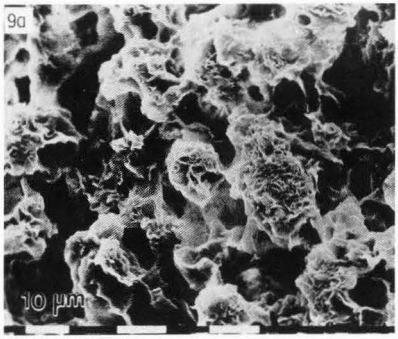
9a
10 µm

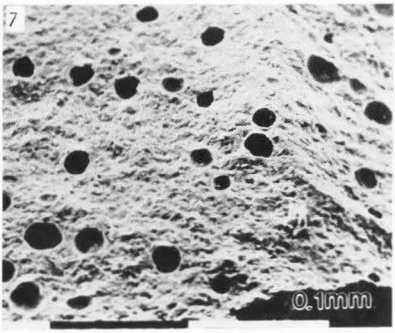
7
0.1mm


9b
10 µm

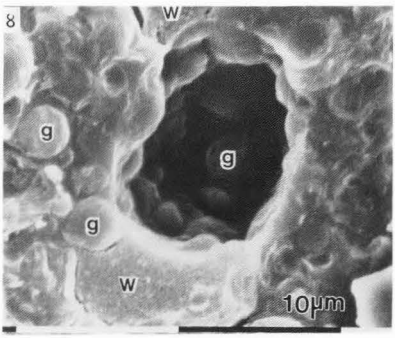
8
w
g
g
g
w
10µm

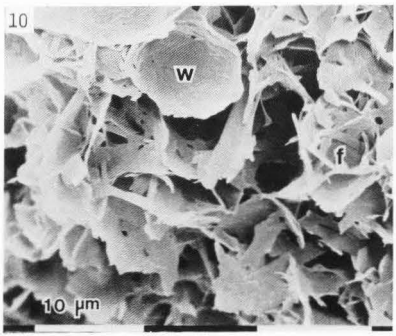
10
w
f
10 µm

The emulsion structure of butter has been a subject of much debate, especially the water continuity of the product (13,14). At the start of butter production, water is the continuous phase. During churning and subsequent working, the fat phase becomes the continuous phase. By more intensive working, the water becomes more finely dispersed in the product. Nevertheless, in contrast to margarine, water continuity in butter is still observed. It has been proposed by Mulder (13) that the water containing membranes of many fat globules lie so close to water droplets that a pathway is offered for transport of water molecules (water channels). This type of structural arrangement can indeed be observed by freeze fracture EM (Fig. 13), although water, as such, cannot be detected.

Water droplets in the final products have sizes between 0.25 and 25 μm. Occasionally small fat globules are incorporated in the water phase (17). The presence of fat crystals around the water droplets in butter is a matter of some debate. A dense surface coverage with high melting butterfat crystals has been reported (17). In other work such a shell formation was not observed (7).

Conclusions

Fat spreads have a microstructure composed of liquid oil, fat crystals, water droplets and sometimes air. A wide variety in ingredients and processes influences the product structure:

- the fat composition determines the amount of fat crystals, the speed of crystallization, as well as the size, the shape and the aggregation of the individual crystals into a network.
- water and water-phase ingredients are emulsified in the fat continuous matrix. Some of the water-soluble ingredients, such as milk proteins (O/W emulsifiers), affect the emulsion stability and consequently the efficiency of emulsification of the water in the product;
- emulsifiers also affect the network structure and the emulsion stability during and after processing;
- processing is another instrument to manipulate crystallization and emulsification conditions such that the desired product properties are obtained. It is clear that these conditions strongly affect structural parameters, such as crystal size, crystal-crystal interactions, network formation, and emulsion stability;
- finally, storage can induce changes in product structure, e.g., as a result of recrystallization.

Recent developments, especially in the area of electron microscopy, have led to a major increase in our understanding of the structure of fat spreads. Hypotheses regarding network formation and distribution of water in various spreads, as they were postulated in the past, have been substantiated. The challenge for the future lies in relating composition and processing variables to changes in product structure, i.e., network structure, fat crystals, cream globules, air cells, water droplets, and shell structure.

References

1. Berger KG, Jewell GG, Pollitt RJM (1979). Oils and Fats. In: Food Microscopy, Vaughan JG (ed.). Academic Press, 471-497.

2. Buchheim W, Precht D (1979). Elektronenmikroskopische Untersuchung der Kristallisationsvorgänge in den Fettkügelchen während der Rahmreifung. Milchwissenschaft 34, 657-662.

3. De Man JM (1983). Consistency of fats: A review. J. Am. Oil Chem. Soc. 60, 82-87.

4. Gupta S, De Man JM (1985). Modification of rheological properties of butter. Milchwissenschaft 40, 321-325.

5. Haighton AJ (1963). Die Konsistenz von Margarine und Fetten. Fette Seifen Anstrichm. 65, 479-482.

6. Haighton AJ (1976). Blending, chilling, and tempering of margarines and shortenings. J. Am. Oil Chem. Soc. 53, 397-399.

7. Heertje I, Leunis M, van Zeijl WJM, Berends E (1987). Product morphology of fatty products. Food Microstruct. 6, 1-8.

8. Larsson K (1986). Physical properties-structural and physical characteristics. In Lipid Handbook, Gunstone FD, Harwood JL, Padley FB (eds.). Chapman and Hall, London.

9. Lucassen-Reijnders EH, Tempel M van den (1963). Stabilization of water-in-oil emulsions by solid particles. J. Phys. Chem. 67, 731-734.

10. Madsen J, Als G (1971). Konsistenz und Kristalltechnische Verhältnisse bei der Herstellung von Ziehmargarine auf Druckkühlern und Kühltrommeln. Fette Seifen Anstrichm. 73, 405-410.

11. Madsen J (1987). Emulsifiers used in margarine, low calorie spread, shortening, bakery compound and filling. Fett Wiss. Technol. Fat Sci. Technol. 89, 165-172.

12. Massiello FJ (1978). Changing trends in consumer margarines. J. Am. Oil Chem. Soc. 55, 262-265.

13. Mulder M (1957). The presence of moisture in butter. Neth. Milk Dairy J. 11, 25-42.

14. Mulder H, Walstra P (1974). Structure and texture of butter. In: The milk fat globule. Emulsion science as applied to milk products and comparable foods. Pudoc, Wageningen, 246-287.

15. Precht D, Buchheim W (1979). Elektronenmikroskopische Untersuchungen über die physikalische Struktur von Streichfetten. I. Die Mikrostruktur der Fettkügelchen in Butter. Milchwissenschaft 34, 745-749.

16. Precht D, Buchheim W (1980). Elektronenmikroskopische Untersuchungen über die physikalische Struktur von Streichfetten. II. Die Mikrostruktur der zwischenglobulären Fettphase in Butter. Milchwissenschaft 35, 393-398.

17. Precht D, Buchheim W (1980). Elektronenmikroskopische Untersuchungen über die physikalische Struktur von Streichfetten. 3. Die wässrige phase in der Butter. Milchwissenschaft 35, 684-690.

18. Precht D (1980). Untersuchungen über die Kristallstruktur und den molekularen Aufbau der Fettphase von Butter. Fette Seifen Anstrichm. 82, 142-147.

19. Precht D, Peters K-H (1981). Die Konsistenz der Butter. I. Elektronenmikroskopische Untersuchungen zum Einfluss unterschiedlicher Rahmreifungstemperaturen auf die Häufigkeit bestimmter Fettkügelchentypen im Rahm. Milchwissenschaft 36, 616-620.

Fig. 11. Differences in water droplet size distribution in margarine as a result of:
(a) low and,
(b) high shear during processing.

Fig. 12. Differences in the survival of fat globules in butter as a result of differences in the ripening procedure in the cream prior to churning.
(a) CWC-ripened cram;
(b) C-ripened cream.

Fig. 13. Freeze-fracture micrograph of butter showing membranes of fat globules in close contact with water droplets. Arrow indicates position of deformation of the globule surface. (w) Water droplet; (F) fat globule.

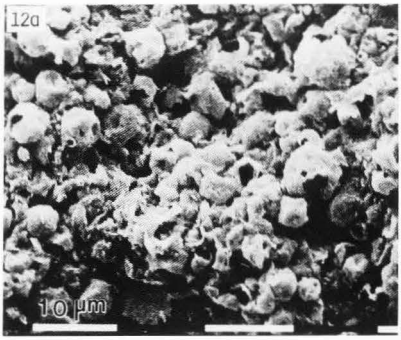

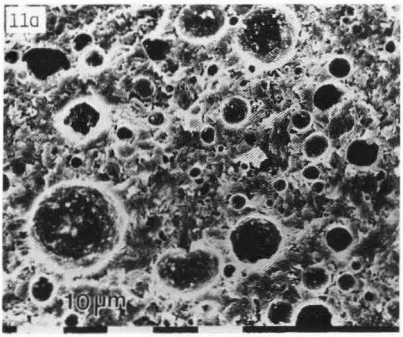

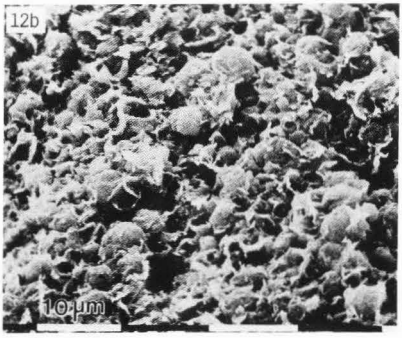

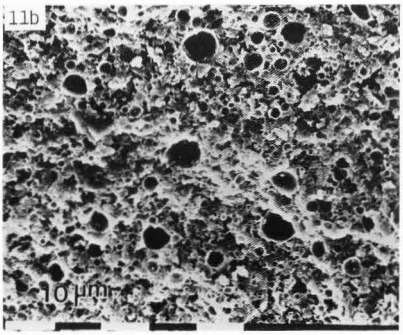

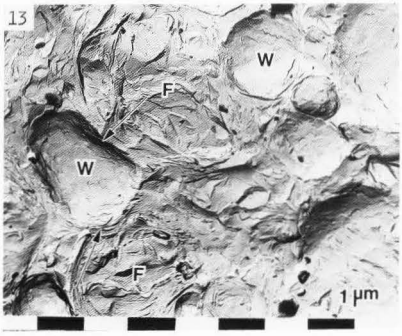

20. Precht D, Peters K-H (1981). Die Konsistenz der Butter. II. Zusammenhänge zwischen der submikroskopischen Struktur von Rahmfettkügelchen sowie Butter und der Konsistenz in Abhängigkeit von speziellen physikalischen Rahmreifungsverfahren. Milchwissenschaft 36, 673-676.

21. Shama F, Sherman P (1970). The influence of work softening on the viscoelastic properties of butter and margarine. J. Texture Stud. 1, 196-205.

22. Verrips CT, Zaalberg J (1980). The intrinsic microbial stability of water-in-oil emulsions. I. Theory. Eur. J. Appl. Microbiol. Biotechnol. 10, 187-196.

23. Verrips CT, Smid D, Kerkhof A (1980). The intrinsic microbial stability of water-in-oil emulsions. II. Experimental. Eur. J. Appl. Microbiol. Biotechnol. 10, 73-85.

24. Walstra P (1974). High-melting triglycerides in the fat globule membrane: an artefact? Neth. Milk Dairy J. 28, 3-9.

Discussion with Reviewers

D. Precht: Is there clear evidence that only the β'- and β-forms are present in spreads or could also less stable forms like the α-form exist due to certain temperature treatments (e.g., rapid cooling)?

Authors: By X-ray diffraction techniques it is shown that, under normal storage conditions, indeed only the β'- and β- modifications are present. During processing, however, under conditions of strong cooling, first the α-modification is formed, which is in general rapidly converted to the β'-modification.

Preservation of α-modification would require the use of low temperature and storage of the product below the melting points of the most abundant α-forms, i.e., below 0°C.

D. Precht and W. Buchheim: According to our own observations the accumulations of fat crystals around the water droplets of butter, margarine, and low-fat dairy and non-dairy spreads is similar, despite strongly varying amounts of surface-active lipids in these products. Could there be another driving force behind this separation process than the one that the authors have mentioned?

Authors: In our opinion shell formation around water droplets is not the same in different products. It can vary between a clear shell and the mere entrapment of the water in the continuous fat matrix, without a clear shell structure. In butter (text reference 7), as well as in some other products, the latter structure is predominant.

It cannot be excluded that freeze-fracture techniques when applied to products containing oil, may lead to erroneous results. Also in fat systems, freezing velocity appears to be very critical. We found that emulsifiers play an important role in shell formation, but certainly other aspects, such as processing conditions, must also be considered. Working may enhance the possibility for transport of fat crystals to the oil/water interface (Heertje et al., this issue). Such a mechanism would, however, not be valid during churning in the normal processing of butter by phase inversion. Also from this background prominent shell formation in butter is not very likely.

D.P. Dylewski: In your opinion how would a close linkage of microscopy, rheology, and sensory help in the formulation and processing of new oil-based products?

Authors: Examples of how microstructure, rheology and product properties are related have been given in this paper and other articles from our laboratory (e.g., see text reference 7; and Heertje et al., the article following this paper in this issue). In this context, it should be mentioned how:

- the nature of the network structure (e.g., continuous versus granular) influences the hardness of a product;
- the emulsion structure influences other sensorial properties.

By deliberately manipulating the structure by the applied processing, it will be possible to induce desired product properties.

FOOD MICROSTRUCTURE, Vol. 7 (1988), pp. 189-193
Scanning Microscopy International, Chicago (AMF O'Hare), IL 60666 USA

0730-5419/88$3.00+.00

THE EFFECT OF PROCESSING ON SOME MICROSTRUCTURAL CHARACTERISTICS OF FAT SPREADS

I. Heertje, J. van Eendenburg, J.M. Cornelissen, A.C. Juriaanse

Unilever Research Laboratorium
P.O. Box 114
3130 AC Vlaardingen, The Netherlands

Abstract

The processing and the composition of fat spreads determine to a large extent the final product properties such as hardness, spreadability, mouthfeel, emulsion stability and salt release. In establishing the relation between composition, processing and final product properties, microstructural studies play an important role. In this context the influence of some process parameters in the production of shortenings and 80% fat spreads on microstructure and product properties has been investigated. Shear, cooling regime and crystallization conditions influence both the emulsion structure and the fat crystalline matrix. In general, working leads to softer products with a more granular crystalline fat matrix, whereas the water droplet size distribution is influenced in a complicated manner by the conditions of shear. This type of work indicates ways to control and manipulate the microstructure and product properties of fat spreads.

Initial paper received September 20, 1988
Manuscript received November 30, 1988
Direct inquiries to I. Heertje
Telephone number: 31 10 4605513

Key words: Processing, microstructure, shear, cooling regime, deformation, A-unit, C-unit, shortening, margarine, crystalline matrix, crystalline shell.

Introduction

Composition and processing are important variables in the manufacture of fat spreads. Much skill is required to find an optimal compromise between fat blend composition, processing and desired product properties (7), such as hardness, spreadability, mouthfeel, emulsion stability and salt release. It is considered that, while on one hand, these functional properties are linked with the product microstructure, on the other hand, composition and processing are the determining factors in the formation of microstructure. Therefore, in order to control and manipulate such properties, the study of product microstructure, and in particular, how the microstructure will be influenced by the composition and the processing conditions, is of vital importance.

In this paper, we investigate how the conditions of shear, crystallization, and deformation effect the product microstructure, in particular, the fat crystalline matrix and emulsion structure. We further investigate the relations with product properties.

Methods

Fat spreads are processed commercially in the A and C-units of a votator line (2,7). An A-unit consists of a scraped-surface tube cooler in which mixing of the fat and water phase, as well as, partial crystallization of the fat phase occurs, depending on the temperature at the exit of the unit (ex A-temperature). Important parameters are the throughput and the rotational speed, presenting conditions of shear in the early stages of the manufacturing process. After supercooling and partial crystallization in the A-units, further crystallization may occur in the C-units. A C-unit is a cylinder fitted with pins on its inner wall and on the rotor. Application of such a unit induces conditions of strong working.

Shortenings are prepared by processing a fat blend without water phase in a votator line.

The influence of process conditions on the microstructure has been studied in a laboratory votator with about 3 kg of fat, by varying the ex-A temperature and the rotational speed of the A-unit. The effect of a C-unit on microstructure has been investigated by comparison of samples, processed in an A-A and an A-A-C sequence.

Hardness is measured after storage of the products by means of a cone penetrometer (1).

Some samples were rheologically characterized in uni-axial compression. From the margarine discs

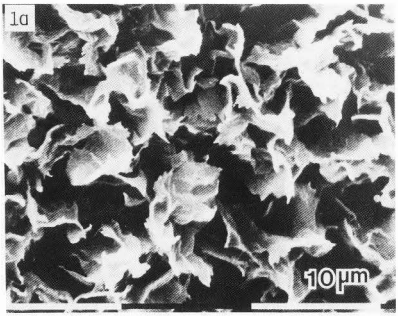

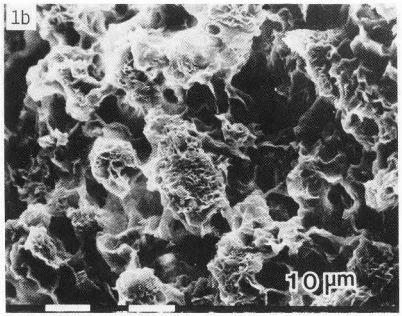

Fig. 1. Microstructure of shortenings. a. Complete crystallization in processing line. b. Partial crystallization in rest.

of 45 mm diameter (with ratios of diameter to height between 3 and 10) were cut using a wire. The samples were compressed between thermostated, approaching parallel plates of 45 mm diameter, using a computer controlled Instron testing machine model 1122. This represents a situation of uniform compression in a macroscopic sense. Stress-strain curves of the material were obtained by eliminating the contribution of friction between the sample and the compressing plates, by performing compression tests with samples of different heights. From such a curve (see Results and Discussion, Fig. 2) three characteristic parameters can be deduced: the maximum stress σ_{max}, the deformation at maximum stress ε_{max} and the ratio (σ_{rat}) of the stress at large deformation (σ_{∞}) and σ_{max}. The latter ratio is a measure of the work softening, which, in turn, may be related to the breaking of bonds in the product.

The microstructure was analyzed by Cryo-scanning electron microscopy (SEM) after de-oiling the products (3) at 10°C. For the shortenings and the margarines, a de-oiling time of 28 hours and 20 hours respectively, was applied. Solid phase contents were measured by pulse nuclear magnetic resonance technique.

Results and Discussion

Shortenings

Influence of cooling regime. A model fat blend, containing 14% of a high melting palm oil fraction (melting point 58°C) in sunflower oil, has been processed in a A-unit. A low ex-A temperature (10°C) resulted in complete crystallization of the solid phase (14%) in the A-unit. At a high ex-A temperature (28°C) only partial crystallization of the solid phase (6%) in the A-unit occurs. The remaining part (8%) of the solid phase crystallizes in rest. The microstructure of the solid fat phase is presented in Fig. 1 which shows that complete crystallization in the A-unit results in a homogenous microstructure of small connected plate-like crystals, whereas partial crystallization in rest leads to a nonhomogeneous structure of large clusters interconnected by crystal bridges.

Both products have also been investigated by parallel plate compression. The stress-strain curves (Fig. 2) are in good agreement with the observed microstructure, considering that on deformation more bonds will be broken in the product with the homogeneous microstructure (Figs. 1a and curve a in Fig. 2) than in the other product (Figs. 1b and curve b in Fig. 2), where only crystal bridges between the clusters will be broken. The product with the homogeneous microstructure has the highest value of σ_{max} (greater hardness) and shows the greatest work softening (σ_{rat} = 0.08 whereas the other product has an σ_{rat} of 0.41).

Influence of deformation. In order to obtain better insight into the effects of deformation, the microstructure of the model fat blend, processed via an A-unit and partially crystallized in rest, has been further investigated before and after uniform compression between parallel plates. Before deformation (Fig. 3a) the structure is composed of crystalline clusters interconnected by a fat-crystalline network. After deformation (Fig. 3b) the structure between the clusters is more open. Crystal bridges have apparently been broken and the interconnecting network is, at least partly, being removed. The stress-strain behavior for this product is given in Fig. 2 (curve b).

On the basis of this information the following picture emerges: the region where only elastic deformation occurs is extremely small. Already at very low deformation, breakdown of crystal bridges between clusters occurs and both elastic deformation and fracture take place. At high deformation, after breakdown of the bonds, the deformation is a plastic one, depending on smoothness, shape, and elasticity of the clusters.

Influence of shear. The influence of C-unit (conditions of strong working during fat crystallization) is illustrated in Fig. 4. When the supercooled fat blend is worked in a C-unit, the samples obtained show a more granular structure than samples exclusively processed in A-units (which show a more continuous structure). This observation agrees well with the idea that during working in a C-unit continuous structure formation is prevented, as well as with the

Fig. 2 (at right). Stress strain curves obtained from parallel plate compression after elimination of friction. h_0 and h: height of sample before and after compression respectively. Products shown in Fig. 1 (T = 20°C).
a. Complete crystallization in processing line.
b. Partial crystallization in rest.

Fig. 3 (at center of page). Influence of deformation (parallel plate compression) on microstructure.
a. Before deformation, presence of crystal bridges;
b. After deformation, absence of crystal bridges.

Fig. 4 (at bottom of page). Influence of shear (C-unit) on microstructure of shortenings.
a. Without shear (A-A units only), continuous structure;
b. With shear (A-A-C processing), granular structure.

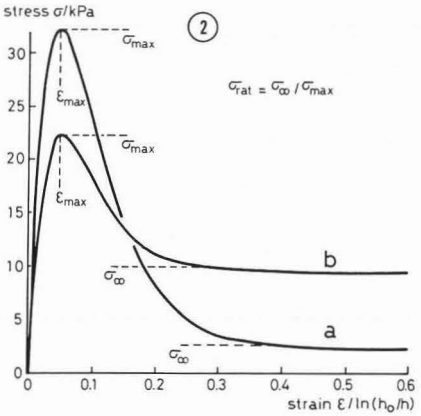

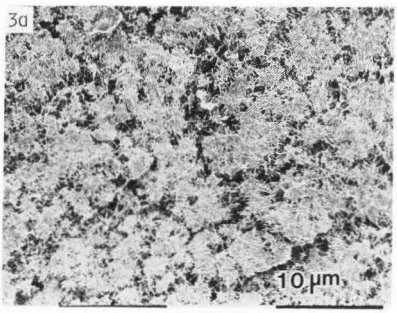

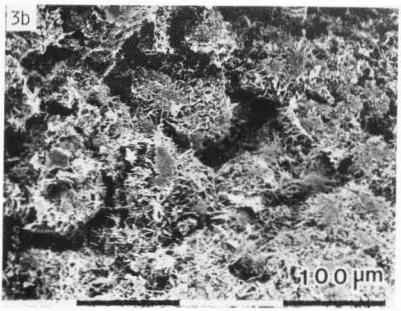

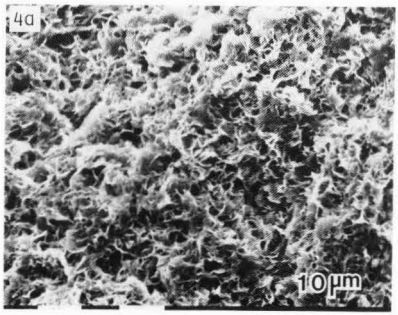

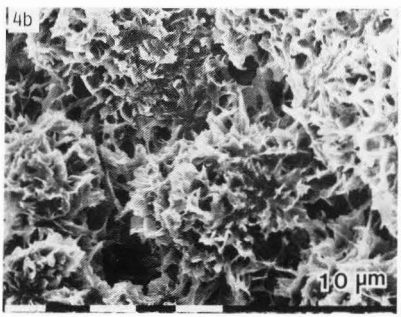

finding that A-A-C processed samples are much softer than A-A processed samples (hardness at 10°C of 600 g/cm² and 2900 g/cm² respectively). It should, be realized that the large grains (up to 40 μm) visible in Fig. 4b would not survive a C-unit and are apparently formed after the processing in the C-unit. Postcrystallization is responsible for this phenomena; this is indicated by the influence of the ex-A temperature on granularity: at high temperatures granularity is more prominent. In this respect there is a resemblance with the structure observed after crystallization in rest (Fig. 2, curve b).

Margarines

Microstructures of spreads containing 20% water after A-A and A-A-C processing are given in Fig. 5. A very distinct influence of the C-unit is observed:

- the fat structure is much more granular, as was observed for shortenings;
- shell formation around water droplets is more pronounced.

In addition, larger water droplets are observed (coarsening). Also in this case A-A-C processed samples are much softer than A-A processed samples (hardnesses at 10°C of 600 g/cm² and 2300 g/cm² respectively). Apparently the influence of the water phase on product hardness is limited.

The better shell formation around the water globules on working may be connected with the enhanced possibility of transport of fat crystals to the oil-water interface. It has been discussed (4-6) that stirring strongly accelerates the rate of adsorption of crystals onto the emulsion droplets. A similar effect is induced by the presence of surfactants (5). When no stirring or working is applied, or in the absence of an emulsifier, free diffusion of crystals will be hindered due to the rapid formation of a solid crystalline network. Consequently the main part of the crystals will stick together to form a network and will not be available for this so called Pickering stabilization of the emulsion droplets. When the emulsion is worked in a C-unit, however, during the crystallization stage crystals will adhere to the emulsion droplets and form a crystalline shell around the water droplets. In addition, smaller crystals, induced by working, can better accommodate and consequently better adhere to the droplet surface.

The coarsening of the emulsion droplets after C-unit processing may also be ascribed to the influence of working. As a result of fat crystallization (in particular in the applied C-unit), the viscosity increases, which may lead to deformation of droplets and subsequent coalescence. Coalescence under the influence of a C-unit is, however, not always observed.

In contrast, a strong shear influence on droplet size can be realized by varying the shear rate in the A-unit. Under conditions of high shear (Fig. 6a) a much finer emulsion is formed than at low shear (Fig. 6b). This difference in behavior should be ascribed to the more liquid-like character of the emulsion in the A-unit, which is still in a supercooled α-crystalline state (2). In this case, higher shear just gives a stronger emulsification; coalescence of droplets, due to a high viscosity of the continuous phase as observed in applying a C-unit, does not occur.

Concluding remarks

The microstructure of fat spreads can be manipulated and controlled by the applied processing. Microstructure and perceived macroscopic properties appear to be related. This opens up the possibility to intentionally prepare products with desired physical and sensorial properties.

References

1. Haighton AJ (1959). The measurement of the hardness of margarines and fats with cone penetrometers. J. Am. Oil Chem. Soc. 36, 345-348.

2. Haighton AJ (1976). Blending, chilling, and tempering of margarines and shortenings. J. Am. Oil Chem. Soc. 53, 397-399.

3. Heertje I, Leunis M, van Zeijl WJM, Berends E (1987). Product morphology of fatty products. Food Microstruct. 6, 1-8.

4. Lucassen-Reijnders EH (1962). Stabilization of water-in-oil emulsions by solid particles. Thesis, Rijksuniversiteit Utrecht.

5. Lucassen-Reijnders EH, Tempel M van den (1963). Stabilization of water-in-oil emulsions by solid particles. J. Phys. Chem. 67, 731-734.

6. Overbeek JThG (1952). Kinetics of flocculation. In: Colloid Science Vol. I, Kruyt HR (ed.), Elsevier, Amsterdam, 289-292.

7. Poot C, Biernoth G (1986). Margarine and butter production. In: The Lipid Handbook, Gunstone FD, Harwood JL, Padley FB (eds.). Chapman and Hall, London, 219-225.

Discussion with Reviewers

D.P. Dylewski: How does fat crystal distribution and shell formation around water globules in margarine change with time?

Authors: We cannot give a general answer to this question. It is highly dependent on blend composition and storage regime. On heating and subsequent cooling of certain fat blends (so called cycling), fractionation effects are observed, in general accompanied by coarsening of fat crystals and changes in water droplet structure.

K. Sato: Do you think that different polymorphic modifications of triacylglycerols such as α, β, and β' are present in the structures presented in your figures?

Authors: By X-ray diffraction techniques we found the predominant modification in fat spreads to be β' (see Juriaanse and Heertje, this issue). In special cases β-crystals may be found, sometimes giving rise to such adverse properties as sandiness. During processing (rapid cooling!) first the α-modification is formed, which is, in general, rapidly converted to β' modification.

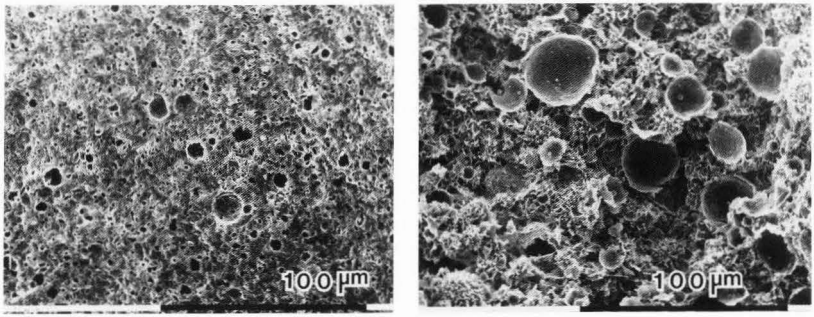

Fig. 5. Influence of shear (C-unit) on microstructure of margarines.
a. Without shear, continuous structure, fine emulsion, no shells around interface;
b. With shear, granular structure, a more coarse emulsion, shells around interface.

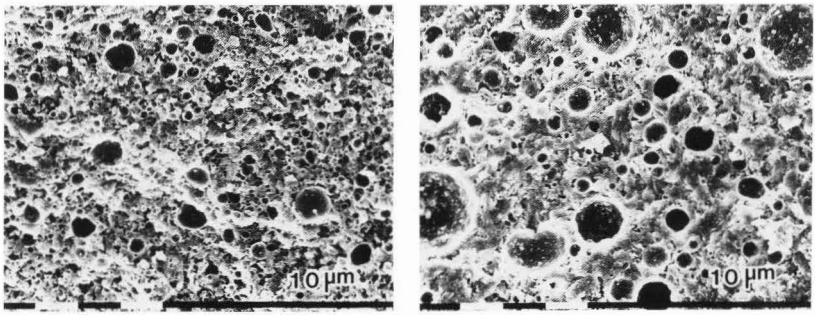

Fig. 6. Influence of shear (rotational speed of A-unit) on microstructure of margarines.
a. Rotational speed 600 rev./min., fine emulsion;
b. Rotational speed 100 rev./min., coarse emulsion.

FOOD MICROSTRUCTURE, Vol. 7 (1988), pp. 195-203
Scanning Microscopy International, Chicago (AMF O'Hare), IL 60666 USA

0730-5419/88$3.00+.00

THE EFFECT OF STORAGE, PROCESSING AND ENZYME TREATMENT ON THE MICROSTRUCTURE OF CLOUDY SPARTAN APPLE JUICE PARTICULATE

D.-L. McKenzie and T. Beveridge

Agriculture Canada Research Station
Summerland, British Columbia, Canada
VOH 1ZO

Abstract

The effect of blanching, post-harvest refrigerated (4°C) storage and enzyme treatment with polygalacturonase on the microstructure of Spartan apple juice was examined by thin sectioning and negative staining transmission electron microscopy. Particles were categorized as granules (3-54 nm), spheres (20-368 nm) and aggregates (12-2519 nm). Enzyme treatment with polygalacturonase significantly decreased granule size ($p \leq 0.01$). Storage of apples significantly decreased both granule size ($p \leq 0.01$) and aggregate length ($p \leq 0.05$) and also resulted in a web-like aspect in the microscopic appearance of juice particulate. The web-like aspect of the particulate was removed either through enzyme treatment with polygalacturonase or by blanching. Blanching of puree significantly increased granule ($p \leq 0.05$) and sphere size ($p \leq 0.01$), while significantly decreasing aggregate length ($p \leq 0.01$). In addition, blanching stabilized suspended particulate by what appeared to be the formation of a protective colloid which prevented particle aggregation through electrostatic repulsion.

Initial paper received May 27, 1988
Manuscript received August 19, 1988
Direct inquiries to T. Beveridge
Telephone number: 604 494 7711

Key words: Apple juice, Spartan Apples, enzyme treatment, storage, processing, post-harvet refrigeration, blanchung, polygalacturinase, microstructure, juice particles.

Introduction

Production of apple juice in Canada has centered mainly around the clarified, amber type of juice (Atkinson and Strachan, 1949a; Beveridge et al., 1986). In Japan, however, the majority of fruit juices are sold in the cloudy, unoxidized, 'natural' state (I. Yamashita, personal communication, 1987). A 'natural' apple juice can be produced through the inactivation of polyphenol oxidase by blanching the apple puree at 90°C in combination with an ascorbic acid or sulfite pretreatment (Holgate et al., 1948; Atkinson and Strachan, 1949b; Beveridge et al., 1986). Blanching successfully inhibits the development of the brown colour and cider-like flavour characteristic of oxidized juice, producing a naturally coloured, opalescent juice with a fresh apple flavour characteristic of the variety processed (Bauernfeind, 1958). The opalescence or cloud formed as a result of blanching is very stable with only a slight sediment being deposited during storage. On the other hand, the cloud formed in oxidized juice is very unstable, readily flocculating to form an undesirable thick layer of sediment at the bottom of the container (Atkinson and Strachan, 1949b).

The thermal stabilization of the juice cloud by blanching offers the possibility of marketing a 'natural', unoxidized juice in either the opalescent form or, upon cloud destabilization, in the clarified form allowing for further expansion of the apple juice market (Carpenter and Walsh, 1932; Atkinson and Strachan, 1949b). An understanding of the factors contributing to stabilization or destabilization of the cloud formed in apple juice is required to enable the manufacturer to efficiently produce either a cloudy or clarified unoxidized 'natural' apple juice. The objective of the present study was to use electron microscopy to gain a better understanding of the effects of blanching, refrigerated (4°C) storage and enzyme treatment with polygalacturonase on the nature of the cloud particulate present in juice from Spartan apples.

Materials and Methods

Apple Juice preparation

This study examined unoxidized apple juice processed with a blanching step, and oxidized juice processed without a blanching step. Oxidized juice was obtained from Spartan apples harvested at the Summerland Research Station in 1985. Both fresh and stored apples were examined, where 'fresh'

apples were stored at 4°C for two weeks after harvest and then processed, while 'stored' apples were stored for nine months at 4°C before processing. Apple maturity was measured by testing firmness and starch content. Fresh Spartan apples had an average starch rating of five (Lau, 1985), and an average firmness of 69.3 N as tested by a Magness-Taylor pressure tester with a 7.8 mm probe. Stored Spartan apples had an average starch rating of nine and an average firmness of 44.4 N as tested by a Magness-Taylor pressure tester with a 7.8 mm probe. The starch test involved transversely bisecting 10 apples perpendicular to the core and immersing the freshly cut surface of the top half of the fruit in a dilute iodine solution for one minute. The starch test gave a measure of apple maturity based on a nine-point scale where a rating of one represented an immature apple with the whole cut surface reacting to turn blue, while a rating of nine corresponded to an overmature apple in which none of the cut surface turned blue (Lau 1985).

A smooth puree was produced from 10 kilograms of apple by blending batches of 500 g of destemmed apple cut into two centimeter cubes with 200 ml of a 200-500 ppm sulfite solution (sulfite as potassium metabisulfite). The concentration of sulfite was adjusted within the range stated so that browning was only just inhibited prior to blanching. Juice was expressed from the puree by centrifugation at 7700 x g for 10 min with a Sorvall RC-5 centrifuge equipped with an SS-34 (10.7 cm) rotor. Enzyme-treated juice was prepared by incubation of the puree with 0.1% Irgazyme 100 (CIBA-GEIGY Corp.), a polygalacturonase with lyase and pectinesterase side activities, for 1 hr at 45°C. Juice was expressed from the enzyme-treated puree as described above. Juice and puree were frozen and stored at -18°C until required.

Unoxidized juice was produced as above with batches of the apple puree blanched as described by Beveridge et al (1986). The puree was heated to over 90°C for at least 25 sec, which was sufficient to destroy apple polyphenoloxidase (Beveridge and Harrison, 1986). After processing, the separate batches of puree were mixed together in a Hobart H 600 mixer, frozen and stored at -18°C.

Transmission Electron Microscopy (TEM)

All samples were examined with a Philips EM 300 transmission electron microscope operating at 60 kV. With the exception of thin sectioning, each treatment was performed twice; duplicate samples were prepared within treatments, then representative sections were photographed. Unless otherwise stated, measurements of particle dimensions were taken of 10 randomly selected particles within each particle category. The range and mean of these measurements were recorded along with descriptions of particle stain density.

Thin Sectioning

Duplicate 2 mL aliquots of juice were dialyzed overnight against 4 L distilled water at room temperature. The water was changed after the first hour of dialysis and again before the last hour of dialysis. Dialyzed juice was stored refrigerated (4°C) until used. Pellets of juice cloud were obtained by centrifugation of dialyzed juice at 343,000 x g for 30 min with a Beckman L8-M ultracentrifuge. The pellets were fixed in a 2% osmium tetroxide - 0.01M cacodylate buffer solution at pH 7.0 for 1 h, dehydrated in 50%, 70%, 95%, absolute ethanol and propylene oxide (two times each for 10 min), embedded in Epon 812 and cured at 60°C. Thin sections [60-90 nm (Hunter, 1984)] were obtained using a Reichert OM U2 ultramicrotome. The sections were stained first with 5% uranyl acetate for 20 min, washed in distilled water and then stained with Reynold's lead citrate in combination with 0.01 N NaOH (Sjostrand, 1967) for 10 min, washed with distilled water and placed on filter paper in a covered petri dish to dry.

Negative Staining

Copper grids (400 mesh) were prepared with a collodion support film (0.5% collodion in amyl acetate) and coated with carbon in an Edwards E306A high vacuum coating unit. The grid was placed on a drop of dialyzed juice for 5 min, transferred to a drop of distilled water for 1 min and washed with 10 drops 2% uranyl acetate. Excess stain was removed by touching the edge of the grid with a piece of filter paper. Grids were then air dried in a covered petri dish.

Results and Discussion

Thin Sectioning

Thin sections from pellets of cloud material from oxidized juice of fresh Spartan apples exhibited a high concentration of particles with a variety of structural characteristics and varying affinities for electron dense stains (Fig. 1). The structures were categorized as granules (g), spheres (s), aggregates (a) and vesicles (v) as tabulated in Table 1. Particle classification was complicated by the possible introduction of sectioning artifacts which could affect particle appearance and distribution (Hayat, 1981). Large vesicles with electron dense membranes were the most prevalent structures in sections of oxidized juice cloud (Fig. 1). Smaller structures such as spheres and granules were found not only individually, but also attached to the surface and within the interior of vesicles (Fig. 1). Spheres and granules also appeared to combine to form larger electron dense aggregates (Fig. 1). These structures were likely derived from fragments of cell walls and other cellular debris created during processing.

The varying affinity of vesicles, aggregates, spheres and granules for the electron dense stains was either an artifact of sectioning or indicated these structures were compositionally different. Since structures maintained these relative stain densities from section to section and from block to block, the differences were considered to be primarily compositional. The more electron dense aggregates and vesicular membranes in Figure 1, may have contained a greater number of exposed heavy metal binding sites than the less densely stained spheres and granules. Of the stains used, osmium reacts with proteins, lipids and membranes whereas lead reacts with hydroxyl groups of carbohydrates and sulfhydryl groups of protein, and uranium is bound by carboxyl and phosphoryl groups (Hayat, 1972; 1981). Studies have also shown that 2% uranyl acetate followed by lead citrate effectively stains cellulose (Hayat, 1981). Considering the composition of apple tissue, the most probable binding sites in the juice cloud would be hydroxyl and sulfhydryl groups of proteins from cell cytoplasm and membranes, with hydroxyl groups of polyanionic carbohydrates such as pectin from the middle lamella and phosphoryl groups of phospholipids from membranes

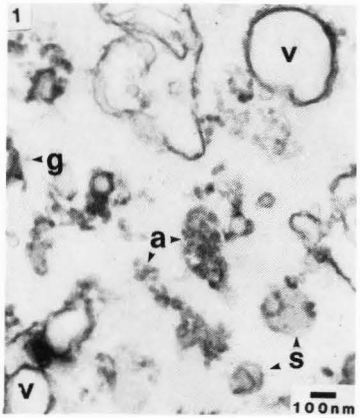

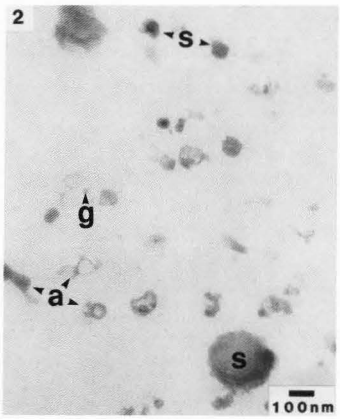

Figs. 1 and 2. Thin Section of pellets of cloud material from oxidized (Fig. 1) and unoxidized (Fig. 2) juice of fresh Spartan apples. Aggregate (a); granule (g); sphere (s); vesicle (v).

Table 1. Characterization of particles in thin sections of cloud material from the juice of fresh Spartan apples

Sample	Particle	Dimension (nm)		Stain density*
		Range	Mean	
Oxidized juice cloud				
	granule	18 - 32	25 diam.	slight-moderate
	sphere	56 - 28	152 diam.	slight-moderate
	aggregate	70 - 679	367 length+	moderate-extreme
		35 - 275	157 width	
	vesicle	96 - 410	273 diam.	
		6 - 39	20 wall	extreme
Unoxidized juice cloud				
	granule	15 - 37	22 diam.	slight-moderate
	sphere	50 - 335	117 diam.	moderate-heavy
	aggregate	12 - 342	180 length+	moderate-heavy
		50 - 157	77 width	

* Extreme = black; slight = just discernible over background.

+ Using the least significant difference test, aggregate particles in cloud from oxidized juice were significantly longer ($p \leq 0.05$) than similar particles in cloud from unoxidized juice.

accounting for a smaller number of the binding sites (Hayat, 1981). Although the formation of aggregates could be an artifact of the dehydration procedure, the presence of heavy metal binding sites suggests aggregation could also be caused by hydrogen bonding between exposed groups on the surfaces of the spheres and granules.

Thin sections of cloud material from unoxidized juice of fresh Spartan apples (Fig. 2) had fewer particles with less variety of structural

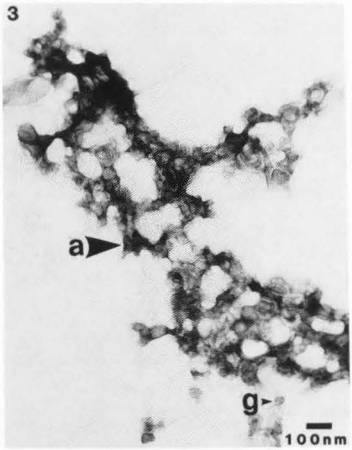

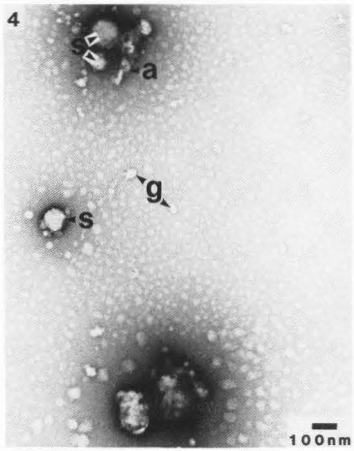

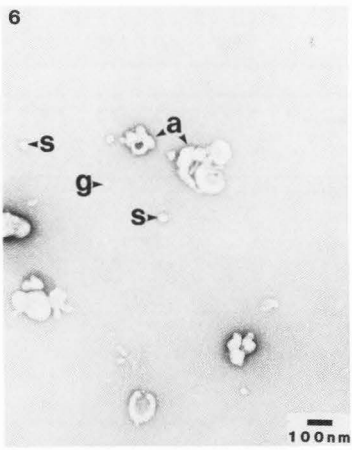

Figs. 3 - 6. Negatively stained particles from oxidized (Figs. 3 and 5) and unoxidized (Figs. 4 and 6) juice of fresh (Figs. 3 and 4) and stored (Figs. 5 and 6) Spartan apples not treated with enzyme. Aggregate (a); granule (g); sphere (s).

characteristics and a more uniform affinity for the electron dense stains than the structures of oxidized juice (Fig. 1 vs 2). Vesicles were not found in cloud from unoxidized juice and a comparison of other structures presented in Table 1 indicated that aggregates in unoxidized juice were significantly smaller ($p \leq 0.05$) and less distinct than those in oxidized juice. Blanching appeared to cause the disintegration and solubilization of aggregates observed in oxidized juice to form relatively smaller structures and more electron dense background in cloud from unoxidized juice (Fig. 1 vs 2).

Negative Staining

The dimensions of particles from negatively

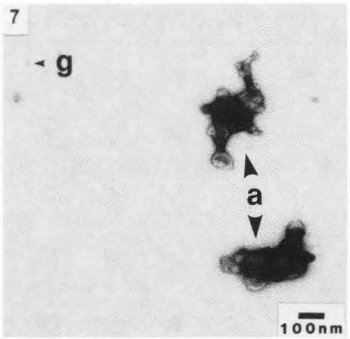

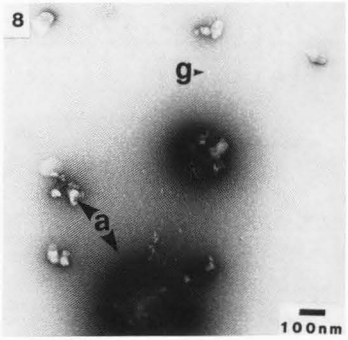

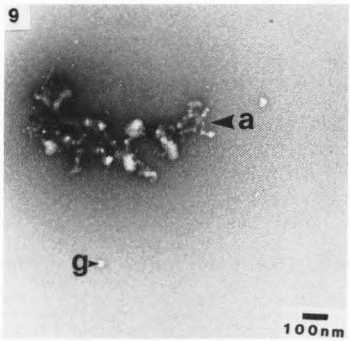

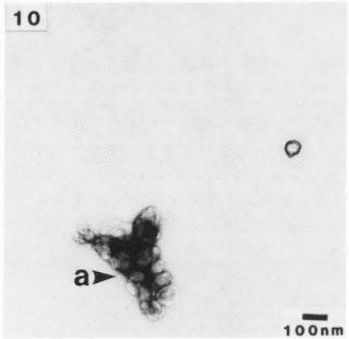

Figs. 7 - 10. Negatively stained particles from oxidized (Figs. 7 and 9) and unoxidized (Figs. 8 and 10) juice of fresh (Figs. 7 and 8) and stored (Figs. 9 and 10) Spartan apples treated with enzyme. Aggregate (a); granule (g).

stained juice samples (Figs. 3-10) are presented in Table 2. The structures were again categorized as granules (g), spheres (s) and aggregates (a) based on dimensions and stain density; no vesicular structures were present. Since vesicles were found only in thin sections of oxidized juice, it is likely that these structures were formed either as artifacts of centrifugation and alcohol dehydration or were cross-sections of spheres. Granules, spheres and aggregates on the other hand, were observed in each preparation of juice, although the relative proportions of the particles varied dramatically between preparations (Fig. 3 vs 4, 7 vs 8). Statistical analyses showed that treatment with enzyme significantly decreased granule size ($p \leq 0.01$), storage of apples also significantly decreased granule size ($p \leq 0.01$) and aggregate length ($p \leq 0.05$), and processing significantly increased granule ($p \leq 0.05$) and sphere size ($p \leq 0.01$) while significantly decreasing aggregate length ($p \leq 0.01$; Table 2).

Examination of Figs. 3-10 revealed several trends. Unoxidized juice from blanched puree not treated with enzyme had a larger number of smaller particles in the form of granules and spheres, whereas similarly prepared samples of oxidized juice consisted of fewer particles mainly in the form of aggregates (Figs. 3 vs 4). Blanching also significantly decreased aggregate length ($p \leq 0.01$), while significantly increasing granule size ($p \leq 0.05$) and sphere diameter ($p \leq 0.01$; Table 2). The aggregates appeared to be agglomerations of spheres and granules and could be an artifact of drying. However, aggregates were formed mainly in oxidized juice not treated with enzyme (Figs. 3, 5) and not in similarly prepared samples of unoxidized juice (Figs.4, 6). Since all grids were prepared in the same manner, the formation of aggregates in certain juice preparations and not in others suggests forces other than surface tension effects were involved in particle aggregation. More likely, the increased aggregation of

Table 2 - Characterization of particles on negatively stained grids of juice from Spartan apples.

Particle	Significant Treatment Effects		Dimensions (nm) Range	Dimensions (nm) Mean	Stain Density+
Granule (diameter)	i) Enzyme**	No enzyme	5 - 54	19	transparent
		Enzyme	3 - 20	12	
	ii) Storage**	Fresh	5 - 54	19	
		Stored	3 - 20	19	
	iii) Processing*	Unoxidized	3 - 54	17	
		Oxidized	5 - 20	14	
Sphere (diameter)	i) Processing**	Unoxidized	35 - 368	110	Slight-moderate with heavy envelope
		Oxidized	20 - 73	47	
Aggregate (length)	i) Processing**	Oxidized	35 - 2519	623	Slight-heavy with extreme envelope
		Unoxidized	60 - 1346	364	
	ii) Storage*	Fresh	35 - 2519	568	
		Stored	59 - 1346	400	
Aggregate (width)	not significantly different		17 - 611	155	

+ Extreme = black; slight = just discernible over background.

** Means significantly different at $p \leq 0.01$; * Means significantly different at $p \leq 0.05$.

particulate in oxidized juice results from the action of endogenous pectin methylesterase. This enzyme converts pectin to pectic acid which can react with calcium and other divalent ions to cause aggregation through the formation of calcium pectate bridges (JA Klavons, personal communication, 1988).

Compositional differences also existed between the particles forming the aggregates as indicated by the variation in stain density of the components within the aggregates (Fig. 3). Although negative staining with uranyl acetate was carried out, it appeared that some particles were negatively stained while other particles were positively stained (Fig. 3). Again, this suggested the presence of binding sites for uranium, e.g., protein carboxyl groups, pectin-like polyanionic carbohydrates which could be involved in hydrogen bonding and particle aggregation. Overall differences in staining were also observed between unoxidized and oxidized juices (Fig. 3 vs 4, 5 vs 6, 7 vs 8, 9 vs 10). Particles in oxidized juice were more heavily stained than similar particles in unoxidized juice which had only slight or moderately stained interiors surrounded by a diffuse layer of densely stained material (Fig. 3 vs 4). The presence of a negatively charged, heavy metal attracting envelope would stabilize the cloud particles in unoxidized juice not treated with enzyme by preventing the aggregation of particles through charge repulsion.

Storage of apples and no enzyme treatment during processing produced cloudy oxidized juice in which a small number of particles were embedded in a densely stained web-like matrix (Fig. 5). The particles also appeared to become less compact and less distinct than their counterparts in fresh juice (Fig. 3 vs 5) probably as a result of the gradual disintegration of cell structure during storage (Hulme, 1958; Hulme and Rhodes, 1971). The affinity of the web-like material for the uranyl acetate stain provided further evidence for the presence of uranium binding sites with potential for hydrogen bonding. The formation of a web-like matrix suggested the establishment of a gel network perhaps due to protein-protein or protein-pectin interactions (Fig. 5). The existence of a gel-like network which allowed for entrapment and imbibition of water, might account for the low yields of juice obtained when pressing stored fruit (Powrie and Tung, 1976; Glunk, 1981). Treatment with heat during blanching or Irgazyme 100 appeared to greatly reduce or eliminate the formation of a web-like matrix (Fig. 5 vs 6, 5 vs 9). The possibility therefore exists for improving juice yields by employing either a blanching step (Beveridge and Harrison, 1986) or an enzyme treatment when processing stored apples. Storage of apples resulted in a significant decrease in granule size ($p \leq 0.01$) and aggregate length ($p \leq 0.05$) in the juice (Table 2). The decrease in aggregate size was evidence for destructive processes occurring during storage.

The treatment of apple puree with Irgazyme 100 resulted in a significant decrease in granule size ($p \leq 0.01$, Table 2) as well as a decrease in the number of

particles present in the juice (Fig. 3 vs 7, 4 vs 8, 5 vs 9, 6 vs 10). The majority of particles present in oxidized juice treated with enzyme were granules most likely formed from the disintegration of larger aggregates (Figs. 7, 9). In contrast, treatment of unoxidized juice with enzyme resulted mainly in the formation of aggregates (Fig. 8). Aggregate formation in unoxidized juice after treatment with enzyme may have resulted from the enzymatic degradation of the intensely stained material surrounding the particles observed in the juice from untreated puree (Fig. 4 vs 8). Degradation of the enveloping material would reduce interparticle repulsion. The resulting interaction of particles would lead to the formation of a larger number aggregates than in untreated juice (Fig. 4 vs 8). Enzyme treatment of unoxidized juice seemed to follow several stages of degradation before reaching the same level of clarification observed in oxidized juice, thus accounting for the longer incubation times or larger amounts of enzyme required to clarify unoxidized juice (Beveridge et al., 1986). In oxidized juice, the enzymes appeared to directly reduce particle size and number (Figs. 3 vs 7). However, in unoxidized juice the enzymes first reduced the thickness of the enveloping material, followed by the formation of numerous aggregates (Fig. 8), before a decrease in particle number and degradation of aggregates became apparent (Fig. 10).

Enzyme treatment of stored apples appeared to be more effective for reducing cloud than enzyme treatment of fresh apples. Juice from stored apples treated with Irgazyme 100 generally had fewer particles than similar preparations of juice from fresh apples (Fig. 8 vs 10).

Conclusions

Particle dimensions as measured in thin sectioned and negatively stained apple juice showed that no significant difference existed with respect to aggregate dimensions ($p \leq 0.05$). However, the dimensions of the spheres and granules in thin sections of apple juice cloud were significantly larger ($p \leq 0.05$) than similar particles in negatively stained preparations (Table 1 vs Table 2). The fixation procedure for thin sectioning is more severe than for negative staining with a greater potential for introduction of artifacts and distortion of particles, possibly accounting for the differences in particle dimensions observed by these two techniques. Although statistical differences were noted, overall the appearance (Fig. 2 vs 4) and dimensions of the particles (Table 1 vs Table 2) observed by these two different techniques were very similar. Of the two techniques, thin sectioning was more time-consuming and therefore impractical for a large number of samples, while negative staining was simple and rapid, supplying substantial structural information as well as compositional information based on particle-stain interactions.

For the apple juice manufacturer, production of a cloudy unoxidized juice appears possible from either fresh or stored apples since stored apples produce juice with more particulate, while unoxidized juice from fresh apples is more resistant to enzyme clarification indicating a more stable suspension. Clarified unoxidized juice could also be made either by filtration of juice from fresh apples or by enzyme treatment of juice from stored apples, allowing the processor to produce several different products from a single raw material.

Acknowledgements

The authors gratefully acknowledge the generous donation of microscope time and associated preparatory and photographic materials by the Agriculture Canada Research Station, Vancouver, B.C. The authors thank Mr. F. Skelton and Dr. F. Leggett for their technical advice and guidance throughout this investigation.

Contribution number 691.

References

1. Atkinson FE, Strachan CC (1949a). Natural Apple Juice. Food Industries of South Africa, June: 37-39.

2. Atkinson FE, Strachan CC (1949b). Production of Juices. Agriculture Canada Technical Bulletin No. 68. 16-32.

3. Bauernfeind JC (1958). The Role of Ascorbic Acid in the Browning Phenomenon of Fruit Juice. F. Hoffmann-La Roche and Company, Ltd. Basil, Switzerland. p. 172.

4. Beveridge T, Harrison J (1986). Pear Juice Production from Heated Pear Mashes. Can. Inst. Food Sci. Technol. J. 19(1): 12-16.

5. Beveridge T, Franz K, Harrison J (1986). Clarified Natural Apple Juice: Production and Storage Stability of Juice and Concentrate. J. Food Sci. 51(2): 411-414, 433.

6. Carpenter DC, Walsh WF (1932). The Commercial Processing of Apple Juice. New York State Experimental Station Technical Bulletin No. 202. 3-21.

7. Glunk U (1981). Increasing the Juice Yield of Pressing with Special Remarks on the Warm Extraction of Apples. Flussiges Obst. 8: 248-255.

8. Hayat MA (1972). Principles and Techniques of Electron Microscopy: Biological Applications. Vol. 2. Van Norstrand Reinhold Co. New York. p. 30-151.

9. Hayat MA (1981). Principles and Techniques of Electron Microscopy: Biological Applications. Aspen Publishers, Inc. Rockville, MD. 301-316.

10. Holgate KC, Moyer JC, Pederson CS (1948). The Use of Ascorbic Acid in Preventing Oxidative Changes in Apple Juice. The Fruit Products J. and American Food Manufacturer 28: 100-112.

11. Hulme AC (1958). Some Aspects of the Biochemistry of Apple and Pear Fruits. Advances in Food Research 8: 297-413.

12. Hulme AC, Rhodes JC (1971). Pome Fruits. In: The Biochemistry of Fruits and Their Products. AC Hulme (Ed.). Academic Press. London. 333-373.

13. Hunter EE (1984). Practical Electron Microscopy: A Beginner's Illustrated Guide. Praeger Publishers. New York. p. 65.

14. Lau OL (1985). Harvest Indices for British Columbia Apples. British Columbia Orchardist July: 7-13.

15. Powrie WD, Tung MA (1976). Food Dispersions. In: Principles of Food Science Part I: Food Chemistry. OR Fennema, (ed.). Marcel Dekker, Inc. New York. p. 554.

16. Sjostrand FS (1967). Electron Microscopy of Cells and Tissues. Vol. 1. Instrumentation and Techniques. Academic Press. New York. p. 300.

Discussion with Reviewers

J.A. Klavons: In citrus juices, "cloud" is defined as particles that scatter visible light, (0.4-0.8 μm). It is generally isolated via centrifugation and therefore contains particles up to approximately 50 μm. Particles larger than 50 μm are considered " pulp". This paper deals with particles (or aggregates) up to approximately 2.5 mm. In the case of citrus juices, the cloud (particles up to 50 μm) have a different composition than do the larger "pulp" particles. As the particle size increases, the ratio of pectin to protein increases. Large "pulp" particles contain much pectin. The physical and chemical properties of pectins are complex and the authors mention them to some degree. However, a very important aspect of cloud stability in citrus juices is the heat inactivation of pectin methylesterase. In unpasteurized (unheated) citrus juices pectin methylesterase converts methoxy pectin to pectic acid. Pectic acid reacts with calcium, or other divalent ions in the juice to form calcium pectate, which destabilizes the cloud and results in cloud loss. Probably, apple juice (and apple puree) that has not been heat inactivated also contains pectin methylesterase (in addition to the pectinase that the authors mention). It would appear that in the cases of non-heat treated apple juice, this phenomenon could account for the aggregation of the particles.
Authors: The particles observed in apple juice ranged from 0.003 μm to 2.5 μm (scales were in nm not μm dimensions). Based on these measurements, the particles can be classified as "cloud" rather than "pulp". A discussion of pectin methylesterase and its possible role in the formation of aggregates through calcium bridging was considered important and so included in the text.

J.A. Klavons: I question the use of such high g-force (343,000 x g) for the isolation of such large particles. In the case of citrus cloud (as defined above) centrifugation at 27,000 x g for 15 minutes is sufficient to reduce the turbidity by 99%. The authors mention that some of the aggregation they are observing could be due to this treatment. I feel that this is a very real possibility.
Authors: We agree that some of the aggregation observed is probably due to this treatment, however, these centrifugal forces are required to completely sediment all cloud particles in the juice.

J.F. Chabot: What was the reason for the dialysis step?
Authors: The dialysis step was used to remove sugars which otherwise caused the collodion support film to split in the presence of the electron beam.

J.F. Chabot: Why not add fixative directly to the juice?
Authors: On negatively stained preparations, addition of fixative directly to juice prior to staining did not improve the quality of the grids so stain alone was used.

J.F. Chabot: Why fix first in osmium tetroxide, instead of glutaraldehyde?
Authors: Since only one fixation step was used, osmium tetroxide (rather than glutaraldehyde) was chosen as a fixative due to its ability to increase contrast.

J.F. Chabot: Do you think there would be a difference in size distribution if you fixed first, and then centrifuged, versus fixing the precipitate after centrifugation?
Authors: There would probably not be a difference, since in negatively stained preparations use of fixative prior to staining did not appear to alter the size distribution of particles present, however, this was not explicitly tested with the centrifuged particles.

J.F. Chabot: There seemed to be no definitive structures that could be related to normal cells in apples. Were no wall found? These usually have a substructure which is characteristic. It was impossible to relate granules and spheres to normal cytoplasm. Were the spheres lipid in nature?
Authors: No walls were found; however, based on the severity of the processing treatments this was not unexpected. Considering the low levels of lipid material present in apple juice, the spheres are more likely to be proteinaceous or pectinaceous in nature.

J.F. Chabot: Did blanching result in a loss of vesicles because of the effect on membranes?
Authors: Blanching could possibly have resulted in a loss of vesicles through heat-induced solubilization of the middle lamella with resulting dispersion of cell wall material.

J.F. Chabot: If all treatments were processed for transmission electron microscopy in the same manner, why would you attribute measured differences between treatments to artifact?
Authors: The fact that measurable differences existed was, on the contrary, used to suggest that the differences were real and not artifact.

J.F. Chabot: Did you examine any sections with different staining procedures, i.e., without lead, or without uranium salts?
Authors: No; however, phosphotungstic acid (PTA) was used with similar results to uranyl acetate in negatively stained preparations.

J.F. Chabot: Why would blanching change staining properties?
Authors: Blanching could lead to conformational changes in the components which might appear as changes in the staining properties of the particulate.

J.F. Chabot: Given the lack of structure in particles in juice, attributing a change as a result of storage to disintegration of cell structure seems unjustified on the basis of the data presented.
Authors: Storage is known to result in degradative changes in the middle lamella binding cells together through the cell walls. What we think we are seeing is a result of these changes in the pectinaceous material of the middle lamella.

J.F. Chabot: Attributing low yield to the formation of a water retaining matrix cannot be done from these pictures. No examination of the apple pulp has been presented.
Authors: This is true, however, it was clear from the centrifuged sediment resulting during yield measurement (3000 x g, 20 minutes) that changes had

occurred which resulted in increased water binding by the material in the pellet.

J.F. Chabot: In Fig. 1, how do you know the "v" is a membrane fragment? Could this structure and the one on the left be fragments of cell wall?
Authors: Yes, it is possible that vesicles could be either fragments of membranes or cell walls.

J.F. Chabot: In Fig.6, how do you distinguish between minor imperfections in the negative stain background from particles?
Authors: Similar structures were seen in other negatively stained grids of this sample as well as in similar samples examined by shadow casting.

K.G. Lapsley: Have other researchers also used the terms granules, spheres, and aggregates to differentiate the structural matter present in apple juice?
Authors: There appears to have been no work done prior to this study on the structure of particulate in apple juice as viewed by electron microscopy. However, electron microscopic investigations of orange juice particulate have used similar descriptors.

K.G. Lapsley: Have you tried any other techniques for compositional analysis?
Authors: Composition of cloud material has been investigated using HPLC and automated nitrogen analysis which suggest that apple juice "cloud" consists mainly of a combination of protein, pectin and cellulose.

G.G. Jewell: Does the quantity of appearance of the particles from the enzyme-treated juice change with either the pH of treatment, or does the presence of enzyme influence the negative stain?
Authors: The effect of treatment at different pH levels was not examined. The presence of enzyme did not appear to alter the effect of the negative stain since particles of similar shapes and dimensions were also obtained by shadow casting.

G.G. Jewell: What effect does incomplete pasteurization have on the structure of the cloud?
Authors: The effect of incomplete pasteurization on the structure of the cloud was not examined, but it would be expected that a gradual shift from a few large aggregate particles to increased numbers of spheres and granules would occur as the severity of the heat treatment increased.

FOOD MICROSTRUCTURE, Vol. 7 (1988), pp. 205-212
Scanning Microscopy International, Chicago (AMF O'Hare), IL 60666 USA

0730-5419/88$3.00+.00

SCANNING ELECTRON MICROSCOPY OF CELLULAR STRUCTURE OF GRANNY SMITH AND RED DELICIOUS APPLES

Gassinee Trakoontivakorn[1], Max E. Patterson[2] and Barry G. Swanson[1*]

[1]Department of Food Science & Human Nutrition
and
[2]Department of Horticulture and Landscape Architecture
Washington State University, Pullman, WA 99164.

Abstract

Immature and mature Granny Smith and Red Delicious apples (*Malus domestica* Borkh.) were studied with scanning electron microscopy (SEM). Parenchyma cells were observed to form a net-like pattern in sections transverse to the stem-calyx of the apple. Bundles of about six intact cells were connected, creating large intercellular spaces. The intercellular spaces were different in shape from different perspectives to the cut surfaces; round in stem-calyx transverse sections and elliptical in stem-calyx cross sections. Cell areas, cell lengths and intercellular space areas were determined with image analysis. The patterns of mature apple cell structure of both cultivars were observed to be similar to the patterns of immature apple cell structure. Both cell area and intercellular space area were larger in mature than in immature apples. Cells of mature apples were longer and more elliptical than cells of immature apples. The patterns of intercellular space area and cell length in Granny Smith and Red Delicious apple cultivars were not the same.

Initial paper received Aug. 04, 1988
Manuscript received Nov. 30, 1988
Direct inquiries to B.G. Swanson
Telephone number: 509 335 4015

Key Words: Apple cellular structure, scanning electron microscopy, Granny Smith apple, Red Delicious apple, *Malus domestica* Borkh., immature apple, mature apple, cell area, intercellular space area, cell length.

*Address for correspondence:
Barry G. Swanson
375 Clark Hall
Department of Food Science and
Human Nutrition
Pullman, WA 99164-6330
(509) 335-4015

Introduction

The cell structure of apple flesh was investigated in the early 1940s (Smith, 1940; Tukey and Young, 1942) with optical microscopes. Later, a more developed stereoscopic microscope was applied by Reeve (1953) to observe apple cellular structures.

During the past 20 years, transmission electron microscopy (TEM) has been the primary instrument used to observe apple cell ultrastructure. TEM ultrastructure studies illustrated cell organelles and cell wall changes of apple tissues as maturity increased (Saikia, 1969; Ben-Arie et al., 1979) and physiological development occurred (Mahanty and Fineran, 1975; Fuller, 1976).

In recent years, scanning electron microscopy (SEM) was applied in a few studies of the physical properties of apple cells (Diehl et al., 1979; Simons and Chu, 1980; Bolin and Huxsoll, 1987; Kovács et al., 1988). With the great depth of focus from the SEM, details of cell concavity and cell arrangement of apple tissues can be observed. More information about apple cell structure is provided with SEM than is available from previous investigations of apple cell structure.

Reeve and Leinbach (1953) and Reeve (1970) related cell structure, size of cells, intercellular spaces and composition as factors influencing textural qualities associated with fresh and processed fruits and vegetables. Reeve and Neufeld (1959) proposed that cell size had a definite effect on canned peach texture. Large cell volumes in peach pieces (19.9-21.8 μm^3) resulted in a coarse, stringy and often ragged texture. Small cell volumes in peach pieces (10.2-12.9 μm^3) resulted in a firm, fine and coherent canned peach texture.

Granny Smith and Red Delicious apples were selected cultivars for this research, since both are principal cultivars produced in Washington State.

Immature apples of both cultivars were investigated to provide baseline cell structure and morphology.

The objectives of this research were to characterize cell structure of Granny Smith and Red Delicious apple fruits, and to study cell size, cell shape and intercellular space area of immature and mature apples.

Materials & Methods

Granny Smith and Red Delicious apples (*Malus domestica* Borkh.) were harvested from trees growing in the Washington State University campus orchard. Immature fruits of both cultivars were picked in the last week of August, 1986. Mature Red Delicious apples were harvested on October 6, 1986. Mature Granny Smith apples (1985 apples) were obtained from the Postharvest Physiology Laboratory, Washington State University. Scanning electron microscopy (SEM) examinations of mature apple tissues were from post-climacteric fruits. Mature Red Delicious apple tissues were analyzed one month after harvesting. Mature Granny Smith apple tissues were analyzed after 7 months of controlled atmosphere storage.

Preparation of apple tissues

Fifteen millimeter diameter cylinders were cut through the center of Granny Smith and Red Delicious apples at right angles to the stem-calyx axis with a cork borer. Prior to punching out a cylinder, a downward arrow (stem to calyx) was marked on the apple skin at the end center of the cylinder as an orientation mark. The cylinder was sliced into 2 mm thick discs, from approximately 1 mm under the skin through the core line. Each side of each disc was labelled; the surface toward the skin was labelled A, and the surface toward the core was labelled B. Small 2 x 4 mm pieces of apple tissue were cut from the center of each disc and labelled by cutting the point from one or two corners with a razor blade. One cut corner on the 4 mm side indicated the upward portion (stem) and two cut corners on the 4 mm side indicated the downward portion (calyx) of apple fruit. As labelled apple tissues on stubs were viewed, one cut on the 2 mm side on the left-bottom corner and two cut corners on the right hand side indicated a surface A perspective. Surface B perspective was indicated with the appearance of one cut corner on the 2 mm side on the right-bottom corner and two cut corners on the left hand side.

Preparation for Scanning Electron Microscopy

Marked apple pieces were fixed with 3% glutaraldehyde in 0.1 M cacodylate buffer (pH 7.3) for 24 h at 4° C. The apple pieces were washed in three changes of 0.1 M cacodylate buffer (pH 7.3) for 10 min each to remove excess glutaraldehyde which will react with osmium tetroxide and leave a dense precipitate on the surfaces of apple tissues (Trump and Ericsson, 1965; Trump and Bulger, 1966). The apple pieces were post-fixed with 2% aqueous osmium tetroxide for 1 h at 4° C. Dehydration was accomplished in an ethyl alcohol series (10%, 20%, 30%, 40%, 50%, 60%, 70% for 10 min each ; 80%, 90% and 95% for 15 min each and 100% 3 times for 15 min each). Ethanol dehydrated apple pieces were critical point dried (Bomar SPC-1500) using carbon dioxide as the transitional fluid. The dried apple pieces were sputter coated (Hummer-Technics) with 300 Å gold and observed with an ETEC U-1 scanning electron microscope (Hayward, CA) operated at 20 kV.

Cell measurement

Cell area, intercellular space area and cell length were measured using a Bioquant II image analysis system (Boyle Instruments, Gig Harbor, WA). Cell area and intercellular space area were measured from SEM micrographs of surface A and/or B of apple discs. The cut corners on apple tissues were observed as diagonal cut areas and used to measure cell length.

Results & Discussion

The gross cell structures of Granny Smith and Red Delicious apples were generally similar. As seen in Fig. 1A-D and 2A-D, parenchyma cells are loosely arranged in a net-like pattern in the outer and middle regions of the apples. Bundles of about six intact cells are attached together to create large intercellular spaces. However, the intercellular space sizes became smaller as the distance from the skin increased toward the core line in stem-calyx transverse sections (Fig. 1A-F, 2A-F). Long elliptical cell shape and an increase in the number of cells in the inner area are related to reduction in size of intercellular spaces. The shapes of intercellular spaces change from round to ellipsoid from different perspectives to the cut surfaces. The stem-calyx transverse section SEM micrographs illustrate round intercellular spaces (Fig. 1A-F, 2A-F, 3A-F, 4A-F). The stem-calyx cross sections SEM micrographs illustrate ellipsoid intercellular spaces (Fig. 5A-F). Observations of apple intercellular space shapes are in agreement with intercellular space shapes previously observed by Reeve (1953) under a stereoscopic microscope.

The cell area from stem-calyx transverse sections became slightly smaller as the distance increased from the skin to the core line (Fig 1A-F, 3A-F). The shape of cells appeared to be

isodiametic within 6 mm beneath the skin. Overall, apple cell shapes tend to become more elliptical and longer toward the core line (Fig. 5A-F).

Cell structure of Granny Smith and Red Delicious apples

Cell area Table 1 illustrates that cell areas of immature Red Delicious apples were larger than cell areas of immature Granny Smith apples. Cell areas of immature Granny Smith apples were smallest in the region 2 - 4 mm above the core line compared to cell areas closer to the skin (Table 1, Fig. 3D,E). However, cell areas were nearly the same size among different regions overall. Cell areas of outer cells near the skin of immature Red Delicious apples (.021 - .024 mm^2) appeared larger than the middle cells (.015 - .018 mm^2) or the cells near the core (.015 - .018 mm^2) (Fig. 4A-F).

Cell areas from all sections of mature Red Delicious apples were larger than cell areas of mature Granny Smith apples (Table 1). Cells throughout mature Granny Smith apples were nearly the same size. Cells approximately 3 mm beneath the skin of mature Red Delicious apples were observed to be the largest in size compared to cells in the rest of Red Delicious apples.

In general, the outer cells of immature and mature apples of both cultivars were slightly larger than cells in the middle or inner regions (Table 1). The observations of consistently larger cells near the skin were in contrast to previous observations that cells towards the skin were slightly smaller than cells located farther away from the skin in apple cultivars examined by Reeve (1953).

In both cultivars, cells of immature fruits were smaller in area than cells of mature fruits (Table 1). Increase in cell size is pronounced in mature Red Delicious apple cells compared to immature Red Delicious apple cells. The ratio of mature:immature cell area of Red Delicious apples illustrated that cells in the middle region of mature apples are approximately two times larger in size than cells in the middle region of immature Red Delicious apples.

Overall, the cell areas of Granny Smith apples were smaller than the cell areas of Red Delicious apples in both immature and mature apples.

Intercellular space area Immature Granny Smith and Red Delicious apples contained a similar percentage of intercellular space area (ISA), ranging from 11 to 32% in an SEM micrograph area of 3.04 mm^2. The percentage ISA in the outer regions (21-32%) of Granny Smith and Red Delicious apples was greater than the percentage ISA in the middle regions (11-17%) or the percentage ISA in the inner regions (11-15%) of both cultivars.

Table 1. Cell area of immature and mature Granny Smith(GS) and Red Delicious(RD) apples.

cultivar	sample region	cell area[a] (mm^2) immature	mature	ma:im ratio
GS	outer	.017<1A>	.022<1A>	1.3
		.019<1B>	.020<1B>	1.1
	middle	.019<2B>	.019<3B>	1.0
		.012<4B>	.017<4B>	1.4
	inner	.015<5B>	.019<7B>	1.3
		.020<6B>	.018<8B>	0.9
RD	outer	.024<1A>	.027<1A>	1.2
		.021<1B>	.042<1B>	2.0
	middle	.018<2B>	.033<3B>	1.8
		.015<3B>	.033<4B>	2.2
	inner	.018<4B>	.027<7B>	1.5
		.015<5B>	.022<8B>	1.5

a) means of 17-40 cells
<> slice no. and surface of perspective

Table 2. Intercellular space areas(ISA) of immature and mature fruits of Granny Smith(GS) and Red Delicious(RD) apples.

region	ISA[a](%) GS immature	GS mature	RD immature	RD mature
outer	27.25	43.23	26.51	30.39
middle	12.18	27.88	15.71	35.97
inner	13.06	28.02	12.24	13.64

a) calculated from

$$\frac{\text{total intercellular space area}\,(mm^2)}{3.04\ mm^2\ \text{SEM picture area}} \times 100$$

Table 3. Cell length of immature(im) and mature(ma) Granny Smith(GS) and Red Delicious(RD) apples.

cultivar	region	slice No. im	ma	cell length[a] im	ma	ma:im ratio
GS	outer	1	1	0.227	0.250	1.1
		2	2	0.186	0.248	1.3
	middle	3	4	0.208	0.278	1.3
		4	5	0.203	0.304	1.5
	inner	5	7	0.196	0.340	1.7
		6	8	0.233	0.442	1.9
RD	outer	1	1	0.237	0.327	1.4
		2	2	0.201	0.334	1.7
	middle	3	5	0.197	0.287	1.5
	inner	4	7	0.266	0.340	1.3
		5	8	0.201	0.354	1.8

a) means of 25 cells, measured in mm

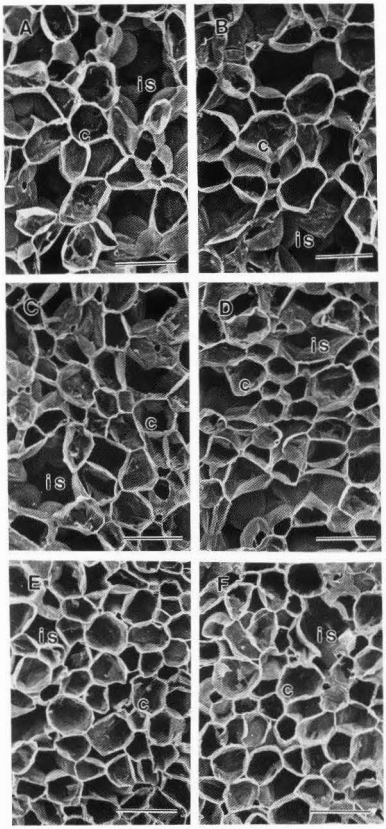

Fig. 1 Scanning electron micrographs showing cells (c) and intercellular spaces (is) of mature Granny Smith apples. A and B illustrate outer region, C and D illustrate middle region, E and F illustrate inner region. Bar = 250 μm.

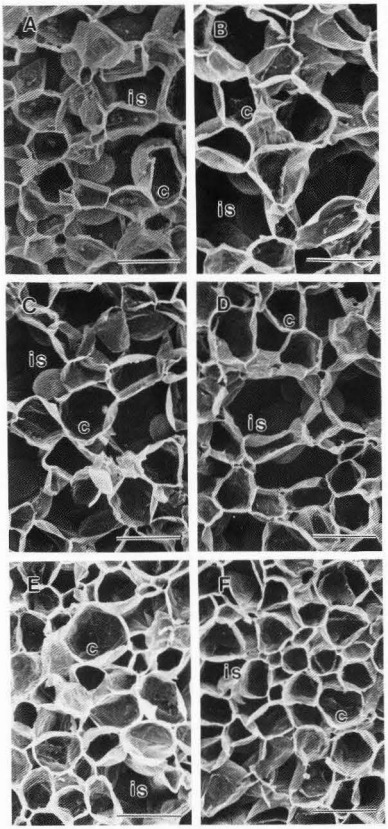

Fig. 2 Scanning electron micrographs showing cells (c) and intercellular spaces (is) of mature Red Delicious apples. A and B illustrate outer region, C and D illustrate middle region, E and F illustrate inner region. Bar = 250 μm.

However, no differences were noted among percentages of intercellular space areas between cultivars or regions of the immature apples.

Mature Granny Smith apples exhibited an intercellular space pattern different from mature Red Delicious apples. The ISA from outer and inner regions of Granny Smith apples were larger than the ISA from outer and inner regions of Red Delicious apples (Table 2). In Granny Smith apples, the ISA in the middle (27.88%) and inner (28.02%) regions were fairly similar, but the ISA in the outer region (43.23%) was larger (Table 2). In Red Delicious apples, the ISA from the outer region (30.39%) was similar to the ISA from the middle region (35.97%), which were larger than the ISA from the inner region (13.64%) (Table 2).

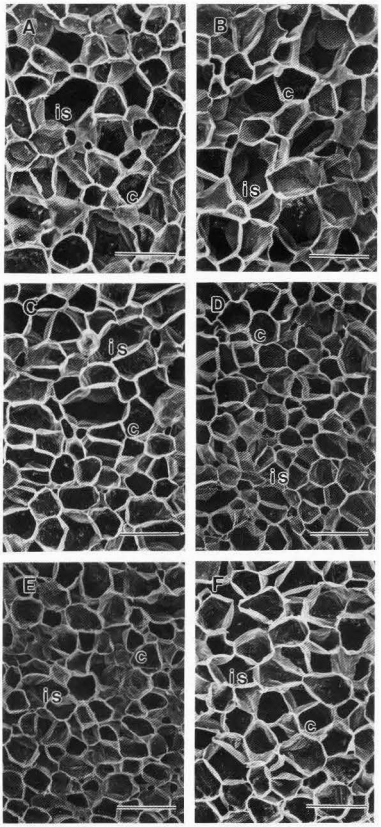

Fig. 3 Scanning electron micrographs showing cells (c) and intercellular spaces (is) of immature Granny Smith apples. A and B illustrate outer region, C and D illustrate middle region, E and F illustrate inner region. Bar = 250 μm.

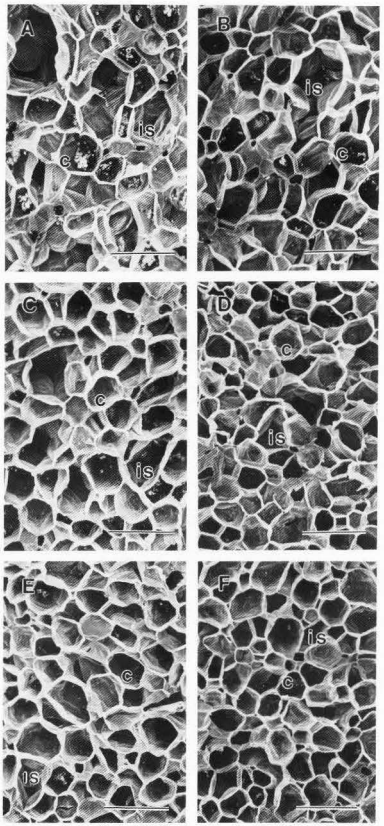

Fig. 4 Scanning electron micrographs showing cells (c) and intercellular spaces (is) of immature Red Delicious apples. A and B illustrate outer region, C and D illustrate middle region, E and F illustrate inner region. Bar = 250 μm.

The intercellular space patterns of mature Granny Smith and Red Delicious apples followed the same pattern as immature apples (Table 2). The percentage intercellular space of Granny Smith apples increased with increasing maturity in the outer, middle and inner areas observed (Table 2). Tukey and Young (1942) proposed that intercellular spaces increase greatly during the two months preceding fruit maturity. However, only the intercellular spaces in the middle region of mature Red Delicious apples were larger than the intercellular spaces in the middle region of immature Red Delicious apples (Table 2).

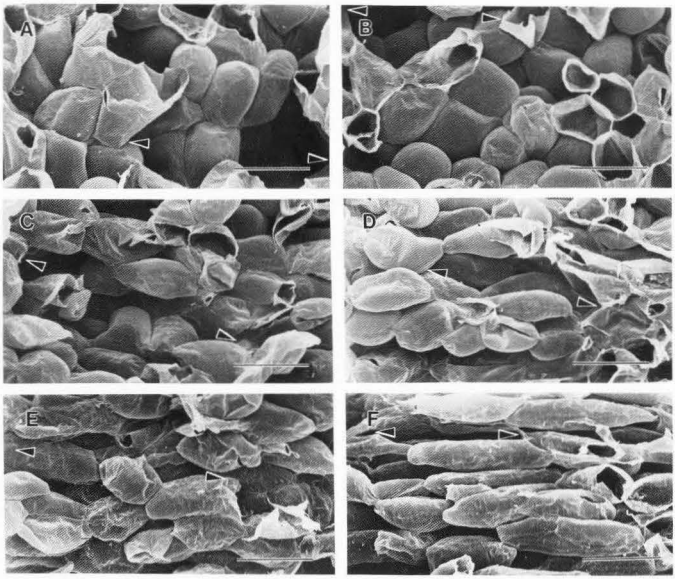

Fig. 5 Scanning electron micrographs showing cell shape changed from skin to the core of mature Granny Smith apples. A and B illustrate outer region, C and D illustrate middle region, E and F illustrate inner region. Bar = 250 μm. Arrows indicate intercellular boarders.

Cell length Cell length in the inner region of immature Granny Smith and Red Delicious apples exhibited the longest cells compared to cell length in other regions (Table 3). Cells in the outer region of immature Red Delicious apples were longer than cells in the outer region of immature Granny Smith apples (Table 3).

The cells became significantly longer as both Granny Smith and Red Delicious apple fruits aged, except in the 3 mm portion of Granny Smith apples near the skin (Table 3). Granny Smith apples exhibited a different cell pattern than Red Delicious apples. Granny Smith apple cells tended to increase in length, 0.250 to 0.442 mm, as distance of cells increased from the skin to the core line. Red Delicious apple cells were longest in the region under the skin and above the core line and shortest in the middle region of the apple.

The patterns of cell area, cell length and percentage intercellular space

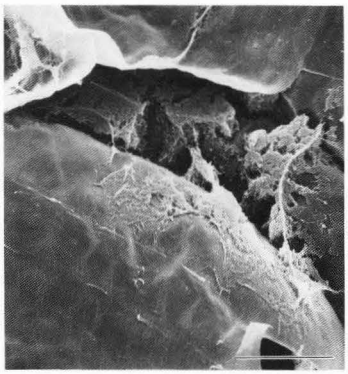

Fig. 6 Scanning electron micrograph showing apparent solids leakage in intercellular spaces of Granny Smith inner area. Bar = 50 μm.

of mature Granny Smith and Red Delicious apples were similar to the patterns of cell area, cell length and intercellular

space of immature Granny Smith and Red Delicious apples. The cell areas and intercellular spaces became larger and cell lengths became greater as maturation increased. Mature Red Delicious apple cells were larger and longer than Granny Smith apple cells.

MacArthur and Wetmore (1941) reported that cell differentiation of apple fruits was completed by the end of June. Three weeks were necessary to complete cell differentiation in McIntosh after full bloom (Tukey and Young, 1942). Immature apples of both cultivars in this study were in the enlargement period of fruit growth. Enlargement of fruit results primarily from an increase in intercellular spaces, cell lengths and/or cell sizes. Yamaki et al.(1979) proposed that the total polysaccharide content of Japanese pear cell wall per cell (DNA content basis) increased rapidly during the pre-enlargement period and remained almost constant during the enlargement period, while the pear fruits enlarged dramatically. The accumulation of polysaccharide substances in the cell walls during the pre-enlargement was necessary for increasing cell size and length.

Granny Smith apple tissues increased significantly in intercellular space area and cell length, but not in cell area during maturation. Red Delicious apple tissues increased significantly in cell length and cell area, but not in intercellular space area during maturation. Theoretically, cell walls of immature apples will be thicker than cell walls of mature apples, since immature apple cells have less surface area than mature apple cells with almost constant total polysaccharide content (Yamaki et al., 1979). Davis and Gordon (1980) reported that cell walls of carrot phloem in early developmental stage were thick with fibrous material. The cell walls of phloem in fully mature carrots were thin and firm with no fibrous material. Cell wall thickness was not measured in this research, however, cell walls of mature apples (Fig 1,2) appeared thicker than immature apple cell walls (Fig 3,4).

Solids leakage into intercellular spaces was observed in the inner region of mature Granny Smith apples (Fig. 6). Saikia (1969) observed transmission electron micrographs with accumulated solids in apple intercellular spaces during the climacteric increase in respiration rate. The accumulation of solids in intercellular spaces suggested that changes in cell membrane structure occurs without changes in cell morphology.

Conclusions

Characterization of the tissue and cell structure of Granny Smith and Red Delicious apples was achieved through use of scanning electron microscopy and image analysis. General cell arrangement and morphology of Granny Smith and Red Delicious apples remained the same during maturation while cell area, intercellular space area and cell length increased. Changes of cell shape and size suggest that the angle of observation for apple tissue must be precise to avoid misinterpretation of cell changes.

Acknowledgements

The authors acknowledge the use of the facilities of the Electron Microscopy Center, Washington State University.

References

Ben-Arie R, Kistev N, Frenkel C. (1979). Ultrastructural changes in the cell walls of ripening apple and pear fruit. Plant Physiol. 64, 197-202.

Bolin HR, Huxsoll CC. (1987). Scanning electron microscope/ image analyzer determination of dimensional post-harvest changes in fruit cells. J. Food Sci. 52, 1649-1650, 1698.

Davis EA, Gordon J. (1980). Structural studies of carrots by SEM. Scanning Electron Microscopy. 1980; III: 601-611.

Diehl KC, Hamann DD, Whitfield JK. (1979). Structural failure in selected raw fruits and vegetables. J. Texture Stud. 10, 371-400.

Fuller MM. (1976). The ultra-structure of the outer tissues of cold-stored apple fruits of high and low calcium content in relation to cell breakdown. Am. Appl. Biol. 83, 299-304.

Kovács E, Keresztes A, Kovács J. (1988). The effects of gamma irradiation and calcium treatment on the ultrastructure of apples and pears. Food Microstructure 7, 1-14.

MacArthur M, Wetmore RH. (1941). Development studies of the apple fruit in the varieties McIntosh Red and Wagener. II. An analysis of development. Can. J. Bot. 19, 371.

Mahanty HK, Fineran BA. (1975). The effects of calcium on the ultrastructure of Cox's Orange apples with reference to Bitter Pit disorder. Aust. J. Bot. 23, 55-65.

Reeve RM, Leinbach LR. (1953). Histological investigations of texture in apples. I. Composition and influence of heat on structure. Food Res. 18, 592-603.

Reeve RM. (1953). Histological investigations of texture in apples. II. Structure and intercellular spaces. Food Res. 18, 604-617.

Reeve RM, Neufeld CHH. (1959). Observation on the histology and texture of Elberta peaches from trees of high and low levels of nitrogen nutrition. Food Res. 24, 552-563.

Reeve RM. (1970). Relations of histological structure to texture of fresh and processed fruits and vegetables. J. Texture Stud. 1, 247-284.

Saikia BN. (1969). A study of ultrastructural changes during maturation and ripening of the apple fruit. Ph. D. thesis, Washington State University, Pullman, WA. pp. 179.

Simons RK, Chu MC. (1980). Scanning electron microscopy and electron microprobe studies of bitter pit in apples. In: Atkinson D, Jackson JE, Sharples RO, Waller WM. (eds). Mineral Nutrition of Fruit Trees. Butterworths, London, pp. 57-69.

Smith WH. (1940). The histological structure of the flesh of the apple in relation to growth and senescence. J. Pom. Hort. Sci. 18, 249.

Trump BF, Bulger RE. (1966). New ultrastructural characteristics of cells fixed in a glutaraldehyde-osmium tetroxide mixture. Lab. Invest. 15, 368.

Trump BF, Ericsson JLE. (1965). The effect of the fixative solution on the ultrastructure of cells and tissues. A comparative analysis with particular attention to the proximal convoluted tubule of the rat kidney. Lab. Invest. 14, 1245.

Tukey HB, Young JC. (1942). Gross morphology and histology of developing fruit of the apple. Botanical Gazette 104, 4-25.

Yamaki S, Machida Y, Kakiuchi N. (1979). Changes in cell wall polysaccharides and monosaccharides during development and ripening of Japanese pear fruit. Plant Cell Physiol. 20, 311-321.

Discussion with Reviewers

K. G. Lapsley: Do you feel you have examined enough apple tissue to be able to account for the variability in structure within any one apple?
Authors: More apples should be examined. However, the selected immature and mature apples were similar in size, shape and weight. Therefore, we believe the results are representative of the cell structure of Red Delicious and Granny Smith apples.

E. Kovács: How was the degree of ripening determined?
Authors: Apples were harvested after quality tests on color, acidity, pH, soluble solids, starch content and firmness. The respiration rates of apples were examined to predict ripening stage or maturity.

E. Kovács: What sampling method did you use?
Authors: Apples were selected by size, shape and appearance. After the first selections, apples of similar weight and density were selected to represent Granny Smith and Red Delicious cultivars.

E. Kovács: Is there any correlation between the textural changes and the size of cells/ size of intercellular spaces? Have you data on it?
Authors: Yes, fruits consisting of large cells with considerable intercellular space give a coarse or spongy texture. In contrast, fruits consisting of small cells with little intercellular space give a smooth texture (Reeve, 1970). We did not examine the relationship of cell size or intercellular space size to apple texture in this research.

E. Kovács: The quality of fruits are influenced by the weather, nutrition and humidity conditions of soil. How do these factors influence the size of cells and intercellular spaces?
Authors: Cell size, cell number and intercellular space of apples are affected by several factors (Westwood et al., 1970; Proc. Am. Soc. Hort. Sci. 91:51-62). Under adequate soil moisture and excess N fertilizer, apple cells tend to increase in size. The amount of intercellular space is related to fruit size, the larger the fruits the greater amount of intercellular space. Soil with available nutrients and adequate moisture available for growth is expected to provide large fruit from light-cropping trees.

E. Kovács: Do you plan to investigate processed apple products in the same way?
Authors: No, we have no plan to do further research on processed apple products.

K. G. Lapsley: Is 3 dimensional mapping of an apple possible yet?
Authors: Three-dimensional mapping is possible for parenchyma cells in the middle area of an apple perpendicular through the stem-calyx axis. Cell structure mapping at the stem or calyx ends must be based on representative observations of specific areas to complete 3-dimensional mapping of an entire apple.

FOOD MICROSTRUCTURE, Vol. 7 (1988), pp. 213-214
Scanning Microscopy International, Chicago (AMF O'Hare), IL 60666 USA

0730-5419/88$3.00+.00

Technical Note: ENCAPSULATION OF VISCOUS FOODS IN AGAR GEL TUBES FOR ELECTRON MICROSCOPY

Miloslav Kalab

Food Research Center, Agriculture Canada, Ottawa, Ontario, Canada
Telephone: (613) 995-3722 x 7707

(Received for publication Nov 26, 1988, and accepted for publication November 30, 1988)

Abstract

Viscous food is aspirated into a glass capillary tube with the inner diameter of approximately 0.5 mm if the food is to be examined by transmission electron microscopy. If the sample is destined for examination by scanning electron microscopy, it is aspirated into a Pasteur pipette having the diameter of 1.0 mm. In each case, the lower end of the glass tube is sealed with a droplet of 40°C warm 3% agar sol. After the sol solidifies, the pipette is dipped in the same agar sol and a coating, 0.2 to 0.5 mm thick, is formed around the glass tube by manipulating it while the sol is still liquid. Dipping may be repeated in order to form a uniform coating of desired thickness. The agar gel sleeve is then trimmed, and the pipette is withdrawn, whereby the sample slides into the agar gel sleeve. The free upper end of the agar gel tube is then sealed with a drop of the agar sol. The subsequent preparation of the encapsulated sample for electron microscopy is the same as that of a solid sample.

KEY WORDS: Agar gel tubes, Electron microscopy, Encapsulation, Viscous foods.

Introduction

Encapsulation of biological samples in agar gel tubes for subsequent examination by electron microscopy has been described by several authors [1, 3-7]. This technique may be used for scanning electron microscopy (SEM) as well as transmission electron microscopy (TEM). Food samples as diverse as milk [3, 4], orange juice [5], stirred yoghurt [1], and mayonnaise [2] have successfully been examined using this technique.

The techniques developed earlier consist of forming an agar gel tube around a piece of steel wire or a glass rod and using the wire or the glass rod as a piston when aspirating the sample into the agar gel sleeve. In this note, an easier and a more rapid approach is described. Its main features were published earlier [6].

Materials and Methods

Agar sol (3%) was made using distilled water and was stirred continually with a magnetic bar at 40°C.

A glass Pasteur pipette with inner diameter of 1.0 mm was used as obtained from the supplier for samples destined for SEM or was drawn out into a capillary tube to an inner diameter of approximately 0.5 mm for use with samples destined for TEM.

Commercial stirred-style yoghurt samples were aspirated into the thin capillary tubes to a length of approximately 2 mm, or were aspirated into the Pasteur pipettes to a length of 15 to 20 mm. The lower ends of the glass tubes were wiped clean with paper tissue and were sealed with droplets of the agar sol (Fig. 1).

After the sealed end had solidified, the capillary tube or the Pasteur pipette was dipped into the agar sol and then was manipulated to form a thin layer of agar gel on the glass surface around the sample. Dipping was repeated once or twice to form a uniform agar gel layer around each sample. The agar gel sleeve was then trimmed at the upper end of the sample and removed. The capillary tube or the pipette was then withdrawn from the agar gel sleeve, whereby the sample slid from the glass tube into the gel tube. The sample column in the agar gel tube was somewhat shorter than was its initial length in the glass tube following its removal because the inner diameter of the agar gel tube was larger than that of the glass tube. The freed upper end of the agar gel tube was then trimmed with a blade approximately 0.5 mm above the sample and was sealed with a droplet of the agar sol. It was then possible to handle the encapsulated samples as solid samples during the subsequent preparatory steps for electron microscopy.

Results and Discussion

The advantages of encapsulating viscous samples for electron microscopy have already been discussed in the literature [1-5]. However, some of the techniques are quite laborious. A high degree of manual dexterity is required to properly aspirate the sample into the agar gel tube using it as a cylinder while the solid rod around which the tube had been formed is used as a piston. This procedure leads to another problem, that is the need to seal both ends of the tube after the sample is aspirated and the piston is withdrawn.

The suggested technique (Fig. 1) simplifies the encapsulation procedure and markedly increases the productivity of the technician. The manipulation required to form a uniform gel coating by dipping the glass tube

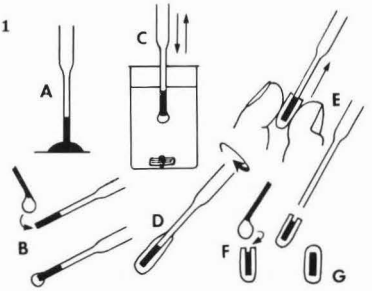

Fig. 1. Encapsulation of viscous food samples in agar gel tubes. A: Aspirate sample, B: Seal lower end of tube, C: Dip into agar sol, D: Rotate tube to form agar gel sleeve, E: Withdraw glass tube, F: Seal upper end of tube, G: Encapsulated sample.

containing the sample into agar sol can easily be learned. Should this appear difficult even after making several attempts, gels may be cast around the glass tubes using a technique that has been described elsewhere [5].

Very viscous samples such as Cream cheese can be encapsulated also provided that the above technique is slightly modified. As it is impossible to aspirate them into the tubes, the samples are placed in the tubes by repeatedly tapping the tubes into the samples which are placed on a firm support such as a microscope glass slide.

The ease with which the sample may be transferred from the glass tube into the agar gel sleeve depends on the viscosity of the sample and also on the quality of the seal at the lower end of the tube. If difficulties are encountered and the agar gel sleeve collapses, the seal should be strengthened with another agar sol droplet and a thicker agar gel sleeve should be formed.

Resin blocks containing food samples which had initially been encapsulated in agar gel tubes must be trimmed in such a way that the entire agar seal is removed along with the bordering area where the food sample and the agar gel may be mixed together.

Food samples encapsulated in agar gel tubes for subsequent SEM examination may be freeze-fractured following their fixation, dehydration, and impregnation with absolute ethanol. The agar gel coating may be left on the sample [1] or may be removed (Fig. 2).

Foods, which disintegrate in aqueous solutions and yet cannot be placed in glass capillaries to be prepared for TEM, may be coated with a thin agar gel layer in a different way. The sample is placed on the tip of a needle and touched with a droplet of warm agar sol (Fig. 3). The sol coats the food particle and immediately solidifies. The bead thus formed is removed from the needle and the exposed area of the food sample is sealed with another agar sol droplet. Again, the encapsulated sample can be treated as a conventional solid particle in any further preparatory steps.

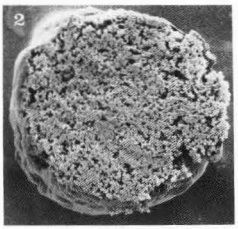

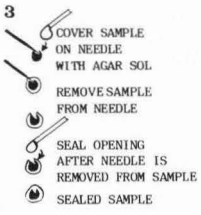

Fig. 2. SEM of stirred yoghurt. The sample was encapsulated in an agar gel tube, fixed, dehydrated, and freeze-fractured. The agar gel tube was removed prior to SEM examination.

Fig. 3. Coating of thick food samples with agar gel for TEM if the sample is too thick to be aspirated into a glass capillary tube.

Acknowledgments

Electron Microscopy Unit, Research Branch, Agriculture Canada in Ottawa provided facilities. Contribution 795 from the Food Research Centre.

References

1. Allan-Wojtas P, Kaláb M. (1984). A simple procedure for the preparation of stirred yoghurt for scanning electron microscopy. Food Microstruc. 3, 197-198.
2. Dylewski DP, Unger RS, Martin RW. (1988). Microstructure of oil-in-water fat spreads. Food Microstruc. 7 (in press).
3. Henstra S, Schmidt DG. (1970). Ultrathin sections of milk by means of the microcapsulation method. (In German). Naturwissenschaften 39, 247.
4. Henstra S, Schmidt DG. (1974). The microcapsule technique. An embedding procedure for the study of suspensions and emulsions. LKB Application Note No. 150.
5. Jewell GG. (1981). The microstructure of orange juice. Scanning Electron Microsc. 1981;III: 593-598.
6. Kaláb M. (1987). Encapsulation of viscous suspensions in agar gel tubes for electron microscopy. Electron Microsc. Soc. Am. Bull. 17(1), 88-89.
7. Salyaev RK. (1968). A method of fixation and embedding of liquid and fragile materials in agar microcapsulae. Proc. 4th Europ. Reg. Conf. Electron Microsc. Rome, II, 37-38.

Discussion with Reviewers

D. P. Dylewski: I would like to express some caution for the application of the above procedure to samples high in their lipid content. I would like to discuss the following three points:
(1) How is a sample, especially one high in lipid content, affected morphologically when it is dipped repeatedly into molten agar at a temperature of 40° to 45°C?
(2) When the removal of the space occupied by the glass tube is completed, how does the sample "pack" into the agar cylinder? Would mayonnaise, for example, retain its native or near natural form, that is, tight packing of lipid droplets?
(3) Using Salyaev's method [7], the sample is drawn in one step into the agar cylinder. Using your method, the sample is handled twice: first it is drawn into the pipette, then blown out into the agar gel cylinder. What are the effects, if any?

Author: The method has been developed in order to facilitate SEM investigation of small hard particles causing grittiness in protein-based milk products such as stirred yoghurt and soft cream cheese. The effect of temperature on high-fat foods such as mayonnaise would have to be tested. If problems are encountered, the agar gel tube around the glass capillary tube may be formed by smearing the agar sol around it rather than dipping the glass tube into the agar sol. This would limit the effect of heat on the sample as the smear cools quite rapidly.

Your concern for the loss of space and the effects of handling are closely related. In my opinion, greater effects on the packing of the sample constituents may be anticipated to originate from the initial aspiration rather than from the subsequent sliding of the sample into the agar gel tube. In viscous samples, there is no continuous matrix that would be at risk of disintegration. The distribution of corpuscular components would not be affected unless air is aspirated along with the samples and a new gas-liquid interface is thus formed in them.

It is advisable, however, that the effects of the factors which you have mentioned be investigated in the case of viscous high-fat foods.

Scanning Microscopy Supplement 2, 1988 ISSN 0892-953X

Proceedings of the Sixth Pfefferkorn Conference held Apr. 28 to May 2, 1987 at Niagara Falls, Canada on

Image and Signal Processing in Electron Microscopy

Edited by: P.W. Hawkes, F.P. Ottensmeyer, A. Rosenfeld and W.O. Saxton

39 papers; 396 + xii pages; hardbound; all papers reviewed (and contain discussion with reviewers); includes subject index and author index. **Price**: $60.00 (US delivery) and $65.00 (outside US delivery)

Contents

Order your copy from: Scanning Microscopy International, P.O. Box 66507 AMF O'Hare, Chicago, IL 60666, USA

Phone: 312 529 6677 FAX: 312 980 6698

DISCUSSION WITH REVIEWERS

Each paper in this journal contains a Discussion with Reviewers (**DWR**). This section follows the text (generally after references) and should be read as a part of the paper. Each paper submitted to Food Microstructure is reviewed by at least three reviewers. The reviewers are asked to separate their comments and questions. The comments are used in determining the acceptability of papers. The comments require no written responses from authors, however, in several cases, the authors prefer to include responses to comments, or to questions phrased from, or based on, these comments (either as a result of editorial suggestion or on the author's own initiative) in DWR.

The questions in DWR, for the most part, originate as a result of statements included in cover letters accompanying papers sent to the reviewers. The reviewers are asked to suppose they are attending a conference where the paper, as written, is presented, and ask relevant questions. From the questions so asked, some are not included with the published paper because the authors attend to them by text revisions. In some cases, editorial and / or space considerations may exclude inclusion of all questions asked by reviewers. The authors prepare the DWR section ready for publication. In some instances the authors edit the questions and / or group several similar questions from different reviewers to provide one answer. While all efforts are made to check that the questions in the printed version faithfully follow the views of the reviewer(s), the editors apologize, if the actual meaning and / or emphasis may have been changed by authors.

The cover letter to the reviewer also states:

"1. Your name will be conveyed to the author with your review UNLESS YOU ASK US NOT TO.

2. The questions published in the Journal will be identified as originating from you UNLESS YOU ADVISE OTHERWISE..."

Reviewers's wishes to remain anonymous are respected; however, in most (though not all) cases, the reviewers allow the identity disclosed to the authors. These reviewers names are included with questions printed with each paper. An overall list of reviewers and their affiliations (for each issue) is provided on the following page. We apologize for any error / omissions. The editors gratefully thank the authors and reviewers for their contributions, invite comments on ways to improve this procedure, and seek qualified volunteers to assist with reviewing papers in the future.

Finally, readers are urged to be cautious regarding the weight they attach to the authors' replies, since the answers to the questions represent the authors unchallenged views. Except for minor editorial changes, the authors generally have the last word. Also, please consider that the questions were, in most cases, relevant to the initially submitted paper, and they may not have the same significance for the revised paper finally published.

If you disagree with the approaches, results, or conclusions in a paper, please send your comments, as a Letter to the Editor, typed in a column format (4-1/8 by 11-1/2 inches or 10.5 by 29.3 cm.). The comments and author's response, will be published in a subsequent issue.

ERRATA: Despite the best efforts of authors, reviewers, and editors, errors may remain. Please help, by providing enough information to locate each error (issue, page, column, line, etc.), and indicating correction.

The Editors

FOOD MICROSTRUCTURE, Vol. 7 (1988)
Scanning Microscopy International, Chicago (AMF O'Hare), IL 60666 USA

REVIEWERS LIST

The help of the following individuals with reviewing of papers included in this years' issues is gratefully acknowledged (the names of editors of the journal, listed on the inside front cover, are excluded):

Akin, D.E.	U.S.D.A. Russell Agri. Res. Ct., Athens, GA
Bechtel, P.J.	University of Illinois, Urbana, IL
Borsa, J.	Radiation Applicatns. Res., Pinawa, Canada
Brooker, B.E.	AFRC Inst. Food Research, Reading, U.K.
Buchheim, W.	Bundes. Milchforschung, Kiel, West Germany
Carroll, R.J.	Emeritus, Norristown, PA
Cartwright, R.	Land O'Lakes Inc., Minneapolis, MN
Chabot, J.F.	Cornell University, Ithaca, NY
Creamer, L.K.	New Zealand Dairy Res. Inst., Palmerston
deMan, J.M.	University of Guelph, Ont., Canada
Dylewski, D.P.	Kraft Research & Dev. Lab., Glenview, IL
Faust, M.	U.S.D.A. Res. Center, Beltsville, MD
Gallant, D.J.	INRA Lab. Tech. Appl. Nutri., Nantes, France
Goll, D.E.	University of Arizona, Tucson
Gordon, J.	University of Minnesota, Saint Paul
Green, M.L.	AFRC Inst. Food Research, Reading, U.K.
Haggis, G.H.	Agriculture Canada, Ottawa, Ont.
Harbers, L.H.	Kansas State University, Manhattan
Heathcock, J.F.	Reading Scientific Serv., Reading, U.K.
Hermansson, A.M.	Swedish Food Institute, Goteborg, Sweden
Irving, D.W.	U.S.D.A.- Western Reg. Res. Lab., Albany, CA
Irwin, P.L.	U.S.D.A.- Eastern Reg. Res. Ctr., Philadelphia, PA
Jewell, G.G.	Quaker Oats Res. and Dev., Southall, U.K.
Jones, S.B.	U.S.D.A.- Eastern Reg. Res. Ctr., Philadelphia, PA
Jung, H.J.G.	University of Minnesota, Saint Paul, MN
Kakuda, Y.	University of Guelph, Canada
Kiss, K.	Stauffer Chemical Company, Dobbs Ferry, NY
Klavons, J.A.	U.S.D.A. Fruit and Veg. Chem. Lab, Pasadena, CA
Kovacs, E.	Central Food Res. Inst., Budapest, Hungary
Krog, N.	Grindsted Products, Brabrand, Denmark
Lapsley, K.	E. T. H., Zurich, Switzerland
Lee, C.M.	University of Rhode Island, Kingston
Lewis, D.F.	Br. Food Mfg. Indust. Res. Asso., Leatherhead, U.K.
Lillard, H.S.	U.S.D.A. Russell Res. Ctr., Athens, GA
Lott, J.N.A.	McMaster University, Hamilton, Ont., Canada
Mandels, M.	U.S. Army Natick Res. and Dev. Labs., MA
Martin, R.W.	Kraft Research & Develop., Glenview, IL
Miller, A.A.	U.S. Army Natick Res. and Dev. Labs., Natick
Monahan-Earley, R.	Beth Israel Hospital, Boston, MA
Moy, J.H.	University of Hawaii, Honolulu
Nath, K.R.	Kraft Research & Develop., Glenview, IL
Ogden, L.V.	Brigham Young University, Provo, UT
Packwood, R.H.	CANMET - EMR, Ottawa, Ont., Canada
Parnell-Clunies, E.M.	Ault Foods Limited, London, Ont., Canada
Pechak, D.G.	Kraft Research & Develop., Glenview, IL
Precht, D.	Bundes. Milchforschung, Kiel, West Germany
Reineccius, G.A.	University of Minnesota, Saint Paul
Richardson, G.H.	Utah State University, Logan
Ruegg, M.W.	Fed. Dairy Res. Institute, Liebefeld, Switzerland
Sargent, J.A.	Electron Micros. Consultn., Oxford, U.K.
Sarwar, G.	Health and Protection Br., Ottawa, Ont., Canada
Sato, K.	Hiroshima University, Fukuyama, Japan
Schmidt, D.G.	Netherlands Inst. Dairy Res., Ede
Schmidt, G.R.	Colorado State University, Fort Collins
Shaffer, E.W.	Brockway Inc. Research Ct., Brockway, PA
Simons, R.K.	University of Illinois, Urbana, IL
Smith, D.E.	University of Minnesota, Saint Paul, MN
Stanley, P.M.	Ecolab Research Center, Saint Paul, MN
Trinick, J.A.	AFRC Food Research Inst., Bristol, U.K.
Tung, M.A.	Technical Univ. Nova Scot., Halifax, Canada
Van Soest, P.J.	Cornell University, Ithaca, NY
Voyle, C.A.	AFRC Inst. Food Research, Bristol, U.K.
Walker, J.	U.S. Army Natick Res. and Dev. Labs., MA
Walstra, P.	Agriculture Univ., Wageningen, Netherlands
Zottola, E.A.	University of Minnesota, Saint Paul, MN

FOOD MICROSTRUCTURE, Vol. 7 (1988) ISSN: 0730-5419
Scanning Microscopy International, Chicago (AMF O'Hare), IL 60666-0507, U.S.A.

SUBJECT INDEX

Cumulative Author Index

FOOD MICROSTRUCTURE
INSTRUCTIONS TO AUTHORS

Papers for publication in the international journal Food Microstructure are invited. Papers can cover all types of foods, including vegetables, grains, sea foods, meat, dairy products and others. Topics of interest are: Fundamental aspects of food microstructure such as the molecular and colloidal forces which determine it, and the practical relationship between food microstructure and processing, ingredient changes, shelf life, consumer acceptability, and other food-related areas. Techniques used may include transmission and scanning electron microscopy, light microscopy, x-ray microanalysis, or other related microscopy/microanalytical methods.

Papers for Food Microstructure (FM) may be offered at any time. Papers can be for publication only, or intended for oral presentation at the Annual Food Microstructure meeting in early spring. The latter papers are due two months prior to the start of the meeting; only papers acceptable for publication are allowed oral presentation. Oral presentation of a paper at some other meeting or publication as unreviewed abstract (e.g., in proceedings, etc.) does not preclude consideration of a paper by FM.

The letter accompanying the paper should contain names and complete addresses of at least **four persons competent to review the paper**. Suggested reviewers: **a.** must neither be from author's current or recent affiliations, nor coworkers; **b.** should preferably be active researchers in the field (e.g., whose work is being extensively referred to); and **c.** need not be personally known or contacted by the authors. The editors **will select** the most suitable reviewers irrespective of their location. Each paper will be intensely reviewed by at least three reviewers.

The **initial paper (hereafter referred to as "paper")** should conform to **these Instructions.** However, to be published after reviewing, **the final manuscript (hereafter referred to as "manuscript") should be either a. submitted on the model sheets conforming to the Manuscript Preparation Guidelines (mailed along with the reviewers' comments), or b. sent to SEM Inc. for preparation at a nominal cost (per details mailed with reviews).** In addition to all the text, the **manuscript** may have to contain the author's publishable responses to questions raised by the paper's reviewers (see the Discussion with Reviewers in papers published in FM).

The following types of contributions can be offered. A length limit is not imposed on papers. Short, but complete, papers are welcome.

RESEARCH PAPER: Presents new unpublished findings.

REVIEW PAPER: Includes an extended literature review and complete bibliography, **emphasizes author's new unpublished findings** and in an extended discussion puts the topic in proper perspective.

TUTORIAL PAPER: Contains an **organized comprehensive review** of **ALL** relevant published material as for a teaching lecture.

TECHNICAL TIP: Paper should have no more than 1000 words.

LETTER TO THE EDITOR: Commenting on paper already published in FM.

The author should indicate the type of paper and carefully adhere to the applicable definition, since the reviewers and editors judge the paper accordingly.

INSTRUCTIONS FOR SUBMISSION OF PAPERS

Type paper in **double-spaced** format on standard size paper.

The paper should include title page, abstract, all headings and text. On the **title page** include: **a.** a **short title** which accurately represents the contents of the paper; **b.** an **informative running head** consisting of no more than 50 characters; **c. names and affiliations** of all authors, **name and complete work and home addresses and phone numbers of the person to contact; d. 10 key words/phrases** suitable for subject index; and **e. for review papers, indicate page numbers containing new material** (e.g., "new material will be found on pages __.").

An **Abstract** (of 100-250 words) is required for all papers. The Abstract should be concise and include the purpose of the paper, major results obtained and conclusions. Phrases such as "will be described," "is discussed," "are presented" etc. should be avoided.

The **Introduction** of the paper **must** contain a clear, concise statement of the purpose of the paper and the relationship of this paper to what is already in the literature. As applicable, a **Materials and Methods** section with **complete specimen preparation** information must be included (even if already published elsewhere), so that the work can be duplicated by others.

Equations should be numbered consecutively, using arabic numerals. Each **symbol and abbreviation** should be defined when first used. **SI units must be used;** other metric units or U.S. customary units (English), if used, must be given in parentheses.

REFERENCES

Include all references relevant to paper which are either readily available published works or papers in press. Work in progress, manuscripts submitted or in preparation, unpublished findings, personal communications etc. must be excluded from the reference list but may be acknowledged in the text (in parentheses).

The reference list at the end of the paper must be organized in alphabetical order by the first authors' names. Names of all authors (last names and initials only, with a comma between names and no other punctuation), full titles of papers, appropriate bibliographic information (with standard abbreviations for journals, and editors and publishers for books and proceedings), and inclusive pagination must be included. Availability information must be included for all non-journal references.

When referencing **SEM Inc. publications**, use the following formats only:

SEM Journal: Frederik PM, Busing WM, Persson A. (1984). Surface defects on thin cryosections. Scanning Electron Microsc. 1984; I:433-443.

Food Microstructure: Elgasim EA, Kennick WH. (1982). Effect of high hydrostatic pressure on meat microstructure. Food Microstruc. 1, 75-82.

In the **text, cite references** in one of the following two styles:

a. Cowley (1967) or (Cowley, 1967) or Crewe and Wall (1970). If there are three or more authors, use the form Venables et al. (1978). If more than one paper is published in the same year by the same author (or group of authors) use the form (Rose, 1974a), etc.

b. As long as there is consistency, either superscript[1] or full-size numerals in brackets [1] can be used. In this case, the numbering must be in sequence in the reference list, but the references will generally not appear in sequence in the text.

ILLUSTRATIONS AND TABLES

Number each figure and table with **an arabic numeral and refer to them in sequence in the text.** Several illustrations within a figure must be designated a, b, c, etc. Each table must have a title. ***Each figure must have a caption*** —either on its own page or all captions should be placed together on separate pages. **Very important: Use arrows or letters to identify features referred to, and so indicate in the caption.** Illustrate text with the fewest photographs possible. Indicate magnification on photos by a line of, e.g., 1μm, 10μm, 100μm, or 1 mm length; identify either on the photo or in the caption. Use nm, μm, or mm, not μ, u or -X.

Quality of Illustrations. *Photos should be clear, clean, unscreened* (screened photos are not acceptable), *black and white glossy prints.* **Color photographs** can be published by prior arrangement between author and the managing editor, whereby the author will be asked to pay the additional cost.

Size. For the *manuscript*, illustrations and tables should preferably be 10.5 cm wide. The maximum permissible length for photographs will be 9 cm (3.5"); line drawings and tables may be longer than 9 cm but not wider than 10.5 cm. All letters and symbols on illustrations and tables must be larger than 2.0 mm. **THE ILLUSTRATIONS, TABLES AND LETTERING INCLUDED WITH THE PAPER MUST CONFORM TO THESE SIZES.** *Permission for larger illustrations and/or tables must be requested when the paper is submitted.*

SUBMISSIONS AND COMMUNICATIONS

Submit 4 copies of the paper. Each of the 4 copies must include its own set of illustrations and clear glossy prints of all photographs. (Retain the best set of prints for your manuscript, since illustrations sent with paper may not be returned.) Papers containing photocopies (Xerox, etc.) of photographs will not be processed for reviewing; manuscripts containing photocopies of tables and illustrations are not accepted. All illustrations must be organized in sequence (must not be mounted on cardboards) and placed in separate envelopes. Place each copy of the paper *(together with its envelope of illustrations) in a separate, unsealed, ready-to-mail envelope,* so that the paper can be sent directly to its reviewers.

For **submission** of papers and **inquiries** contact: one of the editors or **Dr. Om Johari**, Managing Editor, **(phone 312-529-6677)**, P.O. Box 66507, AMF O'Hare, IL 60666 USA. (**Street address,** if needed, is: 1034 Alabama Dr., Elk Grove Village, IL 60007, USA).

OTHER IMPORTANT ITEMS

Reprints. 15 complimentary tear sheets are provided. Information for ordering additional reprints is sent with the proofs.

Copyright. Food Microstructure is a copyrighted publication. Letters granting permission to use other copyrighted material must accompany the **manuscript.**

Continued from outside back cover

Cover photo: Low temperature scanning electron microscopy provides a new and potentially very useful technique for the study of food microstructure. Cryo-preservation is an ideal method for arresting the development of dough in order to follow structural changes which occur during their preparation and baking. This figure from the paper "the application of cold stage scanning electron microscopy to food research" by J.A. Sargent (see pages 123-135) shows the structure of a hydrated, part-baked pizza dough; even the delicate strands of gluten are well preserved. Photo-width = 190 micrometers.

FOOD MICROSTRUCTURE

An International Journal on the Microstructure and Microanalysis of Foods, Feeds and their Ingredients

VOL. 7, NO. 2 (1988)

TABLE OF CONTENTS

Continued on inside back cover